ANATOMICAL CHARACTERIZATION OF THE TYPE-1 CANNABINOID RECEPTORS IN SPECIFIC BRAIN CELL POPULATIONS OF MUTANT MICE

Ana Gutiérrez Rodríguez

2016

Pedro Grandes Moreno, MD, PhD

Giovanni Marsicano, VD, PhD

eman ta zabal zazu

Universidad del País Vasco

Euskal Herriko Unibertsitatea

université de BORDEAUX

ANATOMICAL CHARACTERIZATION OF THE TYPE-1 CANNABINOID RECEPTORS IN SPECIFIC BRAIN CELL POPULATIONS OF MUTANT MICE

Ana Gutiérrez Rodríguez

2016

Pedro Grandes Moreno, MD, PhD

Giovanni Marsicano, VD, PhD

Agradecimientos

En primer lugar, agradecer al Dr. Pedro Grandes y al Dr. Giovanni Marsicano por la oportunidad de llevar a cabo mi sueño de dedicarme a la investigación. Les agradezco la confianza depositada en mi para desarrollar el trabajo de esta Tesis Doctoral. En especial a Pedro por su paciencia, consejos y apoyo.

Gracias a mis compañeros de laboratorio: Almudena, Ianire, Juan, Sonia, Leire y Elsa. Especialmente a Nago y a Izas, por ser mis maestras, por escuchar mis dudas y mis preocupaciones, animándome y guiándome siempre en la dirección correcta.

Gracias a Paula, Jon, Naiara, Irantzu, Itziar y Sara. Por todos los ratos juntos dentro y fuera del Laboratorio, por vuestra ayuda, vuestra comprensión y sobre todo, por vuestra amistad. Os voy a echar mucho de menos. Gracias en especial a Sara, que se ha convertido en alguien esencial en mi vida, por todos los kilómetros, alegrías y penas compartidas, nos vemos siempre “alla donde se cruzan los caminos”.

A mis compañeros del departamento por los buenos ratos en las comidas y por los pasillos, por tener siempre una palabra amable, por su ánimoy su energía.

A mis amigas de Reinosa, por hacerme un hueco en vuestro corazón, hace ya algunos años, compartir tantos y tantos momentos y tener siempre una palabra de aliento. Por estar siempre a mi lado, a una llamada de teléfono, sois las mejores. A Alejandra, a Lauri, a Kela, a Miguel, a Dani y a Cata; por compartir conmigo este sueño, por entenderme y por animarme en cada paso del camino.

A toda mi familia, por todo el cariño y apoyo que me habéis dado siempre, en especial a mis abuelos, a Pablo y a Tata. Gracias a mi madre y a mi padre, por su ejemplo, por estar siempre a mi lado, por cogerme de la mano tras una caida y enseñarme como levantarme para seguir luchando. Gracias por todo vuestro amor incondicional, nada de esto habría sido posible sin vosotros. ¡Os quiero mucho!

A Alex, por estar en mi vida y ser mi fuerza. Por compartir todo conmigo, porque contigo soy capaz de todo. Porque esta tesis es tan tuya como mía, te quiero.

Index

1 SUMMARIES 7

1.1 SPANISH SUMMARY 9

1.2 FRENCH SUMMARY 17

2 INTRODUCTION 25

2.1 THE ENDOCANNABINOID SYSTEM 27

2.1.1 ENDOCANNABINOID COMPOUNDS 28

2.1.2 METABOLISM OF ENDOCANNABINOIDS 29

2.1.3 CANNABINOID RECEPTORS 31

2.1.4 PHYSIOLOGICAL ACTIONS OF ENDOCANNABINOIDS 33

2.1.5 EXPRESSION OF CB_1 RECEPTOR IN THE BRAIN 35

2.1.6 ASTROCYTES AND THE CB_1 RECEPTOR 40

2.2 HIPPOCAMPUS 44

2.2.1 DEFINITION OF THE HIPPOCAMPUS 44

2.2.2 DENTATE GYRUS 45

2.2.2.1 Molecular layer. 46

2.2.2.2 Granular cell layer 47

2.2.2.3 Hilus 47

2.2.3 HIPPOCAMPUS 48

2.2.3.1 Stratum oriens 49

2.2.3.2 Pyramidal cell layer 49

2.2.3.3 Stratum lucidum 49

2.2.3.4 Stratum radiatum 49

2.2.3.5 Stratum lacunosum-moleculare 50

2.2.3.6 GABAergic cells of the hippocampus 50

2.2.4 CONNECTIONS OF THE HIPPOCAMPUS 51

2.2.4.1 Afferent connections 51

2.2.4.2 Efferent connections 52

2.2.4.3 Hippocampal synaptic circuit 53

2.3 WORKING HYPOTHESIS 55

3 OBJECTIVES 57

4 MATERIAL AND METHODS 61

4.1 ANTIBODIES 63

4.2 RESEARCH ANIMALS 65

4.2.1 CB_1 RECEPTOR MUTANT LINES 65

4.2.1.1 Generation of the CB_1-KO mice 65

4.2.1.2 Generation of conditional mutant mice bearing a selective deletion of the CB_1 receptor in cortical glutamatergic neurons (hereafter Glu-CB_1-KO) 65

4.2.1.3 Generation of conditional mutant mice bearing a selective deletion of the CB_1 receptor in GABAergic neurons (hereafter GABA-CB_1-KO) 66

4.2.1.4 Generation of conditional mutant mice bearing a selective deletion of the CB_1 receptor in astrocytes (hereafter GFAP-CB_1-KO) 66

4.2.1.5 Generation of Glu-CB_1-RS and GABA-CB_1-RS 67

4.2.1.6 Generation of GFAP-CB_1-RS 67

4.2.1.7 Generation of GFAPhrGFP-CB_1-WT and GFAPhrGFP-CB_1-KO 67

4.3 ANIMAL TREATMENT 68

4.3.1 TRANSCARDIALLY PERFUSION OF THE ANIMALS 68

4.3.2 AVIDIN-BIOTIN PEROXIDASE METHOD FOR LIGHT MICROSCOPY 69

4.3.3 PREEMBEDDING SILVER-INTENSIFIED IMMUNOGOLD METHOD FOR ELECTRON MICROSCOPY 71

4.3.4 PREEMBEDDING DOUBLE LABELING OF SILVER-INTENSIFIED IMMUNOGOLD AND IMMUNOPEROXIDASE METHOD FOR ELECTRON MICROSCOPY 73

4.4 SEMI-QUANTIFICATION OF THE CB1 RECEPTOR IMMUNOGOLD STAINING 75

4.5 SEMI-QUANTIFICATION OF THE DISTANCE FROM ASTROCYTIC CB_1 RECEPTORS TO THE NEAREST SYNAPSE. 77

5 RESULTS 79

5.1 CB_1 RECEPTOR DISTRIBUTION IN THE BRAIN OF GLU-CB_1-RS AND GABA-CB_1-RS MICE. LIGHT MICROSCOPY 81

5.2 CB_1 RECEPTOR DISTRIBUTION IN HIPPOCAMPUS OF Glu-CB_1-RS AND GABA-CB_1-RS MICE. LIGHT MICROSCOPY 81

5.3 SUBCELLULAR LOCALIZATION OF THE CB_1 RECEPTOR IN HIPPOCAMPUS OF GLU-CB_1-RS AND GABA-CB_1-RS. HIGH RESOLUTION ELECTRON MICROSCOPY 83

5.4 SUBCELLULAR LOCALIZATION OF THE CB_1 RECEPTOR IN HIPPOCAMPUS OF GFAP-CB_1-RS AND GFAPhrGFP-CB_1-WT. HIGH RESOLUTION ELECTRON MICROSCOPY 84

5.5 STATISTICS OF THE CB_1 RECEPTOR IN EXCITATORY TERMINALS OF THE Glu-CB_1-RS AND GABA-CB_1-RS HIPPOCAMPUS 86

5.6 STATISTICS OF THE CB_1 RECEPTOR IN INHIBITORY TERMINALS OF THE Glu-CB_1-RS AND GABA-CB_1-RS HIPPOCAMPUS 87

5.7 STATISTICS OF THE CB_1 RECEPTOR IN ASTROCYTIC PROCESSES OF THE GFAP-CB_1-RS AND GFAPhrGFP-CB_1-WT HIPPOCAMPUS 88

5.8 STATISTICAL ANALYSES OF THE DISTANCE FROM ASTROCYTIC CB_1 RECEPTORS TO THE NEAREST SYNAPSE 91

6 DISCUSSION 107

6.1 THE IMPORTANCE OF CB_1 RECEPTOR MUTANTS IN THE STUDY OF CB_1 RECEPTOR 109

6.2 CB_1 RECEPTOR EXPRESSION IN SPECIFIC BRAIN CELL TYPES OF RESCUE MUTANTS 112

6.2.1 CB_1 RECEPTOR EXPRESSION IN SPECIFIC NEURONAL CELL TYPES OF THE RESCUE MUTANT MICE 112

6.2.2 CB_1 RECEPTOR EXPRESSION IN ASTROCYTES OF RESCUE MUTANT MICE 115

6.3 CB_1 RECEPTOR EXPRESSION IN GFAPhrGFP-CB_1-WT MUTANT MICE 117

6.3.1 TRIPARTITE SYNAPSE: ANATOMICAL INTERPLAY BETWEEN CB_1 RECEPTORS IN ASTROCYTES AND THE NEARBY SYNAPSES ... 118

7 CONCLUSIONS 121

8 ABREVIATIONS 125

9 BIBLIOGRAPHY 131

1 SUMMARIES

1.1 SPANISH SUMMARY

INTRODUCCIÓN

El sistema endocannabinoide está compuesto, principalmente, por un grupo de ligandos lipídicos endógenos denominados endocannabinoides, los Receptores Cannabinoide de Tipo 1 (CB_1) y Tipo 2 (CB_2), así como las proteínas que participan en la síntesis, transporte y la degradación de los endocannabinoides (Piomelli, 2003; Marsicano and Lutz, 2006; Katona and Freund, 2012; Pertwee, 2015; Lu and Mackie, 2016). Este sistema se encuentra involucrado en numerosos mecanismos cerebrales, en el desarrollo del sistema nervioso prenatal y en diversas funciones cognitivas (Marsicano and Kuner, 2008; Bellocchio y coils., 2010; Katona and Freund, 2012). Respecto a la expresión del receptor CB_1, se ha descrito como los terminales inhibidores de neuronas GABAérgicas presentan elevados niveles de expresión de este receptor (Katona y coils., 1999; Kawamura y coils., 2006; Ludányi y coils., 2008; Marsicano and Kuner, 2008; Katona and Freund, 2012; De-May and Ali, 2013; Steindel y coils., 2013; Hu and Mackie, 2015) mientras en los terminales axónicos de neuronas glutamatérgicas encontramos niveles de expresión más bajos (Marsicano y coils., 2003; Domenici y coils., 2006; Takahashi and Castillo, 2006; Katona y coils., 2006; Monory y coils., 2006; Kamprath y coils., 2009; Bellocchio y coils., 2010; Puente y coils., 2011; Reguero y coils., 2011; Steindel y coils., 2013; Ruehle y coils., 2013; Soria-Gómez y coils., 2014). Por otro lado, a nivel subcelular, se ha descrito la expresión del receptor CB_1 en las membranas de las mitocondrias del cerebro y del músculo (Bénard y coils., 2012; Hebert-Chatelain y coils., 2014a; b; Koch y coils., 2015). Así mismo, se ha descrito como el receptor CB_1 está también localizado en los astrocitos en

donde desempeña un papel fundamental en el contexto de la sinapsis tripartita (Navarrete and Araque, 2008, 2010; Perea y coils., 2009; Han y coils., 2012; Gómez-Gonzalo y coils., 2014; Navarrete y coils., 2014; Metna-Laurent and Marsicano, 2015; Viader y coils., 2015; Oliveira da Cruz y coils., 2016).

Las diferencias existentes en los niveles de expresión de este receptor entre los diversos tipos celulares (Marsicano and Lutz, 1999), hacen que resulte extremadamente difícil detectar su expresión en tipos de células y / o en compartimentos sub-celulares donde su expresión es fisiológicamente muy baja (Busquets-Garcia y coils., 2015). En ese sentido, en el pasado, la presencia de niveles bajos de receptor CB_1 fue interpretada erróneamente como mera tinción de fondo en análisis anatómicos de ratones de silvestres (*CB_1*-WT) (Freund y coils., 2003).

De esta manera, para la correcta caracterización anatómica de la distribución subcelular de los receptores CB_1 en cualquier tipo celular, independientemente de sus niveles fisiológicos de expresión, se hace necesarias mejores técnicas de análisis. En ese sentido, las estrategias de "rescate" genético mediante el uso del sistema Cre/LoxP (Balthasar y coils., 2005) suponen una gran herramienta de estudio, ya que permiten analizar la expresión del receptor CB_1 endógeno exclusivamente en tipos celulares determinados (Ruehle y coils., 2013; Soria-Gómez y coils., 2014; de Salas-Quiroga y coils.). En concreto, esta estrategia resulta particularmente útil para determinar el patrón de expresión del receptor CB_1 en tipos específicos de células donde sus niveles de expresión son bajos y puedan encontrarse enmascarados por la enorme expresión de este receptor en otros tipos de células. Sin embargo, es de gran importancia comprobar que la re-

expresión del receptor CB_1 mantiene sus niveles endógenos y se limita a las células deseadas.

En mi tesis doctoral se pretende examinar la expresión receptor CB_1 en el hipocampo de ratones rescatados genéticamente los cuales expresan el gen del receptor CB_1 exclusivamente en determinados tipos celulares: neuronas glutamatérgicas telencefálicas dorsales (ratones Glu-*CB_1*-RS) y neuronas GABAérgicas (ratones GABA-*CB_1*-RS).

Así mismo, con el objetivo de conocer la distribución del receptor CB1 de astrocitos, respecto a las sinapsis excitadoras e inhibidoras, se realizará el análisis de la expresión del CB_1 en ratones que expresan el receptor CB1 únicamente en astrocitos, (GFAP-*CB_1*-RS) y en ratones transgénicos que expresan en astrocitos la proteína citoplasmática difusible hrGFP (ratones GFAPhrGFP-*CB_1*-WT) que permite una mejor detección de la superficie de los astrocitos.

MATERIAL Y MÉTODOS

Ratones: CB1-WT, *CB_1*-KO (no expresan receptor CB_1), GABA-*CB_1*-RS, Glu-CB1-RS, GABA-*CB_1*-KO (no expresan el receptor CB_1 en neuronas GABAérgicas), Glu-*CB_1*-KO (no expresan el receptor CB_1 en neuronas glutamatérgicas telencefálicas dorsales), GFAP-*CB_1*-RS, GFAP-*CB_1*-KO (no expresan el receptor CB_1 en astrocitos), GFAPhrGFP-*CB_1*-WT y GFAPhrGFP-*CB_1*-KO (no expresan el receptor CB_1), fueron profundamente anestesiados y sometidos a perfusión transcardiaca.

La técnica de inmuno-oro preinclusión para Microscopía Electrónica fue aplicada a secciones del hipocampo de ratones *CB_1*-WT, *CB_1*-KO, GABA-*CB_1*-RS, Glu-*CB_1*-RS, GABA-*CB_1*-KO y Glu-*CB_1*-KO. Mientras que a las secciones de hipocampo de ratones GFAP-*CB_1*-RS, GFAP-*CB_1*-KO, GFAPhrGFP-*CB_1*-WT y

GFAPhrGFP-*CB1*-KO se les aplicó la técnica de inmuno-oro e inmunoperoxidasa preinclusión para Microscopía Electrónica. En todos los casos los análisis se llevaron a cabo utilizando tres animales de cada tipo. En estos animales se analizó la distribución anatómica del receptor CB_1 en los diferentes tipos celulares y compartimentos subcelulares. Los datos obtenidos fueron analizados aplicando primero la prueba de normalidad de Kolmogorov-Smirnov para posteriormente analizar estadísticamente los datos mediante test no paramétricos de contraste de medias (prueba de Man-Whitney cuando k = 2 o la prueba de Kruskal-Wallis cuando k> 2).

RESULTADOS

La comparación del porcentaje de terminales excitadores marcados con CB_1 en el stratum radiatum del CA1 en el ratón Glu-*CB1*-RS (21,89% ± 1,21) en el ratón *CB1*-WT y en el ratón GABA-*CB1*-KO no fue estadísticamente significativo. Sin embargo, este valor prácticamente desaparece en los ratones Glu-*CB1*-KO, GABA-*CB1*-RS and *CB1*-KO. Además, no se encontraron diferencias significativas entre el valor de la densidad, expresada como el número de partículas del receptor CB_1 por µm del perímetro de la membrana (partículas/µm), entre los terminales excitadores de Glu-*CB1*-RS (0.45 ± 0.02), *CB1*-WT y GABA-*CB1*-KO.

En el tercio interno de la capa molecular del giro dentado similares porcentajes de terminales excitadores que presentan receptor CB_1 se encontraron en Glu-*CB1*-RS (53.19% ± 2.89), *CB1*-WT y GABA-*CB1*-KO. Desapareciendo prácticamente esta proporción en los ratones Glu-*CB1*-KO, GABA-*CB1*-RS and *CB1*-KO. La densidad de inmunopartículas de CB_1 fue estadísticamente similar entre Glu-*CB1*-RS (0.39 ± 0.02) *CB1*-WT y GABA-*CB1*-KO.

El valor del porcentaje de terminales inhibidores marcados positivamente para el receptor CB_1 en los ratones GABA-*CB1*-RS (77.92% ± 2.63), *CB1*-WT y Glu-*CB1*-KO se mantuvo en el stratum radiatum de la región CA1. Sin embargo, esta proporción prácticamente desaparece en los animales GABA-*CB1*-KO, Glu-*CB1*-RS y *CB1*-KO. No se encontraron diferencias significativas tras la comparación de la densidad de partículas de CB_1 en los terminales inhibidores de los ratones GABA-*CB1*-RS (4.33 ± 0.11 partículas/µm), *CB1*-WT y Glu-*CB1*-KO.

En el tercio interno de la capa molecular del giro dentado, no se obtuvieron diferencias significativas comparando los valores obtenidos para el porcentaje de terminales inhibidores marcados con CB_1 en ratones GABA-*CB1*-RS (85.07% ± 1.76), *CB1*-WT y Glu-*CB1*-KO. Solamente valores residuales del receptor CB_1 se hallaron en animales GABA-*CB1*-KO, Glu-*CB1*-RS y *CB1*-KO. No hubo diferencias significativas tras el análisis estadístico de la densidad de partículas de CB_1 en los terminales inhibidores entre los ratones GABA-*CB1*-RS (7.47 ± 0.14), *CB1*-WT y Glu-*CB1*-KO

En el stratum radiatum de la región CA1 el análisis de los procesos astrocíticos que presentaban un marcaje positivo para CB_1 no resulto estadísticamente significativo al comparar los valores obtenidos en el ratón *CB1*-WT y el ratón GFAP-*CB1*-RS (37.12% ± 3.79). Sin embargo, la proporción de procesos astrocíticos positivos para CB_1 en el ratón GFAPhrGFP-*CB1*-WT aumentó hasta alcanzar el valor de 59.91 % ± 3.29, un aumento que resultó estadísticamente significativo al compararlo con *CB1*-WT. Por otra parte, sólo niveles residuales del receptor CB1 se encontraron en los astrocitos de los animales GFAP-*CB1*-KO, *CB1*-KO y GFAPhrGFP-*CB1*-KO.

Así mismo, la densidad de partículas de CB_1 en la membrana de los procesos astrocíticos (partículas/µm) fue similar entre los valores del ratón *CB_1*-WT y del ratón GFAP-*CB_1*-RS (0.128 ± 0.020). Por otro lado, un gran aumento estadísticamente significativo en la densidad del receptor se obtuvo en el ratón GFAPhrGFP-*CB_1*-WT (0.384 ± 0.039).

En la capa molecular del giro dentado del hipocampo, tras analizar el porcentaje de procesos astrocíticos positivos para CB_1 no se obtuvieron diferencias significativas entre los valores del ratón GFAP-*CB_1*-RS (39.84% ± 3.50) y el ratón *CB_1*-WT, mientras que la proporción aumentó significativamente hasta ser del 59.99% ± 3.37 en el ratón GFAPhrGFP-*CB_1*-WT. Por otra parte, solamente se encontraron partículas de oro residuales en los ratones GFAP-*CB_1*-KO, GFAPhrGFP-*CB_1*-KO y *CB_1*-KO. Además, no hubo diferencias significativas tras la comparación de la densidad del receptor en los astrocitos del ratón *CB_1*-WT y el ratón GFAP-*CB_1*-RS (0.138 ± 0.016). Sin embargo, se obtuvieron diferencias significativas al comparar estos valores con el obtenido en el ratón GFAPhrGFP-*CB_1*-WT (0.334 ± 0.033).

Una vez demostrado que una mejor detección del CB_1 en astrocitos es posible al utilizar la proteína hr-GFP como marcador en el ratón GFAPhrGFP-*CB_1*-WT, se analizó la distancia existente entre el receptor CB_1 astroglial y el punto medio de la sinapsis más cercana. Así, en el stratum radiatum de CA1, el 51,07% ± 3,79 de las sinapsis totales que rodean a un proceso astrocítico estaban situadas a una distancia entre 400 y 800 nm del receptor CB_1 astroglial. Por otra parte, el 43% ± 1,01 de estas sinapsis fueron identificados como sinapsis excitadoras mientras que sólo el 9,91% ± 1,93 eran inhibidoras. En la capa molecular del giro dentado el 57,25% ± 3,19 del total de las sinapsis que rodean a un proceso astrocítico se

encontraron entre 400 y 800 nm de distancia del receptor CB_1 de los astrocitos. De estas sinapsis el 46,67% ± 2,17 fueron identificadas como excitadoras mientras que el 10,59% ± 2,18 eran sinapsis inhibidoras.

CONCLUSIONES

Las conclusiones obtenidas en esta Tesis son las que siguen:

1- En el ratón Glu-*CB_1*-RS se mantienen los mismos niveles de expresión de los receptores CB_1 hipocampal que en los ratones tipo silvestre *CB_1*-WT en las neuronas glutamatérgicas del telencéfalo dorsal.
2- En el ratón GABA-*CB_1*-RS se mantienen los mismos niveles de expresión de los receptores CB_1 hipocampal que en los ratones tipo silvestre *CB_1*-WT únicamente en neuronas GABAergicas.
3- En el ratón GFAP-*CB_1*-RS se mantienen los mismos niveles de expresión de los receptores CB_1 hipocampal que en procesos astrocíticos de los ratones tipo silvestre *CB_1*-WT.

4- La utilización de hrGFP como marcador en el ratón mutante GFAPhrGFP-*CB_1*-WT permitió la detección de niveles significativamente mayores de expresión del receptor CB_1 en los procesos astrocíticos hipocampales que los encontrados en los ratones tipo silvestre *CB_1*-WT utilizando como marcador GFAP.
5- En el hipocampo, la distancia más común entre el receptor CB_1 de astrocitos y la sinapsis más cercana se encuentra en el rango de los 400-800 nm, siendo la mayoría de ellas excitadoras.

6- La mayoria de las sinapsis observadas en el CA1 y en la capa molecular del giro dentado rodeadas de astrocitos inmunopositivos para el receptor CB_1 en el rango de 400-800 nm son de naturaleza excitatoria.

7- El estudio de los ratones mutantes rescatados para el receptor CB_1 caracterizados en esta Tesis Doctoral ha demostrado que: 1) la expresión de los receptores CB_1 se produce en tipos celulares específicos; 2) la re-expresión se encuentra limitada a poblaciones neurales concretas o a astrocitos; 3) los niveles endógenos de receptors CB_1 se mantienen en los tipos celulares que re-expresan el receptor.

8- En conjunto, los ratones mutantes estudiados rescatos para el receptor CB_1 son herramientas excelentes para la realización de estudios funcionales y translacionales relativas al papel de los receptores CB_1 en el cerebro en condiciones normales y patológicas.

1.2 FRENCH SUMMARY

INTRODUCTION

Le système endocannabinoïde est principalement formé par des ligands endogènes lipides (endocannabinoïdes), le Récepteur au cannabinoïde de type 1 (CB_1) et de type 2 (CB_2), ainsi que leurs protéines de synthèse, de transport et de dégradation (Piomelli, 2003; Marsicano and Lutz, 2006; Katona and Freund, 2012; Pertwee, 2015; Lu and Mackie, 2016). Ce système est impliqué dans plusieurs fonctions cérébrales, le développement prénatal du cerveau et de nombreuses fonctions cognitives (Marsicano and Kuner, 2008; Bellocchio et al., 2010; Katona and Freund, 2012). L'expression du récepteur CB_1 est très élevée dans les neurones inhibiteurs GABAergiques concentrée sur leurs terminaisons synaptiques (Katona et al., 1999; Kawamura et al., 2006; Ludányi et al., 2008; Marsicano and Kuner, 2008; Katona and Freund, 2012; De-May and Ali, 2013; Steindel et al., 2013; Hu and Mackie, 2015) et faible dans les neurones glutamatergiques avec une localisation rare des récepteurs sur leurs boutons axonaux (Marsicano et al., 2003; Domenici et al., 2006; Takahashi and Castillo, 2006; Katona et al., 2006; Monory et al., 2006; Kamprath et al., 2009; Bellocchio et al., 2010; Puente et al., 2011; Reguero et al., 2011; Steindel et al., 2013; Ruehle et al., 2013; Soria-Gómez et al., 2014). Les récepteurs CB_1 sont aussi localisés dans les membranes mitochondriales dans le cerveau et les muscles (Bénard et al., 2012; Hebert-Chatelain et al., 2014a; b; Koch et al., 2015) et dans les astrocytes où ils jouent un rôle clé dans le contexte de la synapse tripartite (Navarrete and Araque, 2008, 2010; Perea et al., 2009; Han et al., 2012; Gómez-Gonzalo et al., 2014; Navarrete et al., 2014; Metna-Laurent and Marsicano, 2015; Viader et al., 2015; Oliveira da Cruz et al., 2016). En raison de la très grande

différence de niveau d'expression entre les différents types de cellules (Marsicano and Lutz, 1999), il est extrêmenent difficile d'identifier les faibles niveaux du récepteur CB_1 dans ces types cellulaires et/ou dans les compartiments subcellulaires de cerveaux de souris de type sauvage (Busquets-Garcia et al., 2015). En effet, auparavant, de faibles niveaux d'expression du récepteur CB_1 ont été considérés comme bruit de fond (Freund et al., 2003). Pour établir correctement la distribution anatomique des récepteurs CB_1 dans des types cellulaires spécifiques, indépendamment des niveaux d'expression endogènes, de nouvelles techniques d'analyse sont nécessaires. Par conséquent, la stratégie génétique de "sauvetage" (rescue) basée sur l'utilisation du système Cre/loxP (Balthasar et al., 2005) est apparue comme un excellent outil pour la détermination de l'expression du récepteur CB_1 endogène dans des types cellulaires spécifiques (Ruehle et al., 2013; Soria-Gómez et al., 2014; de Salas-Quiroga et al., 2015). Ceci est particulièrement utile pour élucider les niveaux réels des récepteurs CB_1 dans des types cellulaires spécifiques exprimant de faibles niveaux de la protéine CB_1, ce qui élimine les interférences causées par des cellules qui expriment des niveaux élevés de récepteurs CB_1. Cependant, il est très important de vérifier que la ré-expression est limitée aux types de cellules recherchées et qu'elle maintient les niveaux des récepteurs CB_1 endogènes, où les séquences régulatrices du récepteur sont normalement activées.

J'ai examiné dans ma thèse l'expression du récepteur CB_1 dans l'hippocampe de souris mutantes ré-exprimant spécifiquement le gène spécifiquement dans certains types cellulaires du cerveau tels que : les neurones glutamatergiques du télencéphale dorsal (souris Glu-*CB_1*-RS), et les neurones GABAergiques (souris GABA-*CB_1*-RS).

De plus, dans le but de connaître la distribution anatomique exacte des récepteurs CB_1 astrogliaux par rapport aux synapses excitatrices et inihibitrices, j'ai également étudié l'expression des récepteurs CB_1 dans les astrocytes de souris GFAP-*CB_1*-RS (exprimant le récepteur CB_1 seulement dans les astrocytes) et une souris mutante ciblée pour exprimer la protéine cytoplasmique hrGFP diffusible dans les cellules astrogliales (GFAPhrGFP-*CB_1*-WT) ce qui permet une meilleure détection des prolongements astrocytaires.

MATERIEL ET METHODES

Souris: *CB_1*-WT, *CB_1*-KO (absence des récepteurs CB_1), GABA-*CB_1*-RS, Glu-*CB1*-RS, GABA-*CB_1*-KO (portant une délétion sélective du récepteur CB_1 dans les neurons GABAergiques), Glu-*CB_1*-KO (portant une délétion sélective du récepteur CB_1 dans les neurons glutamatergiques du télencéphale dorsal), GFAP-*CB1*-RS, GFAP-*CB1*-KO (portant une délétion sélective du récepteur CB_1 dans les astrocytes), GFAPhrGFP-*CB_1*-WT et GFAPhrGFP-*CB_1*-KO (absence des récepteurs CB_1 dans les astrocytes). Les animaux ont été profondément anesthésiés et perfusés par voie transcardiaque.

Une méthode de pré-enrobage immunogold pour la microscopie électronique a été appliquée aux coupes hippocampales des souris *CB_1*-WT, *CB_1*-KO, GABA-*CB_1*-RS, Glu-*CB_1*-RS, GABA-*CB_1*-KO et Glu-*CB_1*-KO. Egalement, une méthode combinant un pré-enrobage immunogold et une immunoperoxidase a été utilisée pour les coupes hippocampales des souris GFAP-*CB_1*-RS, GFAP-*CB_1*-KO, GFAPhrGFP-*CB_1*-WT et GFAPhrGFP-*CB_1*-KO. Les expériences ont toujours été réalisées sur trois animaux différents pour chaque condition. Afin de déterminer statistiquement la distribution des récepteurs CB_1 dans les différents types de

cellules et compartiments cellulaires étudiés, un test de normalité a été appliqué (test de normalité de Kolmogorov-Smirnov) avant l'exécution des analyses statistiques. Les données ont été analysées à l'aide de tests non-paramétriques (Man-Whitney U test lorsque k=2 ou Kruskal-Wallis test lorsque k>2).

RESULTATS

La proportion de récepteurs CB_1 immunopositifs au niveau des terminaisons synaptiques excitatrices du stratum radiatum de la région CA1 de l'hippocampe des Glu-*CB1*-RS (21.89% ± 1.21), *CB1*-WT et GABA-*CB1*-KO n'est pas statistiquement différente. Cependant, le pourcentage de terminaisons immunopositives disparait virtuellement chez les animaux Glu-*CB1*-KO, GABA-*CB1*-RS et *CB1*-KO. En outre, aucune différence statistique n'est trouvée pour la densité de récepteur CB_1, exprimée comme étant le nombre de particules par µm du périmètre de la cellule (particules/µm), entre les terminaisons synaptiques excitatrices des Glu-*CB1*-RS (0.45 ± 0.02), *CB1*-WT et GABA-*CB1*-KO.

L'analyse du tiers interne de la couche dentée moléculaire montre des pourcentages de récepteurs immuno-positifs au niveau des terminaisons synaptiques excitatrices comparables chez les Glu-*CB1*-RS (53.19% ± 2.89), *CB1*-WT et GABA-*CB1*-KO. Cette proportion est quasi nulle chez les Glu-*CB1*-KO, GABA-*CB1*-RS et *CB1*-KO. La densité d'immunoparticules de récepteurs CB_1 est statistiquement similaire chez les Glu-*CB1*-RS (0.39 ± 0.02) *CB1*-WT et GABA-*CB1*-KO.

Le nombre de récepteurs CB_1 immunopositifs au niveau des terminaisons neuronales des synapses inhibitrices chez les GABA-*CB1*-RS (77.92% ± 2.63), *CB1*-WT et Glu-*CB1*-KO est maintenu dans le stratum radiatum de CA1.

Cependant, la proportion disparait chez les GABA-*CB1*-KO, Glu-*CB1*-RS et *CB1*-KO. Il n'existe pas de différence significative pour la densité des immunoparticules du récepteur CB_1 entre les terminaisons des synapses inhibitrices des GABA-*CB1*-RS (4.33 ± 0.11), *CB1*-WT et Glu-*CB1*-KO.

La proportion de récepteurs CB_1 immunopositifs au niveau des terminaisons des synapses inhibitrices du tiers interne de la couche dentée moléculaire est similaire entre les GABA-*CB1*-RS (85.07% ± 1.76), *CB1*-WT et Glu-*CB1*-KO. Ces valeurs disparaissent quasiment chez les GABA-*CB1*-KO, Glu-*CB1*-RS et *CB1*-KO. Il n'existe pas de différence significative pour la densité de récepteurs CB_1 au niveau des synapses inhibitrices des GABA-*CB1*-RS (7.47 ± 0.14), *CB1*-WT et Glu-*CB1*-KO.

La proportion de récepteurs CB_1 immunopositifs au niveau des prolongements astrocytaires du stratum radiatum n'est pas significativement différente entre les animaux *CB1*-WT et GFAP-*CB1*-RS (37.12% ± 3.79)

Chez les animaux GFAPhrGFP-*CB1*-WT, la proportion d'éléments astrocytaires immunomarqués pour le récepteur CB_1 augmente de 59.91 % ± 3.29, devenant statistiquement différent comparé au *CB1*-WT. A l'inverse, seuls de rares récepteurs CB_1 sont marqués dans les astrocytes des souris GFAP-*CB1*-KO, *CB1*-KO et chez les souris GFAPhrGFP-*CB1*-KO. La densité d'immunoparticule pour le récepteur CB_1 au niveau de la membrane astrocytaire (particules/µm) est également analysée. Nos données montrent qu'il n'y a pas de différence significative entre les *CB1*-WT et les GFAP-*CB1*-RS (0.128 ± 0.020), alors que nous avons une plus forte densité chez les GFAPhrGFP-*CB1*-WT (0.384 ± 0.039).

L'analyse du tiers interne de la couche dentée moléculaire montre des pourcentages de récepteurs immuno-positifs au niveau des prolongements astrocytaires comparables chez les GFAP-*CB1*-RS (39.84% ± 3.50) et les *CB1*-WT alors que cette proportion augmente de manière significative (59.99% ± 3.37) chez les GFAPhrGFP-*CB1*-WT. Seuls des particules résiduelles sont observées chez les souris GFAP-*CB1*-KO, GFAPhrGFP-*CB1*-KO et *CB1*-KO. Enfin, aucune différence significative de densité du récepteur CB1 n'est observée dans les prolongements astrocytaires des souris *CB1*-WT et GFAP-*CB1*-RS (0.138 ± 0.016). On observe une différence significative de densité du récepteur CB_1 dans les prolongements astrocytaires des souris GFAPhrGFP-*CB1*-WT comparée au *CB1*-WT (0.334 ± 0.033).

Grâce à une meilleure détection des astrocytes obtenue avec la protéine hr-GFP en microscopie électronique, nous avons mesuré la distance entre les immunoparticules du récepteur CB_1 astroglial et le point central de la synapse la plus proche entourée par l'élément astrocytaire immunopositif chez les GFAPhrGFP-*CB1*-WT. Dans le CA1, 51.07% ± 3.79 de toutes les synapses entourées par un prolongement astrocytaire se trouvent à une distance de 400 à 800 nm de la particule astrocytaire la plus proche. Parmi celles-ci, 43.33% ± 1.01 sont des synapses excitatrices alors que 9.91%+/-1.93 sont des synapses inhibitrices. Dans la couche moléculaire dentée, 57.25% ± 3.19 des synapses entourées par un prolongement astrocytaire se trouvent entre 400 et 800 nm de la particule du récepteur CB_1 astroglial. 46.67% ± 2.17 sont au niveau de synapses excitatrices alors que 10.59% ± 2.18 se trouvent au niveau de synapses inhibitrices.

CONCLUSIONS

Les conclusions de ce travail de thèse sont les suivantes:

1. Le niveau d'expression et la localisation des récepteurs CB_1 des neurones glutamatergiques de l'hippocampe de souris Glu-*CB_1*-RS est similaire à celui de souris *CB_1*-WT.

2. Le niveau d'expression et la localisation des récepteurs CB_1 des neurones GABAergiques de l'hippocampe de souris GABA-*CB_1*-RS est similaire à celui des *CB_1*-WT.
3. Le niveau d'expression et la localisation des récepteurs CB_1 dans les astrocytes de l'hippocampe de souris GFAP-*CB_1*-RS est similaire à celui des *CB_1*-WT.
4. La détection des récepteurs CB_1 dans les astrocytes de l'hippocampe de souris GFAPhrGFP-*CB_1*-WT est significativement supérieure comparée aux animaux *CB_1*-WT avec un marqueur GFAP.

5. La distance la plus commune entre le récepteur CB_1 astroglial et la synapse la plus proche est de 400 à 800 nm.
6. La majorité des synapses entourées par des astrocytes immunopositifs pour le récepteur CB_1 dans la région CA1 et de la couche moléculaire dentée, est de nature excitatrice.
7. Les souris mutantes réexprimants le récepteur CB_1 caractérisées dans ce travail de thèse montre: 1) expression du récepteur CB_1 dans différents types cellulaires, 2) la réexpression est limitée à une population neuronale particulière ou aux astrocytes, 3) les niveaux endogènes de récepteurs CB_1

sont maintenus dans les différents types cellulaires ré-exprimants le récepteur CB_1.

8. De façon générale, ces résultats nous montrent que les souris mutantes ré-exprimants le récepteur CB_1 sont d'excellents outils pour l'étude fonctionnelle et translationnelles sur le rôle de ce récepteur dans le cerveau sain ou pathologique.

2 INTRODUCTION

2.1 THE ENDOCANNABINOID SYSTEM

The Cannabis plant (*Cannabis sativa* L.) has been used since antiquity, mostly for the manufacturing and fabrication of cordages but also by its psychotropic, analgesic and antispasmodic effects (Piomelli, 2003). Cannabis plants produce a mixture of chemical constituents, which are collectively referred as phytocannabinoids. Cannabinoids have been shown to produce a unique plethora of effects on the behavior of humans and animals which include euphoria, excitement, cognitive impairments, hypothermia, errors of time and space, enhancement of the sense of hearing, fluctuations of emotions, discoordination, illusions and hallucinations, disruption of short-term memory, relaxation, tachycardia, a decreased ability to focus attention, and sleepiness (Block et al., 1992; Chait and Perry, 1994; Heishman et al., 1997; Court, 1998; Mechoulam and Parker, 2011).

Among these compounds, delta (9) - tetrahydrocannabinol (Δ^9-THC or THC) was first isolated in 1964 (Gaoni and Mechoulam, 1964), and was shown to account for the psychotropic effects of cannabis. Δ^9-THC was described to couple with a group of receptors later named as the cannabinoid receptors, which consequently represent the target of a type of endogenous lipidic messengers, the endocannabinoids. Thus, the endocannabinoid system is comprised by the cannabinoid receptors, their endogenous lipid ligands (the endocannabinoids) and also the enzymes for their synthesis and degradation (Piomelli, 2003, 2014; De Petrocellis et al., 2004; Marsicano and Lutz, 2006; Kano et al., 2009; Katona and Freund, 2012; Pertwee, 2015; Lu and Mackie, 2016).

This system is involved in many brain processes ranging from food intake to cognition (Marsicano and Kuner, 2008; Bellocchio et al., 2010; Katona and Freund,

2012). More specifically, endocannabinoids participate in the complex cellular and molecular mechanisms involved in endocannabinoid-mediated synaptic plasticity (Castillo, 2012) which provide important computational properties to brain circuits, such as coincidence detection and input specificity, critical for high brain functions (Castillo et al., 2012).

2.1.1 ENDOCANNABINOID COMPOUNDS

Endocannabinoids are endogenous lipid compounds synthesized from the cellular membranes. Among them, there are two main endocannabinoids which are better identified and characterized, i.e. *N*-arachidonoylethanolamine (anandamide, AEA) (Devane et al., 1992) and 2-arachidonoylglycerol (2-AG) (Mechoulam et al., 1995). AEA is known by triggering the “tetrad” effects (i.e., catalepsy, antinociception, hypolocomotion, and hypothermia) of cannabinoids in rodents (Fride and Mechoulam, 1993) whereas 2-AG plays a key role in most of the Cannabinoid Type I (CB_1) receptor mediation of synaptic transmission (Kano et al., 2009).

Endocannabinoids are synthesized and released *on demand* following physiological and pathological stimuli and, for the best of our knowledge no evidence have been found for their storage in secretory vesicles (De Petrocellis and Di Marzo, 2009a; Pertwee et al., 2010).

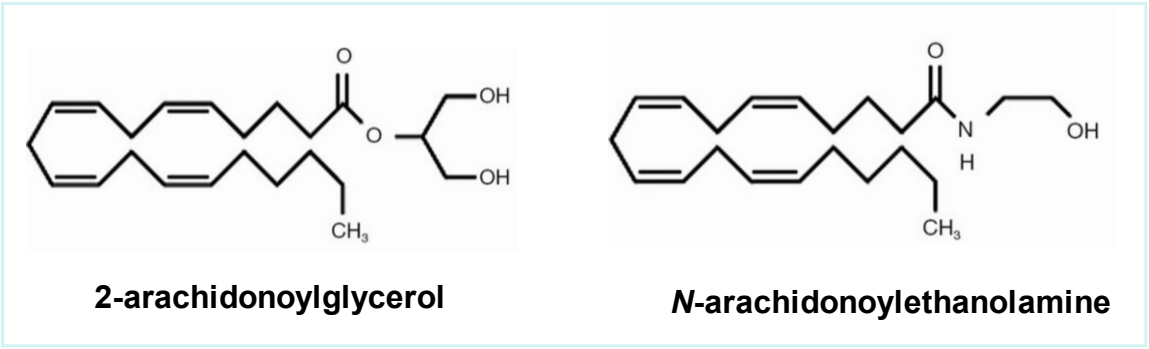

Figure 1. Chemical structures of the two major endocannabinoids. N-arachidonylethanolamide (AEA; "anandamide") and 2-arachidonoylglycerol (2-AG).

Interestingly, other *N*-acyletanolamines such as oleoylethanolamine (OEA) (Fu et al., 2003; Wang et al., 2005; Thabuis et al., 2008) and palmitoylethanolamine (PEA) (Di Marzo et al., 2001; Costa et al., 2008) exhibit a variety of similar biological activities and share with the endocannabinoids certain metabolic pathways. However, it has not been well established if these molecules also share with endocannabinoids their molecular targets (De Petrocellis and Di Marzo, 2009a).

2.1.2 METABOLISM OF ENDOCANNABINOIDS

A wide variety of biochemical pathways for the synthesis, transport, release and degradation of endocannabinoids have been described to date (Piomelli, 2014). In this sense, neuronal membrane depolarization or the activation of G_q-coupled GPCRs triggers the synthesis of 2-AG (Hashimotodani et al., 2005; Kano et al., 2009). It is thought that phospholipase C, β or δ hydrolyses membrane phospholipids to obtain diacylglycerols (DGs), and then the degradation of these DGs by diacylglycerol lipases (DGLs) is driven to the synthesis 2-AG (Gao et al., 2010; Tanimura et al., 2010).

Similarly, it has been described that the Ca^{2+}-dependent enzyme N-acyltransferase (NAT) drives the transfer of arachidonic acid (AA) from phosphatidylcholine to phosphatidylethanolamine, consequently forming the AEA precursor N-arachidonoyl phosphatidylethanolamine (NAPE) (Cadas et al., 1996). Afterwards, the N-acyl phosphatidylethanolamine specific phospholipase D (NAPE-PLD) (Okamoto et al., 2004) catalyzes the release of AEA.

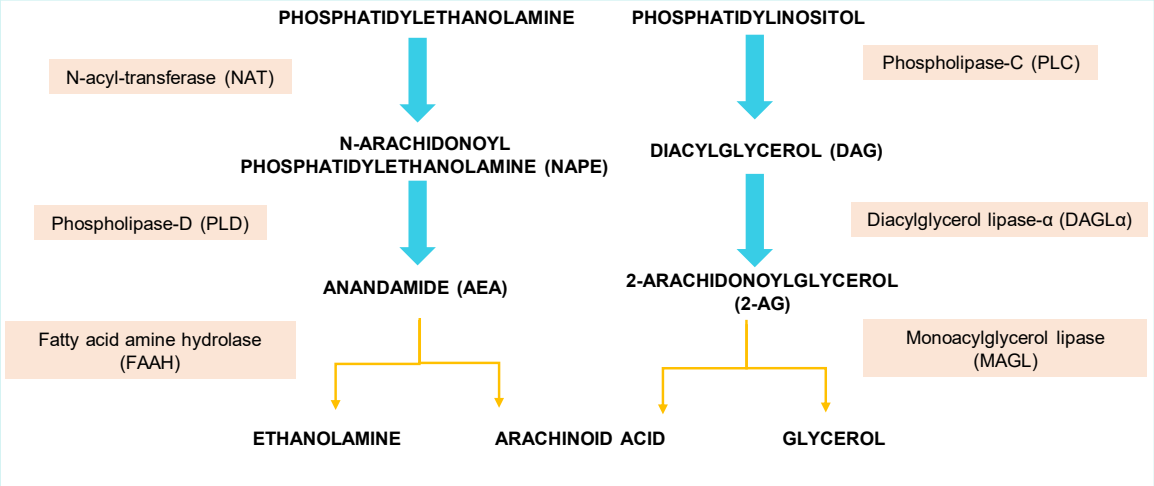

Figure 2. **Major pathways of anandamide and 2-AG synthesis and degradation**. Modified from Lee et al., 2015.

Nevertheless, an alternative pathway for the releasement of AEA includes the hydrolysis of NAPE to phosphoanandamide by the action of the Phospholipase C (PLC) followed by dephosphorylation mediated by phosphatase, such as PTPN22 (Liu et al., 2006).

Conversely, monoacylglicerol lipase (MAGL) and fatty acid amide hydrolase (FAAH) represent the two main catabolic enzymes for the hydrolysis of 2-AG and AEA respectively (Dinh et al., 2002; Ueda, 2002). In this sense, MAGL is mainly found on presynaptic terminals, where it hydrolyses 2-AG molecules bound to presynaptic CB_1 receptors (Straiker et al., 2009; Kano et al., 2009). Furthermore, two other hydrolases, ABHD6 and ABHD12 (α/β-hydrolase domain containing 6

and 12) are also capable of hydrolyzing 2-AG (Blankman et al., 2007). On the other hand, FAAH showing overlap with CB_1 in many brain regions (Egertová et al., 2003; Kano et al., 2009). Moreover, FAAH has also been described to be involved in the metabolism of other bioactive N-acylethanolamines such as OEA and PEA (Di Marzo et al., 2001).

2.1.3 CANNABINOID RECEPTORS

Endocannabinoids receptors are known to be present in many vertebrate species, including rodents and primates, both monkeys and humans, (Elphick and Egertová, 2005). To date, two cannabinoid receptors have been cloned, i.e. the Type I Cannabinoid receptor (CB_1 receptor) (Matsuda et al., 1993) and the Type II Cannabinoid receptor (CB_2 receptor) (Munro et al., 1993).

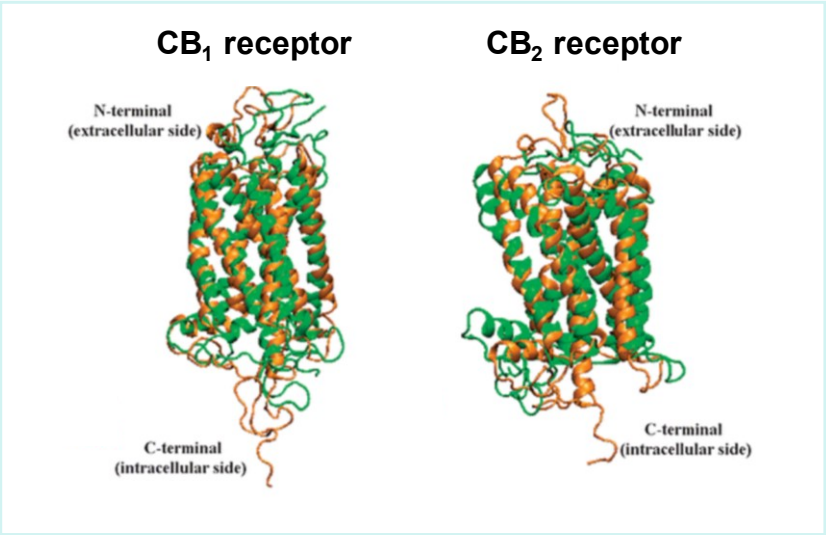

Figure 3. **Three-dimensional representation of CB_1 receptor and CB_2 receptor structure**. Modified from Ramos et al., 2011.

The CB_1 and CB_2 cannabinoid receptors belonging to the G-protein-coupled receptors (GPCRs) superfamily, the largest family of trans-membrane proteins in the human genome, and crucial for many essential physiological processes.

GPCRs are characterized by seven hydrophobic transmembrane segments connected by intracellular and extracellular loops, an N-terminal extracellular domain that possesses glycosylation sites and a C-terminal intracellular domain coupled to a $G_{i/o}$ protein (Howlett et al., 2002).

In the cell, the activation of CB_1 or CB_2 receptor by endocannabinoids triggers intracellular signaling events coupled to these two G-protein-coupled receptors (GPCRs) (Pertwee, 1997). Firstly, stimulation of CB_1 or CB_2 receptor leads to the inhibition of stimulus-induced adenylate cyclase (AC) and, consequently, modulates protein kinase-A-dependent cascades. Moreover, the activation of these receptors provokes the stimulation of mitogen-activated protein kinase signaling. More specifically, the activation of CB_1 receptor also exerts the modulation of ion channels, inducing inhibition of P, Q and N-type voltage-sensitive Ca^{2+} channels and stimulation of rectifying G-protein-coupled K^+ channels. Also, just in the case of CB_1 receptors, the stimulation of this receptor induces the activation of PLC-ɣ, by the βɣ subunits of Gi/o proteins stimulates phosphatidylinositol 3-kinase and intracellular Ca^{2+} mobilization (Devane et al., 1988; Howlett et al., 1990, 2002; De Petrocellis et al., 2004; Pertwee, 2015).

CB_1 receptor is predominantly expressed in the central nervous system (CNS) particularly in brain cortex, basal ganglia, hippocampus, and cerebellum (Hu and Mackie, 2015). Besides, minor levels of expression of CB_1 receptors have been also document in various peripheral tissues (Pertwee, 2000, 2001). On the contrary, CB_2 receptor are localized primarily in immune cells and tissues derived from the immune system (Ameri, 1999; Cabral et al., 2015).

Although CB_1 and CB_2 are well stablished as endocannabionid receptors, there exist other receptors that could be mediating the effects of endocannabinoids

(Pertwee, 2015), such as the Transient Receptor Potential Vanilloid 1, also known as TRPV1, wich can be activated by anandamide (Maccarrone et al., 2008; De Petrocellis and Di Marzo, 2009b; Tóth et al., 2009; Alhouayek et al., 2014; Rossi et al., 2015), as well as for Transient Receptor Potential Ankyrin 1 (TRPA1) receptors (De Petrocellis et al., 2008), Peroxisome Proliferator-Activated Receptors, namely PPAR-α (Sun et al., 2006; Alhouayek et al., 2014) and non-CB_1/CB_2 GPCRs such as G protein-coupled receptor 55 (GPR55) (Ryberg et al., 2007).

2.1.4 PHYSIOLOGICAL ACTIONS OF ENDOCANNABINOIDS

Endocannabinoids are released from the postsynaptic neurons after its depolarization and/or receptor activation. Once released, endocannabinoids bind to the presynaptically located CB_1 (Robbe et al., 2002; Chevaleyre and Castillo, 2003; Kano, 2014). Thus, the binding of the endocannabinoid to its receptor, is able to suppress the elevation of the intracellular free Ca^{2+} concentration induced by the depolarization of the postsynaptic neuron (Sugiura et al., 1997) and consequently regulate the release of different neurotransmitters such as: glutamate (Shen et al., 1996), and gamma-Aminobutyric acid (GABA) (Katona et al., 1999), acetylcholine (Gifford et al., 1997a; b) or noradrenaline (Schlicker et al., 1997). The transient suppression of transmitter release on the presynaptic neuron following the release of endocannabinoid from postsynaptic neurons is known as endocannabinoid-mediated short-term depression or eCB-STD. The transient suppression has been consistently demonstrated to mediate both, depolarization-induced suppression of inhibition (DSI) (Ohno-Shosaku et al., 2001; Wilson and Nicoll, 2001) and of excitation (DSE) (Kreitzer and Regehr, 2001), mechanisms by

which short-term depression of GABA or glutamate release from axon terminals is induced by the depolarization of a postsynaptic neuron (Katona and Freund, 2012; Kano, 2014).

On the other hand, long-term depression (LTD) of GABA or glutamate release is mediated by CB_1 receptor in response to long-lasting synaptic activity, which triggers postsynaptic endocannabinoid releasement and retrograde signaling (endocannabinoid-mediated long-term depression or eCB-LTD) in different types of synapses throughout nervous system (Chevaleyre and Castillo, 2003; Chevaleyre et al., 2006; Castillo, 2012).

In the past years, endocannabinoid signaling have been demonstrated to play a key role in the potentiation of glutamatergic transmission through neuron-glia communication, also known as tripartite synapses, that includes the activation of astroglial CB_1 receptors (Navarrete and Araque, 2008, 2010; Navarrete et al., 2013; Metna-Laurent and Marsicano, 2015; Oliveira da Cruz et al., 2016).

In general, most of the actions of (endo)cannabinoids are mediated by CB_1 receptor ability to modulate synaptic transmission (Kano et al., 2009; Castillo, 2012; Katona and Freund, 2012; Kano, 2014). More specifically, the regulation of synaptic plasticity mediated by CB_1 receptor has been related to the memory-impairment effects of cannabinoids by means of the induction of LTD and the inhibition of LTP in the hippocampus (Stella et al., 1997; Han et al., 2012).

In addition, endocannabinoids have been described to also be involved in cell survival and differentiation processes (Galve-Roperh et al., 2013). In this sense, during embryonary development, the activation of CB_1 and CB_2 receptors participate in the regulation of neuronal progenitor-stem cells self-renewal, proliferation and differentiation. Particularly, the activation of these receptors have

been reported to trigger many different signaling pathways, such as mitogen-activated protein kinase signaling pathways, focal adhesion kinase cascade, phosphatidylinositol 3-kinase, extracellular-signaling regulated protein kinase, and ceramide signaling, among others (Bouaboula et al., 1995b; Derkinderen et al., 1996; Aguado et al., 2005; Ortega-Gutiérrez et al., 2005; Galve-Roperh et al., 2013).

Endocannabinoids are also able to develop neuroprotective roles acting through CB_1 cannabinoid receptors. In this sense, it has been shown that the role developed by the eCBs in retrograde signaling system in glutamatergic synapses (Ohno-Shosaku and Kano, 2014) in the brain could be the origin of its protective role (Wallace et al., 2003; Kano et al., 2009). Importantly, the eCB system would be a pharmacological target for the treatment of diseases characterized by abnormal glutamate homeostasis, such as neurodegenerative disorders (Fernández-Ruiz, 2010; Fernández-Ruiz et al., 2015).

2.1.5 EXPRESSION OF CB_1 RECEPTOR IN THE BRAIN

The CB_1 receptor is the main endocannabinoid signaling protein regarding the CNS (Pertwee, 2009), and, more specifically, the CB_1 receptors represent one of the most abundant GPCRs in the brain (Herkenham et al., 1991; Tsou et al., 1998; Moldrich and Wenger, 2000). Its expression is widespread and heterogeneous, developing crucial roles in brain function, dysfunction and cognition (Marsicano et al., 2002; Monory et al., 2006; Bellocchio et al., 2010; Puente et al., 2011; Castillo, 2012; Katona and Freund, 2012; Steindel et al., 2013; Ruehle et al., 2013; Soria-Gómez et al., 2014, 2015; Hu and Mackie, 2015; Katona, 2015; Martín-García et al., 2015), and it has been reported to palliate numerous pathologies, including

Alzheimer's disease, pain, obesity, and cancer, (Pertwee, 2009). More specifically, the highest levels of CB_1 receptors are present in the substantia nigra, globus pallidus, cerebellum, hippocampus and cortex (Howlett et al., 1990).

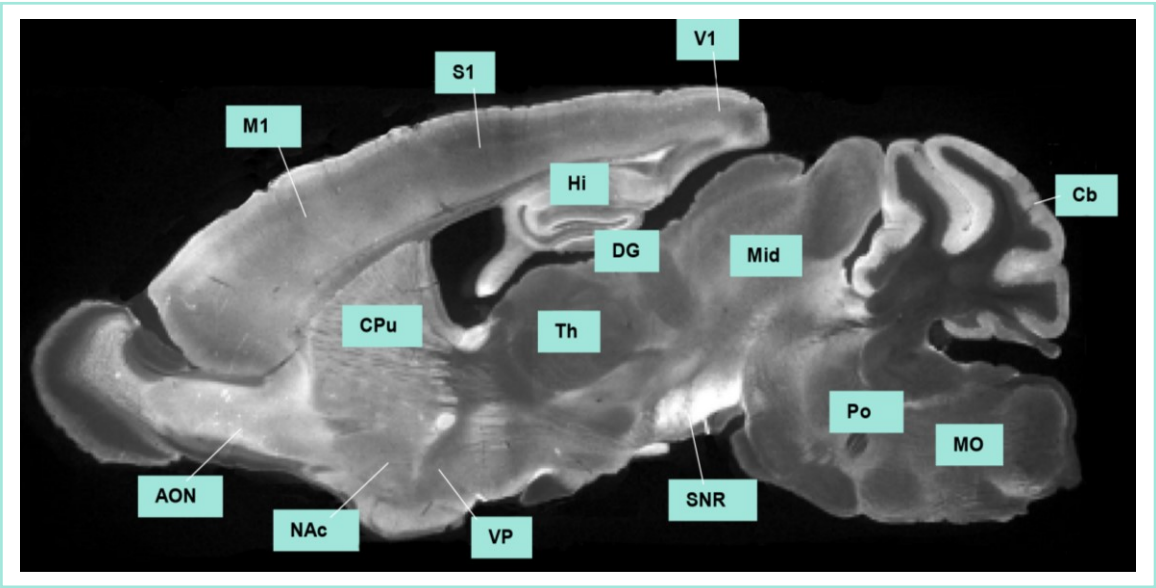

Figure 4. **Distribution of CB_1 receptors in the central nervous system of adult mice.** Primary somatosensory cortex (S1), primary motor cortex (M1), primary visual cortex (V1), hippocampus (Hi), dentate gyrus (DG), cerebellar cortex (Cb), midbrain (Mid), caudate putamen (CPu), thalamus (Th), anterior olfactory nucleus (AON), nucleus accumbens (NAc), ventral pallidum (VP), substantia nigra pars reticulata (SNR), pons (Po), medulla oblongata (MO). Modified from Kano et al., 2009.

At the ultrastructural level, CB_1 receptor expression is very high in inhibitory GABAergic synaptic terminals (Katona et al., 1999; Kawamura et al., 2006; Ludányi et al., 2008; Marsicano and Kuner, 2008; Katona and Freund, 2012; De-May and Ali, 2013; Steindel et al., 2013; Hu and Mackie, 2015) but, to a lower extent, CB_1 receptors are also present in glutamatergic neurons (Marsicano et al., 2003; Domenici et al., 2006; Takahashi and Castillo, 2006; Katona et al., 2006; Monory et al., 2006; Kamprath et al., 2009; Bellocchio et al., 2010; Puente et al., 2011; Reguero et al., 2011; Ruehle et al., 2013; Soria-Gómez et al., 2014) and in brain astrocytes (Navarrete and Araque, 2008, 2010; Stella, 2010; Han et al., 2012; Bosier et al., 2013; Metna-Laurent and Marsicano, 2015; Viader et al., 2015;

Oliveira da Cruz et al., 2016). CB_1 receptors are also constitutively expressed by oligodendrocytes (Molina-Holgado et al., 2002a; Benito et al., 2007; Garcia-Ovejero et al., 2009; Mato et al., 2009; Gomez et al., 2010). Inside the cells, CB_1 receptors, can be subcellularly localized at plasma membranes and intracellular organelles, such as brain mitochondria (Bénard et al., 2012; Hebert-Chatelain et al., 2014a; b; Koch et al., 2015).

Because of the hugely different levels of expression among different cell types (Marsicano and Lutz, 1999), it is extremely difficult to identify low CB_1 receptor expression in cell types and/or in subcellular compartments of wild-type brains (Busquets-Garcia et al., 2015). Actually, former anatomical studies often misinterpreted low CB_1 receptor expression as background staining (Freund et al., 2003).

Pharmacological blockade or genetic ablation of the receptor and its eventual behavioral and neuronal consequences are clear indications of the role of endocannabinoids in the brain. Hence, based on methodological “loss of function” approaches, the use of mutant mice lacking CB_1 receptors in specific cell populations helped to identify the necessary role of the receptor in different brain functions (Marsicano et al., 2003; Monory et al., 2006, 2015; Martín-García et al., 2015; Zimmer, 2015). Moreover, neuroanatomical analysis of these mutant animal models determined the presence of the CB_1 receptor at sites previously not known (e.g. cortical glutamatergic neurons or neuronal mitochondria).

However, these approaches do not provide definitive information concerning the possibly sufficient role of the cell-type expression of CB_1 receptors for a given function. Indeed, distinguishing between low levels (wild-type) and no-expression (mutant mice lacking CB_1 receptors in specific cell populations) is very difficult. To

establish precise causal relationships and to identify low levels of expression, “rescue” strategies utilizing the endogenous genetic locus are needed in order to analyze the function of endogenous CB_1 receptor expression exclusively in specific cell types. To reach this aim the Cre/LoxP system have been previously applied to restore CB_1 receptor expression in a CB_1 receptor-null mutant only in specific cell types (Ruehle et al., 2013; Soria-Gómez et al., 2014; de Salas-Quiroga et al., 2015). In this sense, the rescue approach was first applied to the hypothalamic expression of the melanocortin 4 receptor (Balthasar et al., 2005) using the Cre/loxP system, and was recently applied to the *CB1* gene (Ruehle et al., 2013; Soria-Gómez et al., 2014; de Salas-Quiroga et al., 2015). Briefly, a “stop cassette” flanked by LoxP sites was introduced immediately upstream of the coding sequence of the *CB1* gene by homologous recombination to generate a mutant mouse line. The mice obtained by this approach bore no expression of the CB_1 receptor protein (Ruehle et al., 2013; Soria-Gómez et al., 2014; de Salas-Quiroga et al., 2015), making these mice phenotypically very similar to conventional CB_1 knock-out mice (*CB1*-KO). However, the crossing of these mice with Cre-expressing transgenic mouse lines or the local injection of viruses expressing the Cre recombinase induces a Cre-mediated deletion of the “stop cassette”, causing a specific rescue of expression of the protein in specific cell populations and/or brain regions (Balthasar et al., 2005; Ruehle et al., 2013; Soria-Gómez et al., 2014; de Salas-Quiroga et al., 2015).

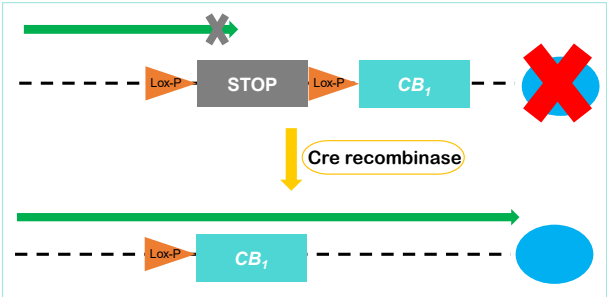

Figure 5. Schematic representation of rescued CB_1 receptor allele after excision of the stop cassette mediated by Cre recombinase.

Moreover, this re-expression is limited to the cell types where the regulatory sequences of the CB_1 receptor are normally activated and the expression levels are the same as in wild-type animals (Ruehle et al., 2013; Soria-Gómez et al., 2014; de Salas-Quiroga et al., 2015).

Furthermore, these rescue mice allowed determining the sufficient causal role of the CB_1 receptor in the anterior olfactory cortex area as well as in dorsal telencephalic glutamatergic neurons (Ruehle et al., 2013; Soria-Gómez et al., 2014; de Salas-Quiroga et al., 2015). However, no studies have addressed so far the subcellular localization of CB_1 receptor in these mutant brains at the electron microscopic level. This is particularly interesting due to the huge expression of CB_1 receptors in specific cell types (e.g. hippocampal GABAergic interneurons) which hinder to appreciate the detailed pattern of expression of the CB_1 receptor in other cell types (e.g. hippocampal glutamatergic pyramidal neurons) in wild-type mouse samples (Freund et al., 2003). Therefore, the conditional rescue mutants emerge as key tools for the detailed anatomical characterization of the subcellular distribution of the receptor in specific cell types, independently of its level of expression.

2.1.6 ASTROCYTES AND THE CB_1 RECEPTOR

Presence of CB_1 receptors in astrocytes has been long debated. Its presence in astrocytes was firstly reported in human and rodent cell cultures (Bouaboula et al., 1995a; Sánchez et al., 1998; Molina-Holgado et al., 2002b; Sheng et al., 2005). However, incongruous results were obtained in mice (Sagan et al., 1999; Walter and Stella, 2003) suggesting that CB_1 receptor expression in astrocytes could vary among different animal species, strains or different cell culture conditions. In addition, low levels of expression of astrocytic CB_1 receptor made it remarkably arduous to detect astroglial *CB_1* mRNA or protein expression by means of in situ hybridization or immunohistochemistry. Fortunately, electron microscopy immunodetection allowed to reveal the presence of astrocytic CB_1 receptor (Rodriguez et al., 2001; Han et al., 2012; Bosier et al., 2013). Moreover, the enzymes for synthesis and degradation of the main endocannabinoids co-localize with Glial Fibrillary Acidic Protein (GFAP) (Suárez et al., 2010). Finally, in light of many different works published during the last years (Navarrete and Araque, 2008, 2010; Stella, 2010; Han et al., 2012; Bosier et al., 2013; Gómez-Gonzalo et al., 2014; Navarrete et al., 2014; Metna-Laurent and Marsicano, 2015; Viader et al., 2015; Oliveira da Cruz et al., 2016) the presence of the CB_1 receptor in astrocytes and its functional importance have been demonstrated.

In this sense, different authors have proposed various signaling pathways in astrocytes after the CB_1 receptor activation. Thus, some authors have proposed the coupling of astrocytic CB_1 to $G\alpha_{i/o}$-protein (Guzmán et al., 2001) whereas other authors suggest that astrocytic CB_1 receptor is able to modulate Ca^{2+} levels in astrocytes and associated signaling by means of $G\alpha_q$ proteins activation (Navarrete and Araque, 2008; Navarrete et al., 2014). In this sense, the

development of different intracellular astrocytic signaling pathways in response to endocannabinoids provides to endocannabinoid-mediated responses with a particular important flexibility in astrocytes (Metna-Laurent and Marsicano, 2015).

Otherwise, astrocytes have long been known for their role as protective elements against injury in the central nervous system and as energetics providers for neurons (Magistretti and Pellerin, 1999; Bélanger and Magistretti, 2009; Yi et al., 2011), not taking a relevant part in the transmission of information for being non-electrically excitable cells. However, this last consideration has already changed, owing to the fact that many signaling systems that are capable to modulate neuronal activity have been described to also regulate astrocytic-neuronal communication (Araque et al., 1999; Haydon and Carmignoto, 2006; Perea et al., 2009; Gómez-Gonzalo et al., 2014). Moreover, these findings lead to the establishment of a new concept: the “tripartite synapse”, which is formed by a presynaptic and a postsynaptic neuronal elements and by the surrounding astroglial processes (Araque et al., 1999) (Fig. 6). In this context, astrocytic CB_1 receptors have been demonstrated to play a key role in the communication between neurons and astrocytes (Navarrete and Araque, 2008, 2010; Navarrete et al., 2013, 2014; Gómez-Gonzalo et al., 2014).

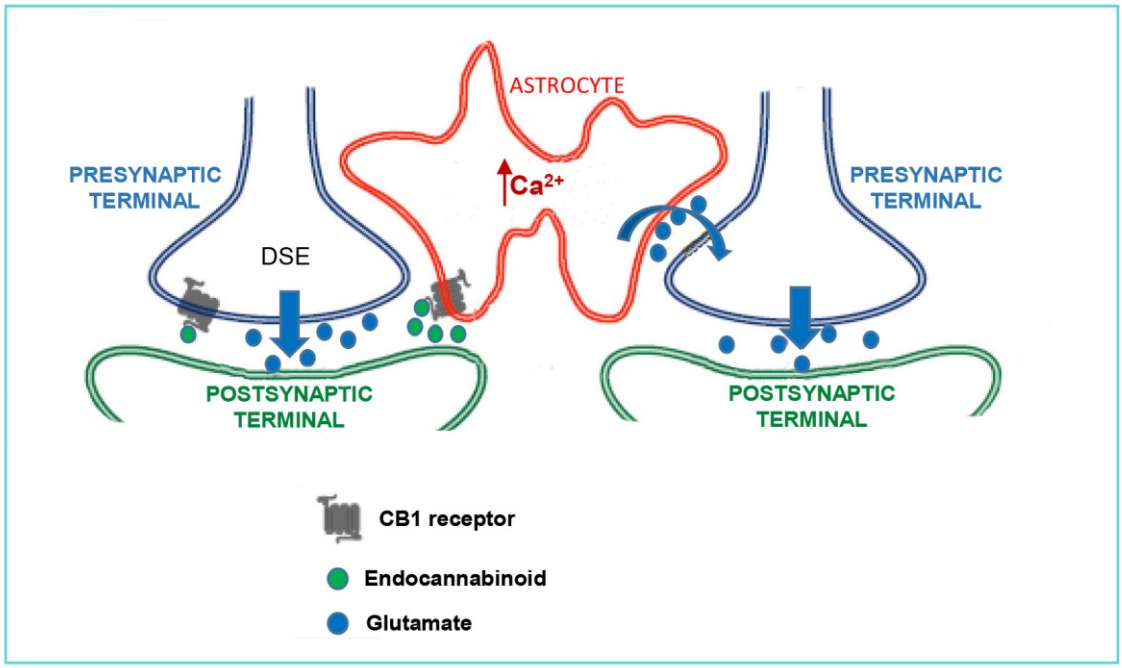

Figure 6. **Signaling mechanisms underlying synaptic regulation by endocannabinoids through stimulation of astrocytes.** Endocannabinoids are released by a postsynaptic neuron acting on presynaptic CB_1 receptors. As a response, a DSE is triggered in homoneuronal synapses. In addition, the released endocannabinoids also are able to activate astrocytic CB_1 receptors. The activation of astrocytic CB_1 receptors increases the intracellular calcium and triggers the release of glutamate by the astrocyte, which stimulates the release of neurotransmitter in hetero-neuronal synapses. Modified from Navarrete et al., 2014.

Moreover, glutamate release is promoted in neurons by the activation of CB_1 receptors in astrocytes (Navarrete and Araque, 2008), and therefore this activation could be improving synaptic transmission (Navarrete and Araque, 2010). Thus, in this context, it has been suggested that the CB_1 receptor would mediate in the development of epileptic seizures (Coiret et al., 2012). In this sense, it has been recently demonstrated that the CB_1 receptor expression in astrocytes is increased in sclerotic hippocampus, which is characterized by refractory temporal lobe epilepsy and both neuronal loss and astrocyte proliferation (Meng et al., 2014).

In astrocytes, GFAP is the principal intermediate filament protein (Eng, 1985; Eng et al., 2000; Hol and Pekny, 2015). However, due to its filament nature the

immunolabeling of GFAP may not show the complete surface of the astrocyte in traditional microscopic preparations. Thus, other methodological approaches have been developed for staining astrocytes in microscopic preparations. In this sense, Green Fluorescence Protein, also known as GFP (Shimomura et al., 1962; Chalfie, 1995), is a cytoplasmically expressed diffusible protein. When inserted in astrocytes, this protein appears distributed throughout the whole cytoplasm, allowing its immunolabeling to be used for a better detection of the whole astrocytic surface (Nolte et al., 2001). More particularly, GFP protein from the sea pansy *Renilla reniformis* (Ward et al., 1978; Ward and Cormier, 1979) and its humanized isoform, known as hrGFP, has been used as a marker in a wide variety of studies (Navarro-Galve et al., 2005; De Francesco et al., 2015; Kerr et al., 2015). More specifically, it has been used as an astroglial marker (Hadaczek et al., 2009).

2.2 HIPPOCAMPUS

2.2.1 DEFINITION OF THE HIPPOCAMPUS

The hippocampus is a structure that includes distinct brain regions differentiated by its cytoarchitecture. The main reason to include these areas under the same anatomical structure is that they are largely connected via unidirectional projections (the perforant path, mossy fibers and Schaffer collaterals). However, as I will describe later, two-way connections may also exist in this region.

The hippocampus can be divided in two cortical structures i.e. the hippocampal formation and the parahippocampal region (Fig. 7). On the one hand, the hippocampal formation is a C-shaped structure localized in the caudal part of the brain. It is comprised by three areas cytoarchitectonically differentiated: the dentate gyrus, the hippocampus properly speaking which is subdivided into three fields (CA1, CA2 and CA3), and the subiculum. On the other hand, the parahippocampal region lies adjacent to the hippocampal formation and comprises five subregions; the perirhinal cortex, the entorhinal cortex, the postrhinal cortex, the presubiculum and the parasubiculum.

The three-dimensional location of the hippocampus in the mouse brain is complex. It appears as an elongated structure, with its septo-temporal C-shaped axis extending towards the temporal lobe in its caudo-ventral end running above and behind the diencephalon. It is delimited by the septal nuclei rostrally and by the lateral ventricles laterally. The longitudinal axis of the hippocampal formation is located in septum-temporal direction, while the transverse or orthogonal axis is extending between temporal lobes. The regions of the hippocampal formation are distributed along the septum-temporal axis so that the dentate gyrus and CA1 and

CA3 regions of the hippocampus appear at more septal levels. The subiculum begins to appear in the first third of septotemporal axis, while the presubiculum and parasubiculum are appearing progressively towards the temporal region. Finally, ventrally in the caudal portion of the hippocampus the entorhinal cortex is confined.

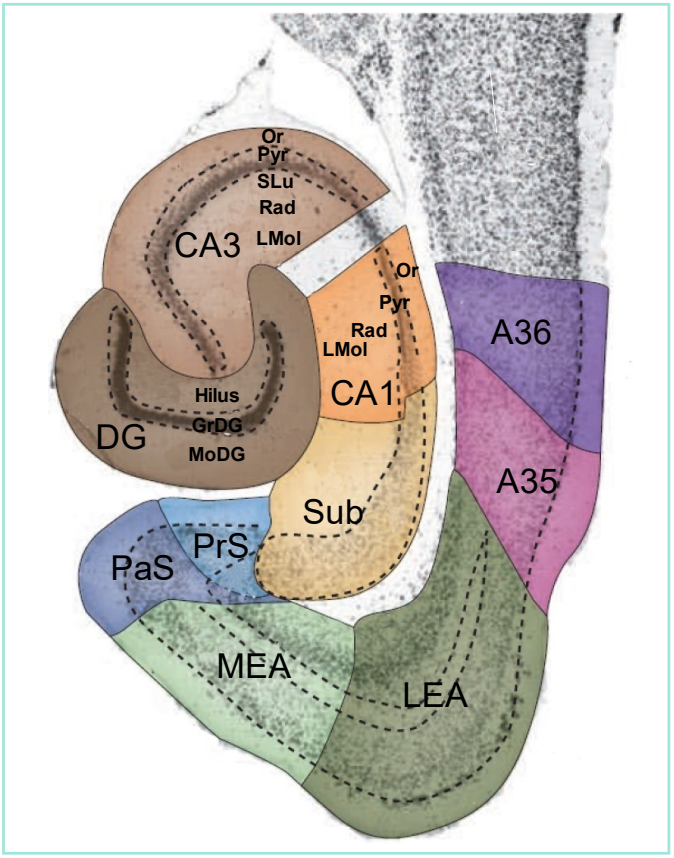

Figure 7. Representation of the hippocampal formation and the parahippocampal region in the rat brain. Dentate gyrus, DG (dark brown); Region 3 of Cornu Ammonis, CA3 (medium brown); Region 2 of Cornu Ammonis CA2 (not indicated); Region 1 of Cornu Ammonis, CA1 (orange). The subiculum, Sub (yellow); presubiculum, PrS (medium blue) and parasubiculum (PaS; dark blue). The entorhinal cortex, which has a lateral, LEA (dark green) and a medial, MEA (light green) areas. The perirhinal cortex (consisting of Brodmann areas: A35 (pink) and A36 (purple). Stratum oriens, Or; Pyramidal cell hippocampus, Py; Stratum radiatum, Rad; stratum lucidum, SLu; Lacunosum moleculare, LMol; Molecular dentate gyrus, MoDG and Granular dentate gyrus, GrDG. Modified from van Strien et al., 2009.

2.2.2 DENTATE GYRUS

The dentate gyrus comprises three layers, the molecular layer, the granular cell layer and the hilus.

2.2.2.1 Molecular layer.

The molecular layer is located edging the hippocampal fissure and contains the perforant path fibers connecting the entorhinal cortex with the dentate gyrus. This layer is mainly occupied by the dendrites of the granule, basket and various polymorphic cells, as well as axon terminals from several sources. Remarkably, synaptic terminals of the commissural/associational system are found in the inner third of the dentate molecular layer, containing a substantial input from the CA3 in addition to the excitatory terminals of the hilar mossy cells (Ribak et al., 1985; Li et al., 1994; Blasco-Ibáñez and Freund, 1997; Scharfman, 2007).

Furthermore, a few neuronal cell types are also present in the molecular layer. The first type of neurons is located in the innermost area, shows a triangular or multipolar soma and present axons projecting to the granular layer basket plexus cells. They are considered as a type of basket cells (Hazlett and Farkas, 1978; Ribak and Seress, 1983; Witter and Amaral, 2004; Jinno and Kosaka, 2006; Witter, 2012).

The other kind of neurons that are localized in the molecular layer are immunoreactive for the neurotransmitter GABA (Celio, 1990), which indicates that they are modulating the activity of granule cells. They are similar to chandelier cells (Kosaka, 1983; Somogyi et al., 1985; Soriano and Frotscher, 1989; Halasy and Somogyi, 1993; Witter and Amaral, 2004; Witter, 2012). Their dendrites remain primarily in the molecular layer, while their axons project from the molecular layer into the granular cell layer and contact with initial axonal segments of granule cells.

2.2.2.2 Granular cell layer

The granule cell layer is situated deeply into the molecular layer. It is constituted mainly of densely packed excitatory glutamatergic neurons known as granule cells. Their dendritic extensions give the cell a characteristic conical appearance and are oriented towards the molecular layer. Furthermore, they have numerous dendritic spines which are able to contact with many axon terminals (Desmond and Levy, 1982, 1985) and increase in length at more distal positions along the dendrite (Stanfield and Cowan, 1979; Vuksic et al., 2008). On the other hand, their glutamatergic axons known as mossy fibers invade the hilar region where they contact with the mossy cells, CA3 pyramidal neurons and GABAergic interneurons (Frotscher et al., 1994). No remarkable morphological differences appeared between granule cells taken from the dorsal or ventral portions, except for the more extensive degree of arborisation found in ventral cells (Vuksic et al., 2008).

Another type of cells in this layer are the GABAergic basket cells (Aika et al., 1994) whose somata are located in the innermost side of the granular cell layer. They owe their name to their axons which form a pericellular plexus surrounding the granule cells bodies (Ribak and Seress, 1983; Ribak et al., 1985) modulating granule cells activity (Meyer et al., 2002; Jinno and Kosaka, 2006).

2.2.2.3 Hilus

Also known as the polymorphic layer, the hilus contains a wide variety of cell types. The most common are the glutamatergic mossy cells (Frotscher et al., 1994; Blasco-Ibáñez and Freund, 1997). Their large cell bodies are oval and their dendrites extend for long distances within the hilus, sometimes being able to reach out the granule cell layer and the molecular layer (Blasco-Ibáñez and Freund,

1997; Fujise and Kosaka, 1999). Remarkably, dendrites of the mossy cells do not leave the confines of the hilus to enter the adjacent CA3 field. The most proximal dendrites are covered by the very large and complex spines called “thorny excrescences”, which establish synaptic contacts with the granule mossy fibers (Ribak et al., 1985; Frotscher et al., 1991; Blasco-Ibáñez and Freund, 1997; Fujise and Kosaka, 1999). Importantly, the axon terminals of the hilar mossy cells contain abundant tightly packed synaptic vesicles and end into the inner third of dentate molecular layer forming asymmetric synapses with granule cell dendrites and dendritic spines (Ribak et al., 1985; Blasco-Ibáñez and Freund, 1997).

Other cell types located in the hilus are the fusiform cells whose dendrites run parallel to the granular cell layer (Bakst et al., 1986; Halasy and Somogyi, 1993), and the multipolar neurons whose axons and dendrites remain within the hilus (Amaral, 1978).

2.2.3 HIPPOCAMPUS

As Llorente de Nó proposed (1934) the hippocampus can be divided into three regions, CA1, CA2 and CA3. The mossy fibers inputs that arrive to CA3 from the dentate gyrus not reaching CA1 and CA2 represent the main anatomical difference among these three regions. In addition to the structural characteristics, different patterns of gene expression also exist among the different regions (Dong et al., 2009; Fanselow and Dong, 2010) that make a real physiological separation between the three different fields.

The hippocampus shows a trilaminar structure, folded on itself. Each of these layers can be defined depending on the cell types that host and their spatial distribution and density. Remarkably, the cellular distribution is correlated with the

performance of specific functions in the hippocampal network (Klausberger and Somogyi, 2008). The ventricular surface of the hippocampus is covered by the alveus, which is a thin layer of myelinated fibers.

2.2.3.1 Stratum oriens

The basal dendritic tree of pyramidal neurons will be part of the stratum oriens, which is a relatively free layer of cells situated in the outer side of the pyramidal layer (Lorente De Nó, 1934).

2.2.3.2 Pyramidal cell layer

The pyramidal cell layer (Lorente De Nó, 1934), consists of glutamatergic cells (Liu et al., 1989) whose somata have a pyramidal look due to the presence of a prominent apical dendrite. Their basal dendritic trees distribute in the stratum oriens while the apical dendritic tree is oriented in ventromedial direction.

There is also an assorted population of basket cells with their cell bodies confined within the pyramidal cell layer (Frotscher et al., 1991; Jinno and Kosaka, 2006). Their axons expand transversely from the cell body forming a basket plexus that innervates the pyramidal cell bodies.

2.2.3.3 Stratum lucidum

This is an acellular CA3 layer just above the pyramidal cell layer that contains the dentate granule mossy fibers axons.

2.2.3.4 Stratum radiatum

The stratum radiatum is located superficial to stratum lucidum in CA3 and above the pyramidal cell layer in CA2.The majority of the CA3 to CA3 associational fibers and the ipsilateral CA3 to CA1 Schaffer collaterals are found in this layer.

2.2.3.5 Stratum lacunosum-moleculare

Finally, the stratum lacunosum-moleculare is located in the vicinity of the hippocampal fissure and the dentate gyrus. About 20% of the dendritic tree of the pyramidal cells reaches the stratum lacunoso-moleculare (Amaral et al., 1990). This layer receives synapses from the entorhinal cortex.

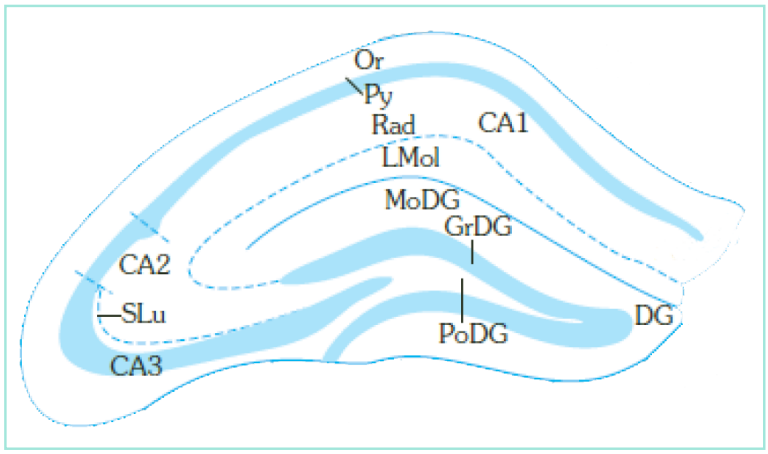

Figure 8. **Representation of a sagittal section of the mouse hippocampal formation.** Laminar structure of the hippocampus. DG, Dentate gyrus; CA1, Region 1 of Cornu Ammonis; CA2, Region 2 of Cornu Ammonis; CA3, Region 3 of Cornu Ammonis; Or, Stratum oriens; Py, Stratum pyramidale; Rad, Stratum radiatum; SLu, stratum lucidum; LMol, Stratum lacunosum moleculare; MoDG, Molecular dentate gyrus; GrDG, Granular dentate gyrus; PoDG, Polymorph dentate gyrus. Modified from Franklin and Paxinos, 2008.

2.2.3.6 GABAergic cells of the hippocampus

Although there are a wide variety of cells in the stratum oriens, stratum radiatum, and stratum lacunosum-moleculare of the hippocampus, most of them are GABAergic neurons (Ribak et al., 1978; Aika et al., 1994). Moreover, there are eight well defined GABAergic subclasses in the hippocampus based on their colocalization with parvalbumin, calretinin, calbindin, neuropeptide-Y, somatostatin, cholecystokinin, vasoactive intestinal polypeptide (VIP), or nitric oxide synthase (NOS) (Morrison et al., 1983; Somogyi et al., 1984; Sloviter and Nilaver, 1987; Sloviter, 1989; Gulyás et al., 1991, 1992, 1999; Miettinen et al., 1992; Tóth and Freund, 1992; Jinno and Kosaka, 2000). Some studies have shown

the relation between chemical phenotypes and electrophysiological properties of the interneurons (Jinno and Kosaka, 2006; Klausberger and Somogyi, 2008) but a clear correlation between them have not been fully established yet and their function in the hippocampal network is still poorly understood (Witter and Amaral, 2004; Witter, 2012)

2.2.4 CONNECTIONS OF THE HIPPOCAMPUS

The hippocampal formation is one of the most important functional structures of the mammalian brain. There exists high connectivity with other brain regions to perform its functions properly. These connections allow playing a key role in memory formation, learning, neurogenesis and cognitive function. Also, they keep informed the hippocampal formation of the brain activity. The connections of the hippocampal formation can be divided into two groups: afferent (connections from other regions) and efferent (connections to other regions) projections.

2.2.4.1 Afferent connections

The hippocampal formation receives main connections from: the neocortex, the septal area, the contralateral hippocampus (commissural fibers), several nuclei of the diencephalon and the reticular formation of the brain stem. The neocortex of the temporal lobe which receives association fibers of different sensory association areas, sends information to the entorhinal cortex of the hippocampal formation. The entorhinal cortex is a transition structure between the neocortex and hippocampal cortex. Then, the entorhinal cortex sends fibers through the subiculum and intersects the hippocampal sulcus to end in the dentate gyrus forming the so-called perforant pathway. Fewer fibers from the entorhinal cortex

form the alveolar via crossing the subcortical white matter as well as the alveus and ending in the hippocampus.

In addition, fibers from the septal nuclei reach the hippocampus through the fornix. Moreover, other afferent fibers also included in the fornix come from the thalami nuclei, hypothalamus, diencephalon and brainstem regions such as the ventral tegmental area (dopaminergic), the locus coeruleus (noradrenergic) and nuclei raphe (serotonergic).

2.2.4.2 Efferent connections

The main efferent pathway from the hippocampal formation is the fornix, which is composed by the axons of the CA1 pyramidal neurons and of the subicular cells. The axons enter the alveus and together constitute the hippocampal fimbria followed by the fornix after leaving the fibers the hippocampus and going into the forebrain.

These glutamatergic fibers travel along the entire fornix which branches near the anterior commissure into two components: precommissural and postcommissural fibers. The precommissural fibers (formed by fibers originating mainly in the hippocampus) extend rostrally, innervating the septal nuclei, the nucleus accumbens and the substantia innominata. Meanwhile, the postcommissural fibers (composed mainly of fibers originating in the subiculum) extend caudally to the diencephalon to finally reach the hypothalamus, where they divide into the medial cortico-hypothalamic tract (that innervates the mammillary bodies, the posterior hypothalamus and other ventromedial hypothalamic nuclei) and the subiculum-thalamic tract (reaching the thalamic nuclei) (Swanson et al., 1987).

A lot of the fimbria fibers are crossed, before being included into the fornix, in the caudal region of the septal nuclei. Most of these fibers are directed to the contralateral hippocampal formation. However, a few of them are integrated into the fornix to innervate the same structures that receive precommissural and postcommissural projections from the ipsilateral fornix.

The fornix is not the only efferent pathway from the hippocampal formation, since there are significant projections from the subicular complex and entorhinal cortex to cortical areas, such as the perirhinal cortex and the parahippocampal gyrus.

2.2.4.3 Hippocampal synaptic circuit

It is well characterized that the hippocampus has a unidirectional pathway that connects all its regions sequentially. The start of the hippocampal circuit is the dentate gyrus which receives the perforant pathway from the entorhinal cortex. Then, the mossy axon fibers of the dentate granule cells project unidirectionally to the proximal dendrites of the CA3 pyramidal cells. In turn, the CA3 pyramidal cell Schaffer collaterals reach the CA1 stratum radiatum. The CA1 hippocampal region projects intensely into the subicular complex which, sends axons back to the entorhinal cortex. Although the circuit forms a loop, each of the hippocampal fields also sends axons out.

However, even though the classical view proposes that the connectivity is unidirectional, several types of retrograde connections also exist in the hippocampal formation (van Strien et al., 2009). For instance, CA3 pyramidal cells are connected with the hilus and the dentate molecular layer (Laurberg, 1979; Buckmaster et al., 1993; Witter, 2007). Furthermore, retrograde connections from CA1 to CA3 through interneurons (Laurberg, 1979; Amaral et al., 1991; Cenquizca

and Swanson, 2007) and from the subiculum to CA1 (Finch et al., 1983) have been identified. Also, recurrent collaterals in CA3 (Laurberg, 1979; Amaral et al., 1990; Buckmaster et al., 1993; Sik et al., 1993; Siddiqui and Joseph, 2005; Wittner et al., 2007) and bidirectional connections between the entorhinal cortex and subiculum have been described.

2.3 WORKING HYPOTHESIS

As I have already described, the CB_1 receptor expression is very high in inhibitory GABAergic synaptic terminals and low in glutamatergic neurons as well as in brain astrocytes. Subcellularly, CB_1 receptors are localized in the plasma membranes and in intracellular organelles, such as brain mitochondria. Due to the hugely different levels of expression among different cell types, it is extremely difficult to identify low CB_1 receptor expression in cell types and/or in subcellular compartments of wild-type brains. This led in the past to consider low CB_1 receptor levels as background staining (see below).

Based on methodological “loss of function” approaches, the use of mutant mice lacking CB_1 receptors in specific cell populations helped identifying the necessary role of the CB_1 receptor for some brain functions. Moreover, neuroanatomical analyses of these mutants determined the presence of the CB_1 receptor at sites previously not known (e.g. cortical glutamatergic neurons or neuronal mitochondria). However, these approaches do not provide definitive information concerning the possibly sufficient role of the cell-type expression of CB_1 receptors for a given function. Indeed, distinguishing between low levels (wild-type) and no expression (conditional mutant) is very difficult.

Therefore, to establish precise causal relationships and to identify low levels of expression, “rescue” strategies are needed to analyze the function of endogenous CB_1 receptor expression exclusively in specific cell types. Indeed, these rescue mice have allowed already determining the sufficient causal role of the CB_1 receptor in the anterior olfactory cortex area as well as in dorsal telencephalic glutamatergic neurons. However, so far no studies have addressed the subcellular

localization of the CB_1 receptor in these mutant brains in the electron microscope. This is particularly important because the huge expression of the CB_1 receptor in specific cell types (e.g. hippocampal GABAergic interneurons) does not appreciate the detailed pattern of expression of the receptor in other cell types (e.g. hippocampal glutamatergic pyramidal neurons) in wild-type mouse samples. Hence, the conditional rescue mutants emerge as key tools for the detailed anatomical characterization of the subcellular distribution of the receptor in specific cell types, independently of its level of expression.

In this study, we have examined the CB_1 receptor expression in the hippocampus of rescue mice modified to express the gene exclusively in specific brain cell types, such as dorsal telencephalic glutamatergic neurons (Glu-*CB1*-RS), GABAergic neurons (GABA-*CB1*-RS) and brain astrocytes (GFAP-*CB1*-RS), for three reasons. First, to elucidate the real levels of CB_1 receptors in specific cell types expressing very little CB_1 protein eliminating the interference of other cells highly expressing CB_1 receptors. Second, to verify that the re-expression is limited to the specific cell types and maintains endogenous levels of CB_1 receptors where the regulatory sequences of the receptor are normally activated. And third, to know whether the rescue mutant mice are good and reliable tools for functional studies of the endocannabinoid system in the brain. Finally, we have also analyzed the CB_1 receptor expression in the hippocampus of transgenic mice expressing the hrGFP protein in astrocytes (GFAPhrGFP-*CB1*-WT and GFAPhrGFP-*CB1*-KO mice) in order to investigate the CB_1 receptor distribution in astrocytes relative to the tripartite synapses.

3 OBJECTIVES

The general goal of this Thesis was the anatomical characterization of new different mutant mice expressing CB_1 receptors in specific brain cells. In particular, the study was focused on the hippocampus processed for a preembedding immunogold method for electron microscopy.

The proposed objectives of the present Thesis work are:

- To study the CB_1 receptor expression in the hippocampus of mice with the CB_1 receptor rescued in dorsal glutamatergic neurons (Glu-*CB*$_1$-RS).
- To investigate the CB_1 receptor expression in the hippocampus of mice with the CB_1 receptor rescued in GABAergic neurons (GABA-*CB*$_1$-RS).
- To determine the CB_1 receptor expression in the hippocampus of mice with the CB_1 receptor rescued in astrocytes (GFAP-*CB*$_1$-RS).
- To compare the CB_1 receptor expression in hippocampal astrocytes of transgenic mice with GFAP or with hrGFP as the astrocytic marker.
- To establish the anatomical distribution of the astrocytic CB_1 receptors relative to the surrounding excitatory and inhibitory synapse forming the tripartite synapse.

4 MATERIAL AND METHODS

I have used specific antibodies in combination with an immunocytochemical technique (immunoperoxidase) for light microscopy; a preembedding silver intensified immunogold method and a double preembedding immunogold and immunoperoxidase method for electron microscopy. In addition, I have done the corresponding quantification and statistical analysis of the data obtained in the electron microscopic experiments.

4.1 ANTIBODIES

Polyclonal Anti-Cannabinoid Receptor Type-1 (anti-CB1 receptor), monoclonal Anti-Glial Fibrillary Acidic Protein (anti-GFAP) and polyclonal humanized *Renilla reniformis* Green Fluorescence Protein (anti-hrGFP) antibodies were used (Table 1).

Table 1. Details of the antibodies used in this Thesis.

ANTIBODY	MANUFACTURER	HOST	CONCENTRATION
Polyclonal Anti-Cannabinoid Receptor Type-1 (CB_1)	Frontier Institute	Goat	1:100
Monoclonal Anti-Glial Fibrillary Acidic Protein (GFAP)	Sigma-Aldrich	Mouse	1:1000
Polyclonal humanized *Renilla reniformis* Green Fluorescence Protein (hrGFP)	Stratagene	Rabbit	1:500

The experiments were done under the same conditions. Moreover, a negative control by omitting the primary antibody was performed. Importantly, the CB_1 receptor antibodies used were tested in *CB_1*-KO brain tissue. Finally, the specificity of the other antibodies has been thoroughly confirmed in previous studies.

CB_1: The sequence of the immunizing peptide used to generate the antibody corresponds with the last 31 amino acids of the C-terminus of the mouse CB_1 receptor (NM007726), as provided by the manufacturer (NCBI Reference Sequence: NP_031752.1; 443-473 amino acid residues: MHRAAESCIKSTVKIAKVTMSVSTDTSAEAL). The specificity of the CB_1 receptor antibody (Frontier Institute; Goat polyclonal; #CB1-Go-Af450) was assessed in previous publications (Bellocchio et al., 2010; Reguero et al., 2011; Bénard et al., 2012; Hebert-Chatelain et al., 2014b; Soria-Gómez et al., 2014; Martín-García et al., 2015). Furthermore, the specificity was tested in this study by applying the antibody to *CB_1*-KO hippocampus. No immunostaining was observed in this tissue in the light microscope. Also, the specificity of the CB_1 receptor pattern was analyzed in hippocampi of *CB_1*-WT and *CB_1*-KO processed together for immunoelectron microscopy. Thus, CB_1 receptor immunoparticles were localized in the inhibitory and excitatory synaptic terminals of *CB_1*-WT mouse while the CB_1 receptor pattern disappeared in *CB_1*-KO tissue, indicating the high specificity of the antibody used. Moreover, the antibody detects a single protein band of 52 kDa on immunoblots (Manufacturer´s provided information, Frontier Science).

- **GFAP:** The specificity of the GFAP antibody (Sigma-Aldrich; mouse monoclonal; #G3893) was established in previous publications (Han et al., 2012; Bosier et al., 2013). This antibody has been tested for the GFAP immunolocalization in human, pig and rat tissues, and specifically detects GFAP on immunoblots. In addition, it does not cross react with vimentin,

which is frequently co-expressed in glioma cells and some astrocytes (Manufacturer´s provided information Sigma-Aldrich).

- **hr-GFP:** The humanized *Renilla reniformis* green fluorescence protein (hr-GFP) antibody (Stratagene; rabbit polyclonal; #240142) has been tested in brain and spinal cord and other tissues previously (Sakata et al., 2009; Zhang et al., 2013; Kerr et al., 2015). Moreover, anti-hrGFP antibody was not observed to bind to any cell in wild type mice.

4.2 RESEARCH ANIMALS

4.2.1 CB_1 RECEPTOR MUTANT LINES

4.2.1.1 Generation of the *CB_1*-KO mice

CB_1-KO mice were generated and genotyped as described (Marsicano et al., 2002). Conditional CB_1 receptor mutant mice were obtained by crossing the respective Cre expressing mouse line with $CB_1^{f/f}$ mice (Marsicano et al., 2003), using a three-step breeding protocol (Monory et al., 2006). All mice were in a predominant C57BL/6N background.

4.2.1.2 Generation of conditional mutant mice bearing a selective deletion of the CB_1 receptor in cortical glutamatergic neurons (hereafter Glu-*CB_1*-KO)

The helix-loop-helix transcription factor NEX is a marker of embryonic neuronal progenitors, which will develop into mature cortical glutamatergic neurons (Wu et al., 2005). In the adult brain, NEX is expressed in mature glutamatergic cortical neurons, but not in cortical GABAergic interneurons and to a much lesser extent in subcortical regions (Bartholomä and Nave, 1994). Cre expression under the control of the regulatory sequences of NEX in mutant mice as generated by knock-in into

the NEX locus (NEX-Cre mice), leads to the specific deletion of ‘‘floxed’’ alleles in forebrain neurons (Kleppisch et al., 2003). Thereby, $CB_1^{f/f;\ NEX\text{-}Cre}$ mice Glu-*CB*$_1$-KO, (Monory et al., 2006) were obtained by crossing $CB_1^{f/f;}$ with NEX-Cre mice (Schwab et al., 2000; Kleppisch et al., 2003). Mutants were obtained by crossing $CB_1^{f/f}$ females with $CB_1^{f/f;\ NEX\text{-}Cre}$ males.

4.2.1.3 Generation of conditional mutant mice bearing a selective deletion of the CB_1 receptor in GABAergic neurons (hereafter GABA-*CB*$_1$-KO)

The *Dlx5/Dlx6* genes are homeobox genes that are expressed in differentiating and migrating forebrain GABAergic neurons during embryonic development (Stuhmer, 2002). Dlx5/6-Cre (Zerucha et al., 2000) were crossed with $CB_1^{f/f}$ to obtain $CB_1^{f/f;\ Dlx5/6\text{-}Cre}$ mice. Thus, the expression of Cre recombinase under the control of the regulatory sequences of *Dlx5/Dlx6* genes drives to a recombination of loxP sites in GABAergic neurons (GABA-*CB*$_1$-KO mice, (Monory et al., 2006). Mutants were obtained by crossing $CB_1^{f/f}$ females with $CB_1^{f/f;\ DLX5/6\text{-}Cre}$ males.

4.2.1.4 Generation of conditional mutant mice bearing a selective deletion of the CB_1 receptor in astrocytes (hereafter GFAP-*CB*$_1$-KO)

Transgenic mice $CB_1^{f/f;\ GFAP\text{-}CreERT2}$ were obtained from crossing mice carrying CB_1 receptor “floxed” sequence (Marsicano et al., 2003) with transgenic mice expressing the inducible version of the Cre recombinase CreERT2 under the control of the human glial fibrillary acid protein promoter, i.e. GFAP-CreERT2 mice (Hirrlinger et al., 2006). This animal model allows the on-demand control of astroglial CB_1 receptor recombination in adult mice (Han et al., 2012).

4.2.1.5 Generation of Glu-*CB$_1$*-RS and GABA-*CB$_1$*-RS

Rescue mice were produced as previously described (Ruehle et al., 2013). Briefly, Stop-CB$_1$ mice were generated by inserting a loxP-flanked stop cassette into the 5'UTR of the coding exon of the *CB$_1$* gene, 32 nucleotides upstream of the translational start codon to obtain *CB$_1$*$^{stop/stop}$ mice, lacking expression of the CB$_1$ protein (Ruehle et al., 2013). Conditional rescue mice were obtained by crossing Stop-CB$_1$ with NEX-Cre or Dlx5/6-Cre mice to generate Glu-*CB$_1$*-RS (rescue) and GABA-*CB$_1$*-RS, respectively. Genotyping was performed as previously described (Ruehle et al., 2013), and rescue mutants were obtained by crossing *CB$_1$*$^{stop/stop}$ females with *CB$_1$*$^{stop/stop;\ Nex\text{-}Cre}$ or *CB$_1$*$^{stop/stop;\ DLX5/6\text{-}Cre}$ males, respectively.

4.2.1.6 Generation of GFAP-*CB$_1$*-RS

To obtain specific CB$_1$ rescue in astrocytes STOP-*CB$_1$* mice (Ruehle et al., 2013) were crossed with GFAP-CreERT2 mice (Han et al., 2012) as previously described (Ruehle et al., 2013). Three weeks before neuroanatomical characterization, deletion of stop cassette for CB$_1$ rescue was achieved by injection of 4-hydroxytamoxifen as previously described (Han et al., 2012).

4.2.1.7 Generation of GFAPhrGFP-*CB$_1$*-WT and GFAPhrGFP-*CB$_1$*-KO

CB$_1$-WT and *CB$_1$*-KO mice received an intrahippocampal injection of a recombinant adeno associated virus expressing humanized Renilla GFP protein under the control of human GFAP promoter (von Jonquieres et al., 2013). Virus production and purification, as well as injection procedure were performed as previously described (Chiarlone et al., 2014). After surgery, mice were allowed to recover for at least 4 weeks before anatomical characterization.

4.3 ANIMAL TREATMENT

The experiments were approved by the Committee of Ethics for Animal Welfare of the University of the Basque Country (CEEA/408/2015/GRANDES MORENO, CEIAB/213/2015/GRANDES MORENO). Animals were treated according to the European Community Council Directive 2010/63/UE and the Spanish legislation (RD 53/2013 and Ley 6/2013). Finally, great efforts were made in order to minimize the number and the suffering of the animals used.

4.3.1 TRANSCARDIALLY PERFUSION OF THE ANIMALS

1. C57BL/6N adult mice (between 60 and 90 postnatal days) of either sex were housed under standard conditions (food and water ad libitum; 12h/12h light/dark cycle). CB_1 wild type (hereafter *CB1*-WT), Glu-*CB1*-KO, GABA-*CB1*-KO, GFAP-*CB1*-KO, *CB1*-STOP, Glu-*CB1*-RS, GABA-*CB1*-RS, GFAP-*CB1*-RS, *CB1*-KO, GFAPhrGFP-*CB1*-WT and GFAPhrGFP-*CB1*-KO mice (at least three animals of 3 each condition) were deeply anesthetized by intraperitoneal injection of ketamine/xylazine (80/10 mg/kg body weight).
2. Animals were transcardially perfused at room temperature (20-25 ºC) with phosphate buffered saline (0.1 M, pH 7.4) for 20 seconds, followed by the fixative solution made up of 4% formaldehyde (freshly depolymerized from paraformaldehyde), 0.2% picric acid, and 0.1% glutaraldehyde in phosphate buffer (0.1 M Phosphate buffer, pH 7.4) for 10-15 minutes.
3. Brains were carefully removed from the skull and post-fixed in the fixative solution for approximately 1 week at 4 ºC. Finally, brains were stored at 4

ºC in 1:10 diluted fixative solution plus 0.025% sodium azide at 4°C until its processing.

4.3.2 AVIDIN-BIOTIN PEROXIDASE METHOD FOR LIGHT MICROSCOPY

This is the protocol applied:

1. Brain coronal sections were cut at 50 µm in a vibratome and collected in 0.1 M Phosphate buffer at room temperature.
2. Preincubation of the hippocampal sections with blocking solution composed by 10% horse serum, 0.1% sodium azide and 0.5% triton X-100 prepared in Tris-Hydrogen Chloride buffered saline 1X, pH 7.4 for 30 minutes at room temperature.
3. Incubation with the primary anti-CB_1 receptor antibody (1:100) prepared in the blocking solution, with continuous gentle shaking for 2 days at 4 ºC.
4. Several washes in 1% horse serum and 0.5% triton X-100 in Tris-Hydrogen Chloride buffered saline for 30 minutes to remove excess of the antibody.
5. Incubation with a secondary biotinylated horse anti-goat Inmunoglobulin-G (1:200, Vector Laboratories, Burlingame, CA, USA) prepared in the washing solution for 1 hour on a shaker at room temperature.
6. Washes with 1% horse serum and 0.5% triton X-100 in Tris-Hydrogen Chloride buffered saline.
7. Incubation in 1:50 avidin-biotin complex (Avidin-biotin peroxidase complex, Elite, Vector Laboratories, Burlingame, CA, USA) prepared in the washing solution for 1 hour at room temperature.

8. Several rinses with1% horse serum and 0.5% triton X-100 in Tris-Hydrogen Chloride buffered saline. Last rinses were done with 0.1M phosphate buffer and 0.5% triton X-100.
9. Incubation with 0.05% diaminobenzidine as a chromogen in 0.1 M phosphate buffer containing 0.5% triton-X100 and 0.01% hydrogen peroxide, for 5 minutes at room temperature.
10. Several washes in 0.1 M phosphate buffer with 0.5% triton-X100.
11. Mounting on gelatinized slides.
12. Dehydration in graded alcohols (50°, 70°, 96°, 100°) for 5 minutes each.
13. Clearing in xylol (3 times of 5 min).
14. Coverslipped with DPX.
15. Tissue sections were observed and photographed with a Zeiss Axiocam light microscope coupled to a Zeiss AxioCam HRc Camera.

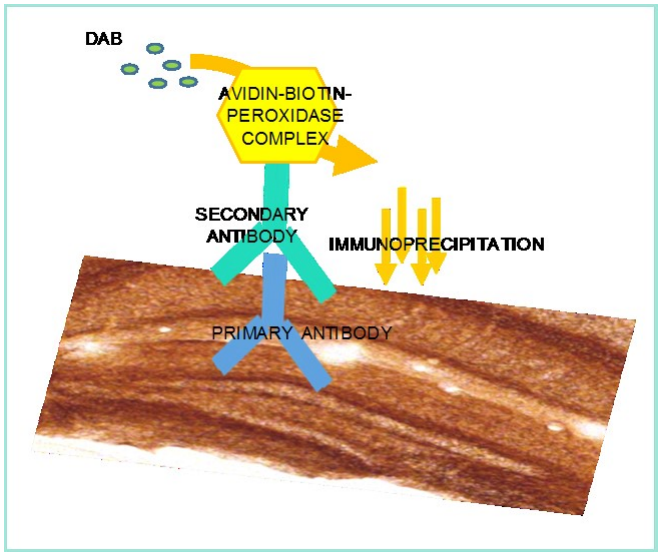

Figure 9. Graphical representation of the Immunoperoxidase method for light microscopy.

4.3.3 PREEMBEDDING SILVER-INTENSIFIED IMMUNOGOLD METHOD FOR ELECTRON MICROSCOPY

The following protocol was applied:

1. Coronal hippocampal vibrosections were cut at 50 µm and collected in 0.1 M phosphate buffer (pH 7.4) at room temperature.
2. Preincubation of the sections in a blocking solution of 10% bovine serum albumin, 0.1% sodium azide, and 0.02% saponin prepared in Tris-Hydrogen Chloride buffered saline 1X, pH 7.4 for 30 minutes at room temperature.
3. Incubation with the primary goat polyclonal anti-CB_1 receptor antibody (1:100) in 10% Bovine Serum Albumin / Tris-Hydrogen Chloride buffered saline containing 0.1% sodium azide and 0.004% saponin on a shaker for 2 days at 4°C.
4. Several washes in 1% Bovine Serum Albumin / Tris-Hydrogen Chloride buffered saline.
5. Incubation in a secondary 1.4 nm gold-labeled rabbit anti-goat Immunoglobulin-G (Fab' fragment, 1:100, Nanoprobes Inc., Yaphank, NY, USA) in 1% Bovine Serum Albumin / Tris-Hydrogen Chloride buffered saline with 0.004% saponin on a shaker for 3 hours at room temperature.
6. Several washes in 1% Bovine Serum Albumin / Tris-Hydrogen Chloride buffered saline overnight on a shaker at 4°C.
7. Post-fixation with 1% glutaraldehyde prepared in Tris-Hydrogen Chloride buffered saline for 10 minutes at room temperature.
8. Several washes in double distilled water for 30 min.
9. Silver intensification of gold particles with a HQ Silver kit (Nanoprobes Inc., Yaphank, NY, USA) for about 12 minutes in the dark.

10. Several washes in double distilled water for 10 minutes.
11. Several washes in 0.1 M phosphate buffer (pH 7.4) for 30 minutes.
12. Osmication (1% osmium tetroxide, in 0.1 M phosphate buffer pH 7.4) for 20 minutes.
13. Several washes in 0.1 M phosphate buffer (pH 7.4) for 30 minutes.
14. Dehydration in graded alcohols (50°, 70°, 96° and 100°) for 5 min each and 3 times of 5 min for 100°.
15. Clearing in propylene oxide 3 times, 5 min each.
16. Embedding in a mixture of 1:1 propylene oxide and Epon resin 812 overnight on a shaker at room temperature.
17. Resin polymerization in a heater at 60°C for 2 days.
18. Cutting 1µm semithin sections in the Reichert-Jung ultracut.
19. Collection of 60nm ultrathin sections on mesh nickel grids.
20. Staining with 2.5% lead citrate for 20 min.
21. Examination under a Philips EM208S electron microscope. Tissue was photographed by using a digital Morada Camera from Olympus coupled to the electron microscope.

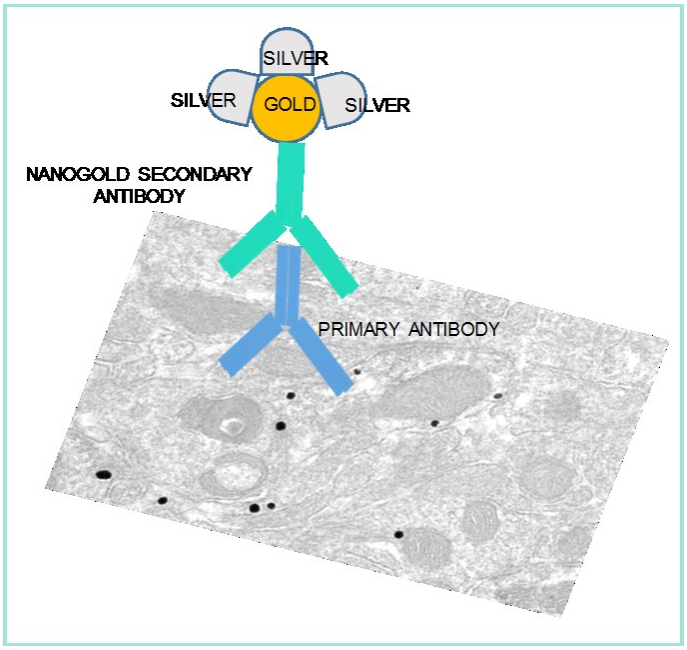

Figure 10. Graphical representation of the Immunoperoxidase method for light microscopy.

4.3.4 PREEMBEDDING DOUBLE LABELING OF SILVER-INTENSIFIED IMMUNOGOLD AND IMMUNOPEROXIDASE METHOD FOR ELECTRON MICROSCOPY

This is the protocol followed:

1. Coronal hippocampal vibrosections were cut at 50 µm and collected in 0.1 M phosphate buffer (pH 7.4) at room temperature.
2. Preincubation in a blocking solution of 10% bovine serum albumin, 0.1% sodium azide, and 0.02% saponin prepared in Tris-Hydrogen Chloride buffered saline 1X, pH 7.4 for 30 minutes at room temperature.
3. Incubation with the primary goat polyclonal anti-CB_1 receptor antibody (1:100) and the primary mouse monoclonal anti-GFAP (1:1000) or the primary rabbit polyclonal hrGFP (1:500) prepared in the blocking solution in 10% Bovine Serum Albumin / Tris-Hydrogen Chloride buffered saline containing 0.1% sodium azide and 0.004% saponin on a shaker for 2 days at 4°C.

4. Several washes in 1% Bovine Serum Albumin / Tris-Hydrogen Chloride buffered saline.
5. Incubation with the corresponding biotinylated secondary antibody (1:200) in 1% Bovine Serum Albumin / Tris-Hydrogen Chloride buffered saline with 0.004% saponin on a shaker for 3 hours at room temperature.
6. Several washes in 1% Bovine Serum Albumin / Tris-Hydrogen Chloride buffered saline overnight on a shaker at 4°C.
7. Incubation in a secondary 1.4 nm gold-labeled rabbit anti-goat Immunoglobulin-G (Fab' fragment, 1:100, Nanoprobes Inc., Yaphank, NY, USA) in 1% Bovine Serum Albumin / Tris-Hydrogen Chloride buffered saline with 0.004% saponin on a shaker for 3 hours at room temperature.
8. Several washes in 1% Bovine Serum Albumin / Tris-Hydrogen Chloride buffered saline for 30 minutes on a shaker at 4°C.
9. Incubation in avidin-biotin complex (1:50) prepared in the washing solution for 1.5 hour at room temperature.
10. Several washes in 1% Bovine Serum Albumin / Tris-Hydrogen Chloride buffered saline overnight on a shaker at 4°C.
11. Post-fixation with 1% glutaraldehyde in Tris-Hydrogen Chloride buffered saline for 10 minutes at room temperature.
12. Several washes in double distilled water for 30 min.
13. Silver intensification of the gold particles was with a HQ Silver kit (Nanoprobes Inc., Yaphank, NY, USA) for about 12 minutes in the dark.
14. Several washes in double distilled water for 10 minutes.
15. Several washes in 0.1 M phosphate buffer (pH 7.4) for 30 minutes.

16. Incubation in 0.05% DAB and 0.01% hydrogen peroxide prepared in 0.1 M phosphate buffer for 5 minutes at room temperature.
17. Osmication (1% osmium tetroxide, in 0.1 M phosphate buffer pH 7.4) for 20 minutes).
18. Several washes in 0.1 M phosphate buffer (pH 7.4) for 30 minutes.
19. Dehydration in graded alcohols (50°, 70°, 96° and 100°) for 5 min each and 3 times of 5 min for 100°.
20. Clearing in propylene oxide 3 times, 5 min each.
21. Embedding in a mixture of 1:1 propylene oxide and Epon resin 812 overnight on a shaker at room temperature.
22. Resin polymerization in a heater at 60°C for 2 days.
23. Cutting 1µm semithin sections in the Reichert-Jung ultracut.
24. Collection of 60nm ultrathin sections on mesh nickel grids.
25. Staining with 2.5% lead citrate for 20 min.
26. Examination under a Philips EM208S electron microscope. Tissue preparations were photographed by using a digital Morada Camera from Olympus coupled to the electron microscope.

4.4 SEMI-QUANTIFICATION OF THE CB1 RECEPTOR IMMUNOGOLD STAINING

With the aim of maximizing the standard conditions, the pre-embedding immunogold method was systematically applied simultaneously to all the sections collected from the all different animals (n=3 of each condition) in each of the three replicated experiments done for each mouse performed.

Immunogold-labeled hippocampal sections were then visualized in the light microscope in order to select portions of the CA1 and the dentate molecular layer with good and reproducible CB_1 receptor immunolabeling. Then the semithin sections were cut with an ultra-microtome and just the first 5 ultrathin sections (60 nm thick) were collected onto two grids. Moreover, to further standardize the conditions between the immunolabeled sections obtained from the different mice, only the first 1.5 µm from the section surface was photographed. All electron micrographs were taken at 18,000x using a Digital Morada Camera from Olympus. Sampling was always performed accurately in the same way for all the animals studied.

The analyzed excitatory and inhibitory synapses were identified by their characteristic ultrastructural features. Hence, excitatory synapses were distinguished by their asymmetric synapses with thick postsynaptic densities and presynaptic terminals containing abundant, clear and spherical synaptic vesicles. Inhibitory synapses were identified by their symmetric synaptic contacts and terminal boutons with pleomorphic synaptic vesicles.

To determine the proportion of the labeled CB_1 receptor terminals, positive labeling was considered if at least one immunoparticle was within approximately 30 nm from the plasmalemma of the synaptic terminal. Metal particles at these synaptic membranes were visualized and counted. Immunopositive astrocytic processes were considered positive if the precipitates of DAB immunoreaction product for hrGFP or GFAP, were inside the astrocytic elements. Image-J software was used to measure the membrane length and distance to synapses. Percentages of CB_1 receptor positive profiles, density (particles/µm membrane) and proportion of CB_1 immunoparticles in terminals versus total CB_1 receptor expression in cellular

membranes were analyzed and displayed as mean ± Standard Error of the Mean using a statistical software package (GraphPad Prism, GraphPad Software Inc, San Diego, USA). The normality test (Kolmogorov-Smirnov normality test) was applied before running statistical tests and subsequently data were analyzed using nonparametric tests (Man-Whitney U test when k=2 or Kruskal-Wallis test when k>2). A potential variability between mice of the same mutant line was analyzed statistically. Since there were no differences between them, all data from each line were pooled.

4.5 SEMI-QUANTIFICATION OF THE DISTANCE FROM ASTROCYTIC CB_1 RECEPTORS TO THE NEAREST SYNAPSE.

Immunogold and immunoperoxidase hippocampal sections were visualized in the light microscope in order to select portions of the CA1 and the dentate molecular layer with good and reproducible immunolabeling. The first 5 ultrathin sections (60 nm thick) were collected onto two grids. Moreover, to further standardize the conditions between the immunolabeled sections obtained from the different mice, only the first 1.5 µm from the section surface was photographed. Once again, all electron micrographs were taken at 18,000x using a Digital Morada Camera from Olympus. Sampling was always accurately done in the same way for all the animals studied.

Positive astrocytic processes were considered by the presence of immunoprecipitation of DAB in the cytoplasm (see above). Moreover, to determine the proportion of labeled CB_1 receptor astrocytic processes, positive labeling was

considered if at least one immunoparticle was within approximately 30 nm from the plasmalemma.

Afterward, the nearby synapses surrounding the immunopositive astrocytic process were identified, the distances were measured using the Image-J software, and the nearest synapse to the astrocytic CB_1 receptor immunogold particle was selected. The data from all the nearest synapses to the astrocytic CB_1 receptor particles were tabulated, analyzed and displayed as mean ± S.E.M. using a statistical software package (GraphPad Prism, GraphPad Software Inc, San Diego, USA).

5 RESULTS

5.1 CB_1 RECEPTOR DISTRIBUTION IN THE BRAIN OF GLU-*CB1*-RS AND GABA-*CB1*-RS MICE. LIGHT MICROSCOPY

The pattern of CB_1 receptor immunostaining was first analyzed in the Glu-*CB1*-RS and GABA-*CB1*-RS brains by light microscopy (Figs. 11 and 12). As expected, a much weaker and diffuse CB_1 receptor pattern was observed in Glu-*CB1*-RS than in GABA-*CB1*-RS, in accordance with the distribution of CB_1 receptor in glutamatergic and GABAergic cells, respectively (Figs. 11 and 12). Thus, noticeable CB_1 receptor staining was observed in the striatum, cortex, olfactory tubercle and amygdala of Glu-*CB1*-RS (Fig. 11). In GABA-*CB1*-RS, strong CB_1 receptor immunoreactivity was detected in the cortex, anterior olfactory nucleus, piriform cortex, globus pallidus, entopeduncular nucleus, amygdala and the substantia nigra (Fig. 12). The striatum exhibited moderate to strong immunostaining (Fig. 12). Altogether, the overall CB_1 receptor pattern in Glu-*CB1*-RS and GABA-*CB1*-RS matches the known receptor distribution in the brain.

5.2 CB_1 RECEPTOR DISTRIBUTION IN HIPPOCAMPUS OF GLU-*CB1*-RS AND GABA-*CB1*-RS MICE. LIGHT MICROSCOPY

We particularly focused on the pattern of the CB_1 receptor immunostaining in the hippocampus (Fig.13). In *CB1*-WT, a distinct intensity pattern was observed throughout the layers (Fig. 13a). Thus, the strongest CB_1 receptor immunostaining was revealed in the stratum pyramidale and at the limit between the strata radiatum and lacunosum-moleculare. Also, a dense neuropil labeling was seen throughout

the strata radiatum and oriens. In the dentate gyrus, the most prominent CB_1 receptor staining localized in the innermost third of the stratum moleculare whereas a remarkable but weaker staining was found in the outer 2/3 of the layer. Finally, immunoreactive fibrous processes surrounding the granule cell bodies were visible in the stratum granulosum (Fig. 13a).

In the Glu-*CB_1*-RS hippocampus, a faint CB_1 receptor immunoreactivity was observed throughout the strata oriens and radiatum of the hippocampal Ammon´s horn (Cornu ammonis, CA) (Fig. 13b). Remarkably, a strong band of CB_1 receptor immunostaining appeared in the innermost third of the dentate molecular layer which corresponds to the zone of the synapses of the commissural/associational system (Fig. 13b) (Monory et al., 2006; Ruehle et al., 2013). In GABA-*CB_1*-RS, heavy CB_1 receptor immunoreactivity was distributed throughout the CA stratum radiatum and the dentate molecular layer (Fig. 13c). However, a stronger CB_1 receptor staining was found in the pyramidal cell layer and at the limit between strata radiatum and lacunosum-moleculare of the CA1, as well as in the molecular innermost third and the infragranular zone of the dentate gyrus (Fig.13c). Importantly, the CB_1 receptor immunostaining was absence in the *CB_1*-KO hippocampus, indicating the specificity of the CB_1 receptor antibody used (Fig. 13d).

5.3 SUBCELLULAR LOCALIZATION OF THE CB_1 RECEPTOR IN HIPPOCAMPUS OF GLU-*CB1*-RS AND GABA-*CB1*-RS. HIGH RESOLUTION ELECTRON MICROSCOPY

To study the localization of CB_1 receptor in detail, a preembedding immunogold method for electron microscopy was used. Hence, hippocampal sections of *CB1*-WT, *CB1*-KO, Glu-*CB1*-RS, GABA-*CB1*-RS, STOP-*CB1*, Glu-*CB1*-KO and GABA *CB1*-KO mice were used to investigate the cellular and subcellular localization of the receptor in the CA1 stratum radiatum (Fig.14) and in the inner third of the dentate molecular layer (Fig.15). As expected in *CB1*-WT, presynaptic inhibitory terminal membranes forming symmetric synapses were decorated with a high density of CB_1 receptor immunoparticles, whereas a much lower labeling was observed in excitatory terminals making asymmetric synapses. CB_1 receptor immunoparticles were located at a distance from the active zones of the symmetric and asymmetric synapses formed with postsynaptic dendrites and dendritic spines, respectively (Figs.14a and 15a). Noticeably, the CB_1 receptor pattern virtually disappeared in *CB1*-KO meaning that the CB_1 receptor antibody used was highly specific (Figs. 14b and 15b).

In Glu-*CB1*-RS, the CB_1 receptor was re-expressed in excitatory synapses identified by their typical ultrastructural features, namely, axon boutons with abundant, clear and spherical synaptic vesicles forming asymmetric synapses with postsynaptic dendritic spines, whereas CB_1 receptor immunolabeling was absent in symmetric synapses (Figs. 14 d and 15d). CB_1 receptor was also re-expressed in synaptic terminals of the commissural/associational system in the inner third of

the dentate molecular layer that contained abundant tightly packed synaptic vesicles and forming asymmetric synapses with granule cell dendrites and dendritic spines (Fig. 15d) (Ribak et al., 1985; Li et al., 1994; Blasco-Ibáñez and Freund, 1997; Scharfman, 2007). By contrast, in Glu-*CB1*-KO CB_1 receptor immunonegative excitatory synapses but numerous CB_1 receptor immunoparticles accumulated in terminals with pleomorphic synaptic vesicles and symmetric synapses with dendrites were observed (Figs.14e and 15e).

In the case of GABA-*CB1*-RS, rich CB_1 receptor immunolabeling was restricted to presynaptic terminal plasma membranes making symmetric synapses with dendrites; no immunoparticles were found at excitatory synapses (Figs.14f and 15 f). On the other hand, only presynaptic boutons forming asymmetric synapses with spines were CB_1 receptor immunopositive in GABA-*CB1*-KO (Figs.14g and 15g). No immunolabeling was observed in excitatory or inhibitory synapses of STOP-*CB1* hippocampus (Figs.14c and 15c). In addition, CB_1 receptor immunoparticles were also observed in mitochondrial membranes of *CB1*-WT and the conditional mutants, but not in *CB1*-KO (Figs.14b and 15b)

5.4 SUBCELLULAR LOCALIZATION OF THE CB_1 RECEPTOR IN HIPPOCAMPUS OF GFAP-*CB1*-RS AND GFAPhrGFP-*CB1*-WT. HIGH RESOLUTION ELECTRON MICROSCOPY

For the study in detail of the localization of CB_1 receptors in astrocytes of the hippocampus, a preembedding immunogold and immunoperoxidase method for electron microscopy were applied. In order to investigate the cellular and

subcellular localization of the receptor in the CA1 stratum radiatum (Fig.16) and in the the dentate molecular layer (Fig.17), hippocampal sections of *CB1*-WT, *CB1*-KO, GFAP-*CB1*-RS, STOP-*CB1* and GFAP-*CB1*-KO mice were used. Besides, *CB1*-WT and *CB1*-KO mice expressing hrGFP in astrocytes (GFAPhrGFP-*CB1*-WT and GFAPhrGFP-*CB1*-KO respectively) were also analyzed.

As expected, CB_1 receptor immunoparticles were distributed in astrocytic processes membranes and terminal plasmalemma of *CB1*-WT (Figs.16a and 17a) and of GFAPhrGFP-*CB1*-WT (Figs 16f, 16g, 17f and 17g). However, in GFAP-*CB1*-RS, CB_1 receptor immunoparticles appeared only in astrocytic processes but not in synaptic terminals (Figs. 16c and 17c). Conversely in GFAP-*CB1*-KO (Figs. 16d and 17d), CB_1 receptor labeling disappeared from astrocytes membranes whereas the pattern of the CB_1 receptor in synaptic terminals remained unchangeable relative to *CB1*-WT (Figs. 16a and 17a). Importantly, there was not CB_1 receptor immunolabeling in synaptic terminals nor in astrocytic processes of STOP-*CB1* hippocampus (Figs.16e and 17e). Furthermore, the CB_1 receptor staining pattern disappeared in *CB1*-KO (Figs. 16b and 17b) and in GFAPhrGFP-*CB1*-KO (Figs. 16h and 17h) hence demonstrating the great specificity of the anti-CB_1 receptor antibody used.

5.5 STATISTICS OF THE CB_1 RECEPTOR IN EXCITATORY TERMINALS OF THE GLU-*CB1*-RS AND GABA-*CB1*-RS HIPPOCAMPUS

The proportion of CB_1 receptor immunopositive excitatory synaptic terminals in the CA1 stratum radiatum of *CB1*-WT (24.29% ± 1.09), Glu-*CB1*-RS (21.89% ± 1.21) and GABA-*CB1*-KO (21.37% ± 1.13) was not significantly different (Fig. 18a). However, the percentage of positive terminals greatly decreased in Glu-*CB1*-KO (2.50% ± 0.76) and virtually disappeared in STOP-*CB1*, GABA-*CB1*-RS and *CB1*-KO (Fig. 18a). Furthermore, no statistical differences were found in CB_1 receptor density (particles/µm) between excitatory synaptic terminals of *CB1*-WT (0.45 ± 0.01), Glu-*CB1*-RS (0.45 ± 0.02) and GABA-*CB1*-KO (0.46 ± 0.02) (Fig. 18b). Finally, the proportion of CB_1 receptor gold particles in asymmetric terminals versus total CB_1 receptor expression in plasmalemmal structures was analyzed in CA1 stratum radiatum. 88.78% ± 1.96 of the total CB_1 receptor immunoparticles were located in excitatory terminals of Glu-*CB1*-RS, while 12.35% ± 1.04 and 27.30% ± 3.34 were found in *CB1*-WT and GABA-*CB1*-KO respectively. Only residual CB_1 receptor immunoparticles were observed in STOP-*CB1*, GABA-*CB1*-RS, Glu-*CB1*-KO and *CB1*-KO (Fig. 18c).

The analysis of the inner third of the dentate molecular layer showed comparable percentages of CB_1 receptor immunopositive excitatory synaptic terminals in *CB1*-WT (55.98% ± 2.51), Glu-*CB1*-RS (53.19% ± 2.89) and GABA-*CB1*-KO (52.12% ± 3.00) (Fig. 19a). The proportion decreased in Glu-*CB1*-KO (5.48% ± 1.70) and practically disappeared in STOP-*CB1*, GABA-*CB1*-RS and *CB1*-KO (Fig. 19a). CB_1 receptor immunoparticle density, expressed as the number of particles per µm of

cell perimeter, was statistically similar in *CB1*-WT (0.39 ± 0.02), Glu-*CB1*-RS (0.39 ± 0.02) and GABA-*CB1*-KO (0.39 ± 0.02) (Fig. 19b). Furthermore, the proportion of CB_1 receptor immunogold particles in glutamatergic terminals versus total CB_1 receptor expression in plasmalemma was 12.80% ± 1.39 in *CB1*-WT, 88.64% ± 1.71 in Glu-*CB1*-RS, 29.22% ± 3.65 in GABA-*CB1*-KO and only residual CB_1 receptor immunoparticles were found in excitatory terminals of GABA-*CB1*-RS, Glu-*CB1*-KO, STOP-*CB1* and *CB1*-KO mice (Fig. 19c). Altogether, these results indicate that the subcellular CB_1 receptor distribution and expression levels at excitatory synapses were preserved in the Glu-*CB1*-RS and GABA-*CB1*-KO mutants relative to the wild type, remaining residual at the same synapses of Glu-*CB1*-KO and GABA-*CB1*-RS mice.

5.6 STATISTICS OF THE CB_1 RECEPTOR IN INHIBITORY TERMINALS OF THE GLU-*CB1*-RS AND GABA-*CB1*-RS HIPPOCAMPUS

As to the inhibitory synapses, the amount of CB_1 receptor immunopositive terminals in *CB1*-WT (78.50% ± 2.44), GABA-*CB1*-RS (77.92% ± 2.63) and Glu-*CB1*-KO (79.63% ± 2.35) was maintained in the CA1 stratum radiatum (Fig. 20a). However, this proportion drastically decreased in STOP-*CB1*, GABA-*CB1*-KO and Glu-*CB1*-RS and virtually disappeared in *CB1*-KO (Fig. 20a). There were not statistically significant differences in CB_1 receptor immunoparticle density between inhibitory synaptic terminals of *CB1*-WT (4.57 ± 0.13), GABA-*CB1*-RS (4.33 ± 0.11) and Glu-*CB1*-KO (4.50 ± 0.15) (Fig. 20b). Furthermore, 44.06% ± 2.67 of the total immunoparticles in *CB1*-WT, 97.10% ± 0.46 in GABA-*CB1*-RS and 54.87% ± 3.94

in Glu-*CB1*-KO were located in inhibitory terminals. Just residual particles were observed in STOP-*CB1*, Glu-*CB1*-RS, GABA-*CB1*-KO and *CB1*-KO mice (Fig. 20c).

The proportion of CB_1 receptor immunopositive inhibitory synaptic terminals in the inner third of the dentate molecular layer was found to be similar between *CB1*-WT (84.27% ± 2.38), GABA-*CB1*-RS (85.07% ± 1.76) and Glu-*CB1*-KO (88.02% ± 1.93) (Fig. 21a). These values almost disappeared in STOP-*CB1*, GABA-*CB1*-KO, Glu-*CB1*-RS and in *CB1*-KO (Fig. 21a). No statistical differences in labeling density were found between inhibitory terminals of *CB1*-WT (7.54 ± 0.16), GABA-*CB1*-RS (7.47 ± 0.14) and Glu-*CB1*-KO (7.69 ± 0.21) (Fig. 21b). Moreover, 45.38% ± 3.18 of the total immunoparticles in the inner third of the dentate molecular layer were located in GABAergic terminals of *CB1*-WT, 93.87% ± 0.93 in GABA-*CB1*-RS and 59.45% ± 4.00 in Glu-*CB1*-KO, whereas only residual particles were found in inhibitory terminals of STOP-*CB1*, Glu-*CB1*-RS, GABA-*CB1*-KO and *CB1*-KO mice (Fig. 21c). Hence, the subcellular distribution and expression levels of CB_1 receptors at inhibitory synapses were kept in the GABA-*CB1*-RS and Glu-*CB1*-KO mutants relative to the wild type, remaining residual at the same synapses of STOP-*CB1*, GABA-*CB1*-KO and Glu-*CB1*-RS mice.

5.7 STATISTICS OF THE CB_1 RECEPTOR IN ASTROCYTIC PROCESSES OF THE GFAP-*CB1*-RS AND GFAPhrGFP-*CB1*-WT HIPPOCAMPUS

The analysis of the percentage of CB_1 receptor immunopositive astrocytic processes (Fig. 22a) did not show statistical differences between *CB1*-WT (42.06% ± 3.56) and GFAP-*CB1*-RS (37.12% ± 3.79) in the CA1 stratum radiatum. In GFAPhrGFP-*CB1*-WT, the proportion of astrocytic elements immunolabeled for

CB_1 receptors increased to 59.91% ± 3.29 being the difference statistically significant when compared with *CB_1*-WT. Conversely, only scarce CB_1 receptor immunolabeling was found in astrocytes of GFAP-*CB_1*-KO, STOP-*CB_1*, *CB_1*-KO and in GFAPhrGFP-*CB_1*-KO mice.

Additionally, CB_1 receptor immunoparticle density on astrocytic membranes (particles/µm) was analyzed (Fig. 22b). Our data showed statistically similar densities in *CB_1*-WT (0.135 ± 0.019) and GFAP-*CB_1*-RS (0.128 ± 0.020), whereas a great statistically significant increase was found in GFAPhrGFP-*CB_1*-WT (0.384 ± 0.039). Nevertheless, only residual unspecific particles were found in GFAP-*CB_1*-KO (0.005 ± 0.003), in STOP-*CB_1* (0.005 ± 0.003), in *CB_1*-KO (0.001 ± 0.001) and in GFAPhrGFP-*CB_1*-KO (0.004 ± 0.002).

Finally, the proportion of CB_1 immunogold particles in astrocytic processes versus total CB_1 expression in plasmalemma was analyzed in CA1 stratum radiatum (Fig. 22c). 95.45% ± 1.82 of the total CB_1 immunoparticles were located in astrocytic processes of GFAP-*CB_1*-RS, while 23.08% ± 1.99 of the total immunogold particles were in the astrocytic elements of *CB_1*-WT. This proportion reached 33.71% ± 2.75 in GFAPhrGFP-*CB_1*-WT. As expected, only residual CB_1 receptor immunoparticles were located in astrocytes of GFAP-*CB_1*-KO, STOP-*CB_1*, GFAPhrGFP-*CB_1*-KO and *CB_1*-KO mice.

Furthermore, 75.13% ± 4.06 of the total CB_1 immunoparticles in plasmalemma were in terminal membranes of GFAP-*CB_1*-KO, while 65.52% ± 2.44 were in C*B_1*-WT, and 56.32% ± 2.73 in GFAPhrGFP-*CB_1*-WT (Fig. 22d). As expected, only residual CB_1 receptor immunoparticles were located in astrocytic processes of GFAP-*CB_1*-RS, STOP-*CB_1*, GFAPhrGFP-*CB_1*-KO and *CB_1*-KO mice (Fig. 22d).

The analysis of the hippocampal dentate molecular layer showed comparable percentages of CB_1 receptor immunopositive astrocytic processes between *CB1*-WT (44.67% ± 3.85) and GFAP-*CB1*-RS (39.84% ± 3.50), whereas the proportion significantly increased to 59.99% ± 3.37 in GFAPhrGFP-*CB1*-WT. The proportion decreased in GFAP-*CB1*-KO, STOP-*CB1*, GFAPhrGFP-*CB1*-KO and *CB1*-KO mice (Fig. 23a).

Besides, no statistical differences were found between the CB_1 receptor density (particles/µm) on astrocytic processes of *CB1*-WT (0.112 ± 0.011) and GFAP-*CB1*-RS (0.138 ± 0.016) mice but there was when compared with GFAPhrGFP-*CB1*-WT (0.334 ± 0.033) (Fig. 23b). However, only residual particles were observed in GFAP-*CB1*-KO (0.006 ± 0.003), STOP-*CB1* (0.006 ± 0.003), GFAPhrGFP-CB_1-KO (0.002 ± 0.002) and CB_1-KO mice (0.004 ± 0.002) (Fig. 23b).

Furthermore, we examined the proportion of CB_1 receptor labeling in astrocytic processes versus total CB_1 receptor expression (Fig. 23c). The values were 22.40% ± 2.28 in *CB1*-WT, 95.61% ± 1.56 in GFAP-*CB1*-RS and 32.57% ± 2.09 in GFAPhrGFP-*CB1*-WT. Only non-specific CB_1 receptor immunoparticles were found in astrocytic processes of GFAP-*CB1*-KO, STOP-*CB1,* and GFAPhrGFP-*CB1*-KO and CB_1-KO mice (Fig. 23c).

Finally, CB_1 gold labeling in terminal membranes versus total CB_1 expression was also studied. 76.17% ± 4.70 of the total CB_1 immunoparticles were located in terminals of GFAP-*CB1*-KO, 64.27% ± 2.88 in *CB1*-WT and 57.17% ± 2.19 in GFAPhrGFP-*CB1*-WT (Fig. 23d). Just residual particles were in astrocytic processes of GFAP-*CB1*-RS, STOP-*CB1*, GFAPhrGFP-*CB1*-KO and *CB1*-KO mice (Fig. 23d).

5.8 STATISTICAL ANALYSES OF THE DISTANCE FROM ASTROCYTIC CB_1 RECEPTORS TO THE NEAREST SYNAPSE

Taking advantage of the better detection of astrocytes achieved with the hr-GFP protein in the electron microscope, the distance between the astrocytic CB_1 receptor immunoparticles and the midpoint of the nearest synapse surrounded by the immunopositive astrocytic element was measured in GFAPhrGFP-*CB_1*-WT.

In CA1 (Fig 24a), 50.76% ± 4.10 of the total synapses surrounded by astrocytic processes were at a distance between 400-800 nm away from the nearest astrocytic immunoparticle. Of those, 40.89% ± 2.57 were excitatory synapses whereas 9.86% ± 1.97 were inhibitory synapses. 20.60% ± 6.1 of the synapses were found to be located in a range of 0 nm to 400 nm from the astrocytic CB_1 receptor to the nearest synapse. Of these, 17.52% ± 5.63 were excitatory synapses and only 3.08% ± 0.49 were inhibitory synapses. 18.46% ± 2.53 of the synapses were found to be located in a range of 800 nm to 1200 nm of which 13,96% ± 1,60 were excitatory and 4.50% ± 0.95 were inhibitory synapses. Only 10.18% ± 7.81 synapses were found at more than 1200 nm from the astrocytic CB_1 receptor metal particle, being 9.62% ± 8.01 of them excitatory and only 0.56% ± 0.56 were inhibitory synapses.

In the dentate molecular layer (Fig 24b), 57.25% ± 3.19 of the synapses surrounded by astrocytic processes were at 400-800 nm from the astrocytic CB_1 receptor particle, 46.67% ± 2.17 of them were excitatory synapses and the other 10.59% ± 2.18 were inhibitory synapses. 19.83% ± 0.58 of the synapses were in a range of 0 nm to 400 nm from the astrocytic CB_1 receptor metal particle of which

16.67% ± 1.31 were excitatory and 3.16% ± 0.82 inhibitory synapses. Finally, 16.42% ± 4.37 of the total synapses were found between 800 nm and 1200 nm; 13.22% ± 3.19 being excitatory and 3.21% ± 2.25 inhibitory synapses. Only 6.48% ± 2.31 synapses were found at more than 1200 nm from the astrocytic CB_1 receptor. 5.16% ± 2.72 of them were excitatory and 1.32% ± 0.66 inhibitory synapses.

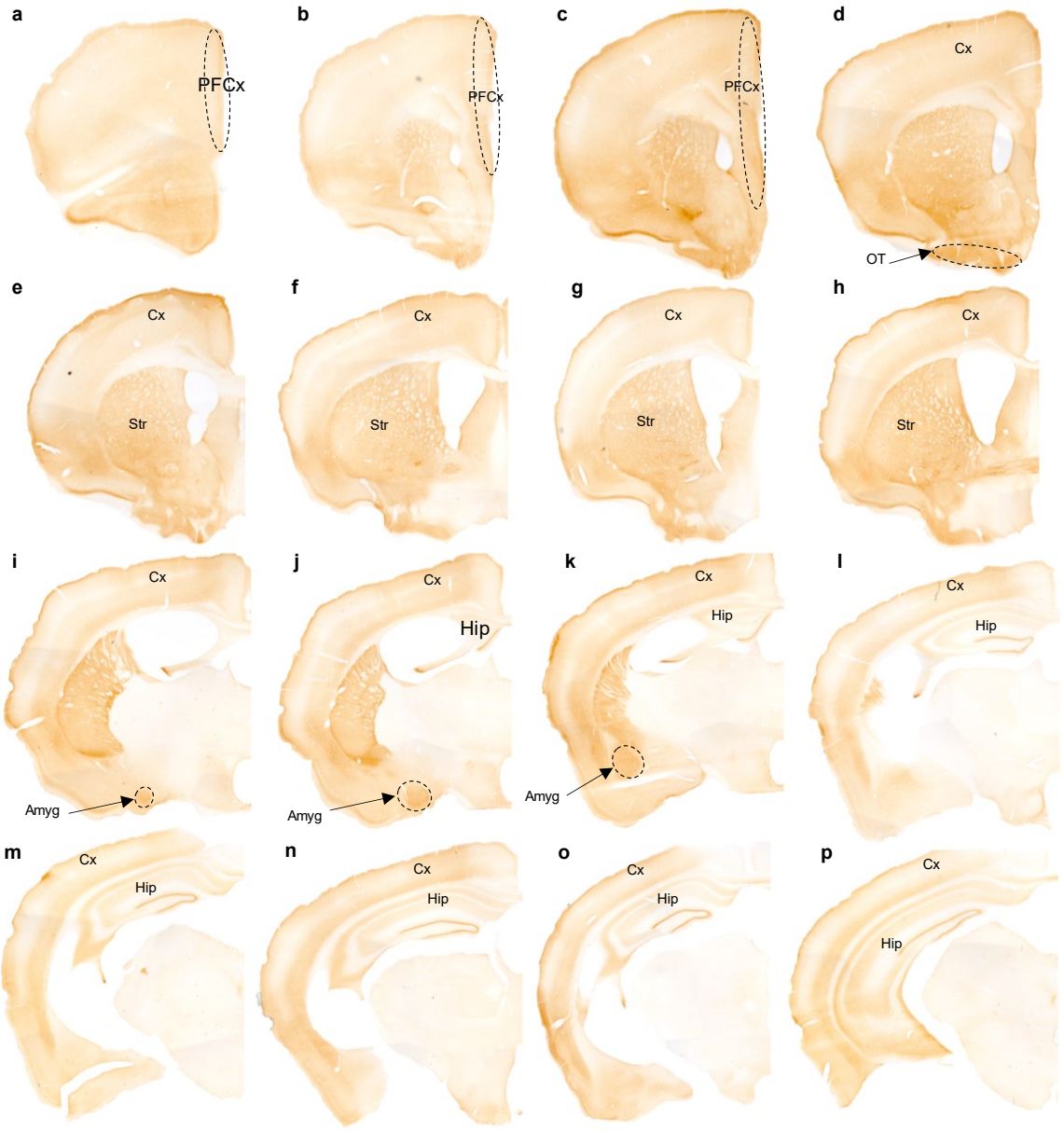

Figure 11. CB_1 receptor immunostaining in the Glu-*CB_1*-RS mouse brain.

An immunoperoxidase method for light microscopy was used for CB_1 receptor immunostaining detection in the Glu-*CB_1*-RS mouse brain. Representative rostro-caudal coronal brain sections stained with the CB_1 antibody (left to right and top to bottom). Observe a diffuse CB_1 receptor staining throughout but somehow more detectable in OT, Cx, Str, Amyg and hippocampus.

PFCx, Prefrontal cortex; OT, Olfactory tubercle; Cx, Cortex; Str, Striatum; Amyg, Amygdala; Hip, Hippocampus; a to d: Bregma 2.34 to 1.34 mm; e to h: Bregma 0.98 to 0.14 mm; i to l: Bregma -0.46 to -1.70 mm; m to p: Bregma -2.46 to -2.80 mm.

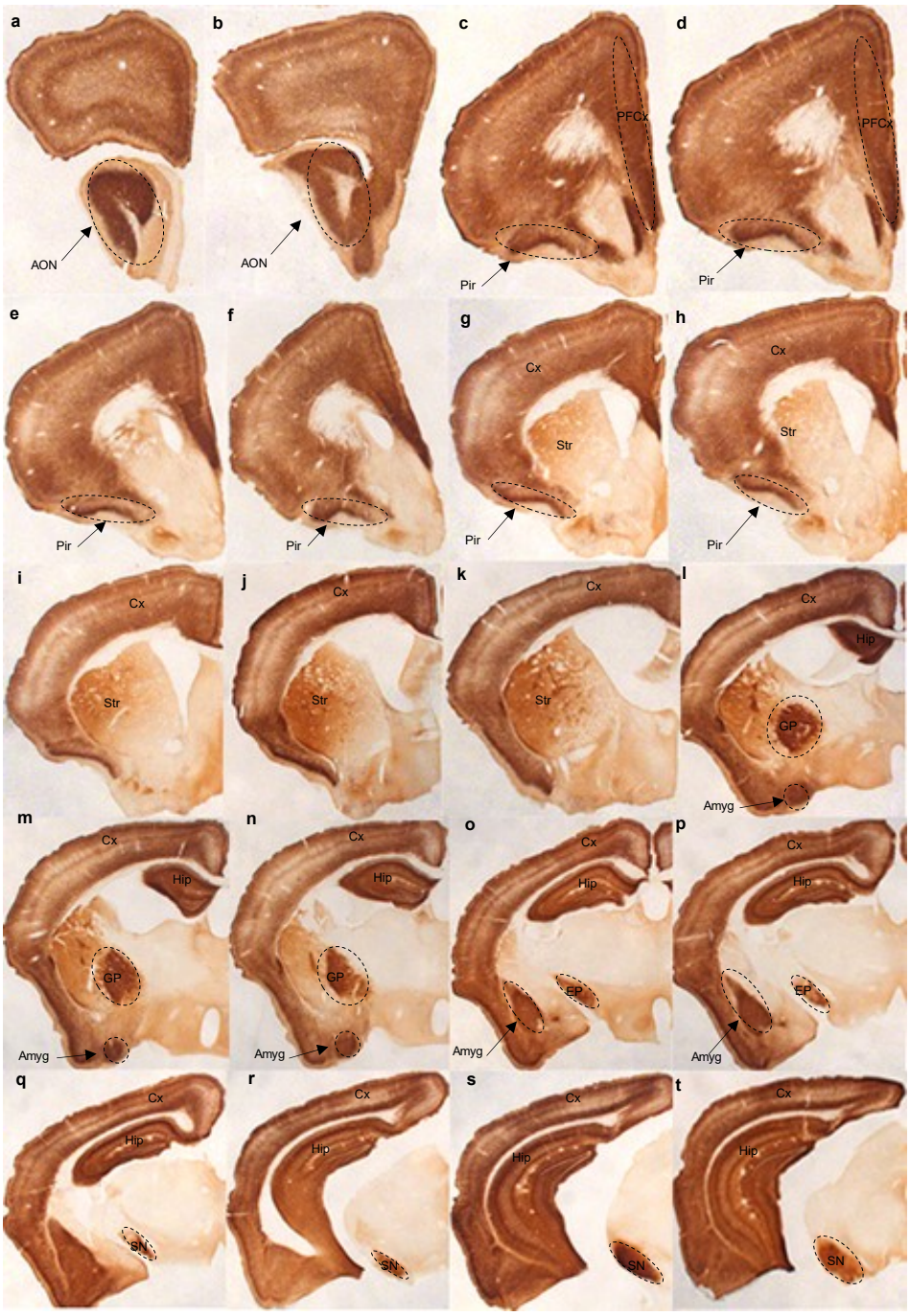

Figure 12. **CB_1 receptor immunostaining in the GABA-*CB_1*-RS mouse brain.**

An immunoperoxidase method for light microscopy was used for CB_1 receptor immunostaining detection in the GABA-*CB_1*-RS mouse brain. Representative rostro-caudal coronal brain sections (left to right and top to bottom). Strong CB_1 receptor immunostaining is found in AON, Pir, PFCx, Cx, Str, GP, EP, Amyg, SN and hippocampus.

AON, Anterior olfactory nucleus; Pir, Piriform cortex; PFCx, Prefrontal cortex; Cx, Cortex; Str, Striatum; GP, Globus pallidus; Amyg, Amygdala; Hip, Hippocampus; EP, Entopeduncular nucleus; SN, Substantia nigra; a to d: Bregma 2.80 to 1.70 mm; e to h: Bregma 1.54 to 1.18 mm; i to l: Bregma 0.74 to -0.94 mm; m to p: Bregma -1.22 to -1.58 mm; q to t: Bregma -2.46 to -2.92.

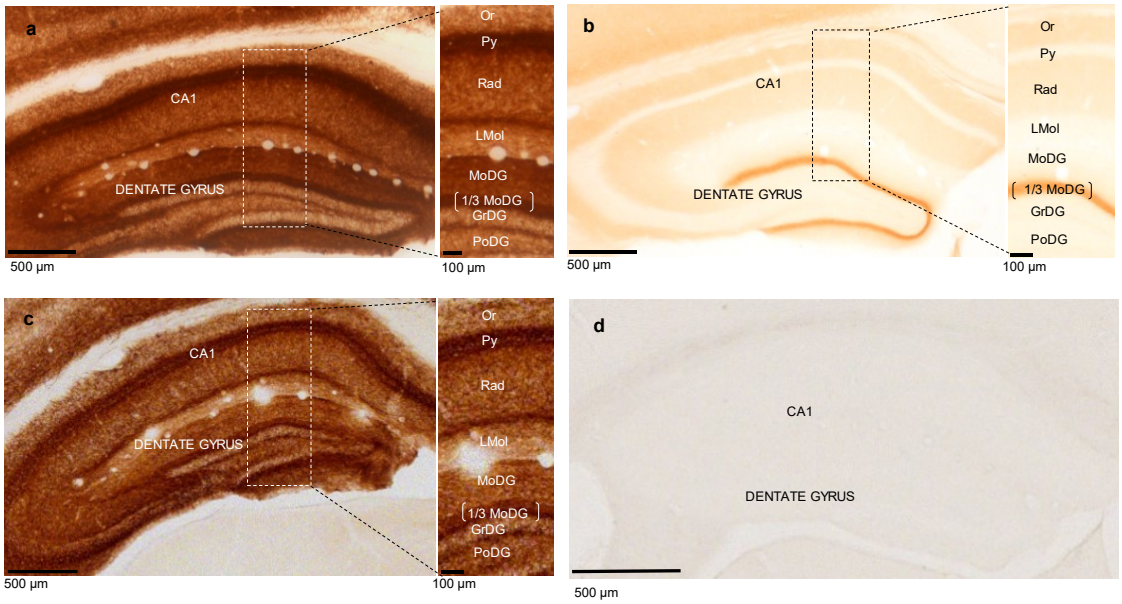

Figure 13. CB_1 receptor immunostaining in the hippocampus of *CB1*-WT, Glu-*CB1*-RS and GABA-*CB1*-RS and *CB1*-KO mice.

An immunoperoxidase method for light microscopy was used. In the *CB1*-WT hippocampus a stronger immunolabeling is observed in Py and at the limit Rad and LMol than throughout the Or and Rad. In the dentate gyrus, the densest immunolabeling is found in the inner third of MoDG whereas less staining, although intense, was found in the outer parts of this layer. Fibrous processes surrounding the granule cell bodies are observed in GrDG (**a**). Detailed magnification of the Glu-*CB1*-RS hippocampus: noticeable CB_1 receptor neuropil labeling is detected in Or and Rad. A dense band of immunostaining is observed in the inner third of MoDG (**b**). Detailed magnification of the GABA-*CB1*-RS hippocampus: a denser labeling area is seen in Py and also at the limit between Rad and LMol. MoDG is heavily CB_1 receptor immunoreactive exhibiting a conspicuous band at its inner third (**c**). Detailed magnification of the *CB1*-KO hippocampus: immunostaining completely disappears in all the *CB1*-KO layers demonstrating that the CB_1 antibody is highly specific (**d**).

CA1, Region 1 of Cornu Ammonis; Or, Stratum oriens; Py, Pyramidal cell hippocampus; Rad, Stratum radiatum; LMol, Lacunosum moleculare; MoDG, Molecular dentate gyrus; 1/3 MoDG, inner third of molecular dentate gyrus; GrDG, Granular dentate gyrus; PoDG, Polymorph dentate gyrus.

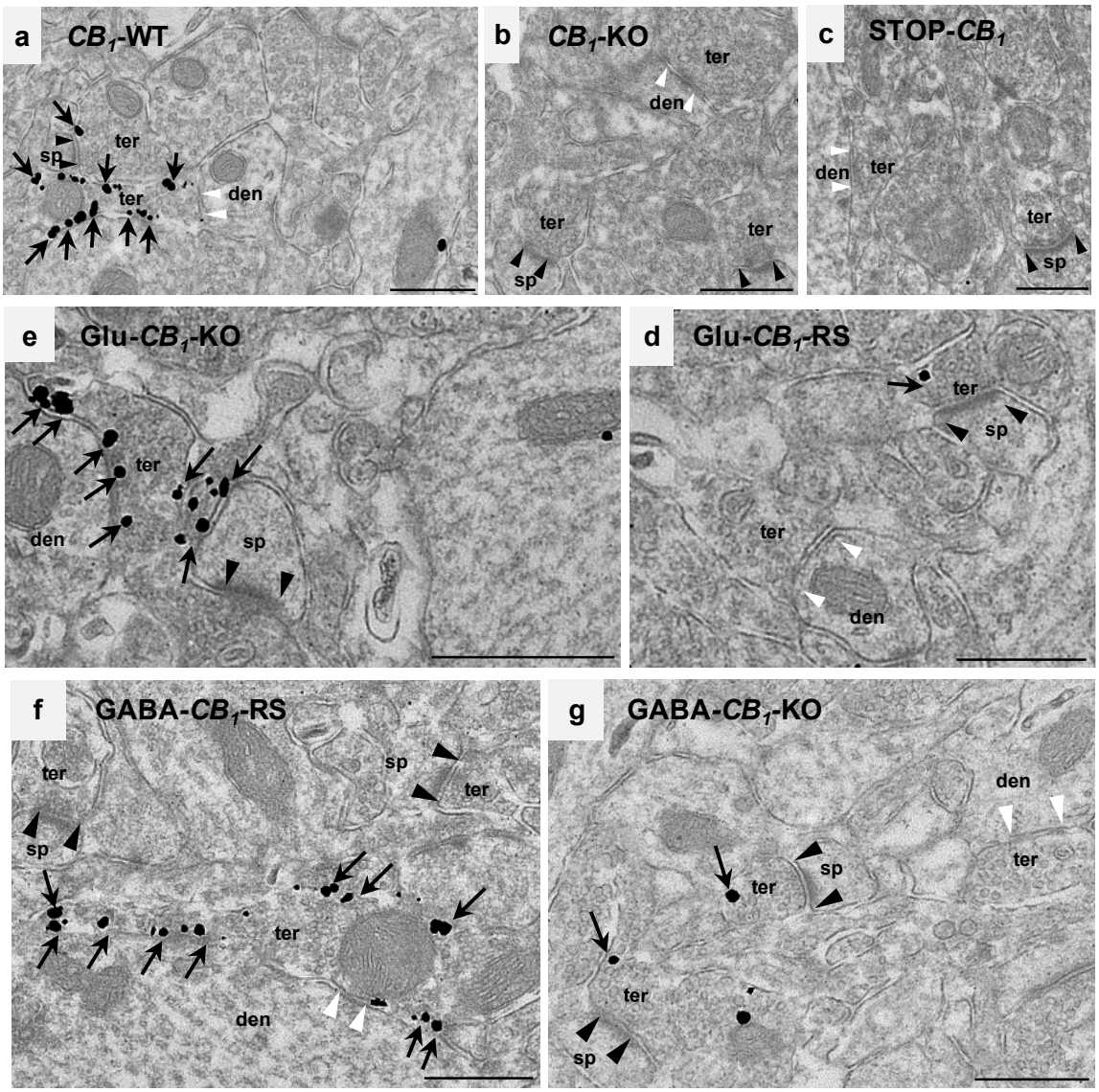

Figure 14. **Subcellular CB_1 receptor localization in synaptic terminals of the CA1 stratum radiatum. Preembedding immunogold method for electron microscopy.**

In *CB1*-WT, immunoparticles are localized on excitatory (asymmetric synapses) and inhibitory (symmetric synapses) terminal membranes making synaptic contacts with dendritic spines or dendrites, respectively (**a**). No CB_1 receptor immunolabeling is detected in *CB1*-KO, indicating that the CB_1 receptor antibody used is specific (**b**). In STOP-*CB1*, no CB_1 receptor labeling is observed in excitatory or inhibitory terminals (**c**). In Glu-*CB1*-RS, CB_1 receptor immunoparticles are at asymmetric but not symmetric synapses (**d**). On the contrary, CB_1 receptor immunolabeling is distributed on inhibitory presynaptic terminal membranes and not on membranes of excitatory boutons in Glu-*CB1*-KO (**e**). Similarly, many CB_1 receptor immunoparticles are confined to symmetric synapses in GABA-*CB1*-RS (**f**). However, synaptic CB_1 receptor immunoparticles are observed on excitatory presynaptic terminal membranes and not in inhibitory terminals of GABA-*CB1*-KO (**g**). Note the presence of CB_1 receptor labeling in mitochondria (a, d-g).

Black arrowheads: excitatory synapses; white arrowheads: inhibitory synapses; black arrows: CB_1 receptor immunoparticles. ter, terminal; den, dendrite; sp, dendritic spine. Scale bars: 0.5 µm.

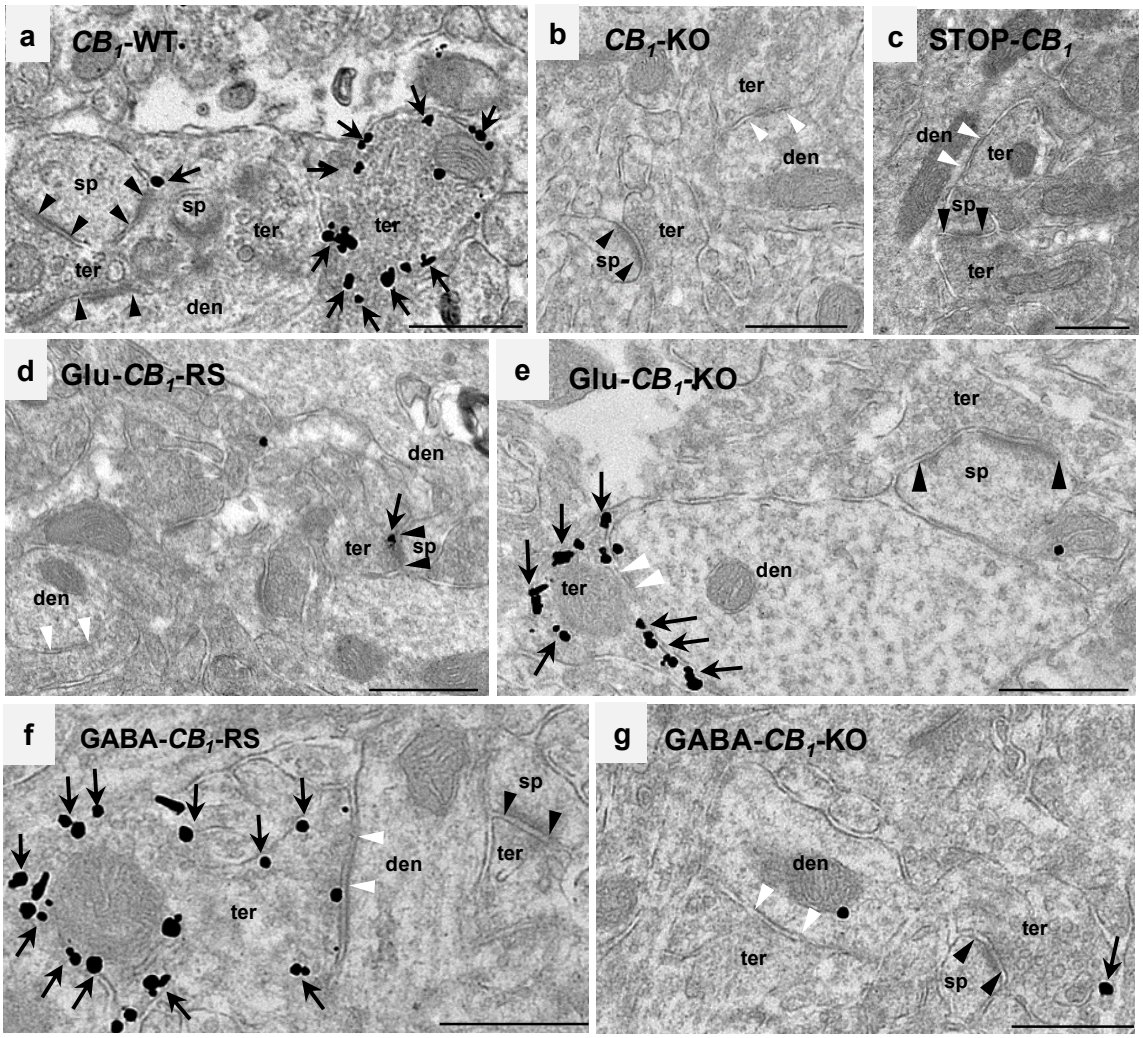

Figure 15. Subcellular CB_1 receptor localization in synaptic terminals of the dentate inner 1/3 molecular layer. Preembedding immunogold method for electron microscopy.

In *CB1*-WT, scarce CB_1 receptor immunoparticles are localized on presynaptic terminal membranes making excitatory synapses (asymmetric) with dendritic spines while numerous metal particles are at inhibitory terminals (**a**). The CB_1 receptor labeling pattern is neither observed in *CB1*-KO (**b**) nor in STOP-*CB1* mice (**c**). In Glu-*CB1*-RS, CB_1 receptor gold particles are only seen on presynaptic mossy cell axon boutons and not on presynaptic inhibitory terminal membranes (**d**). However, in Glu-*CB1*-KO, excitatory mossy cell terminals are immunonegative but inhibitory boutons contain abundant CB_1 receptor labeling (**e**). In GABA-*CB1*-RS, numerous CB_1 receptor immunoparticles are only on presynaptic inhibitory axon terminals but not at excitatory synapses (**f**). In contrast, immunolabeling is not observed in GABAergic terminals but it is present in excitatory boutons of GABA-*CB1*-KO (**g**). Observe CB_1 receptor immunoparticles on mitochondria (a, d-g).

Black arrowheads: excitatory synapses; white arrowheads: inhibitory synapses; black arrows: CB_1 receptor immunoparticles. ter, terminal; den, dendrite; sp, dendritic spine. Scale bars: 0.5 µm.

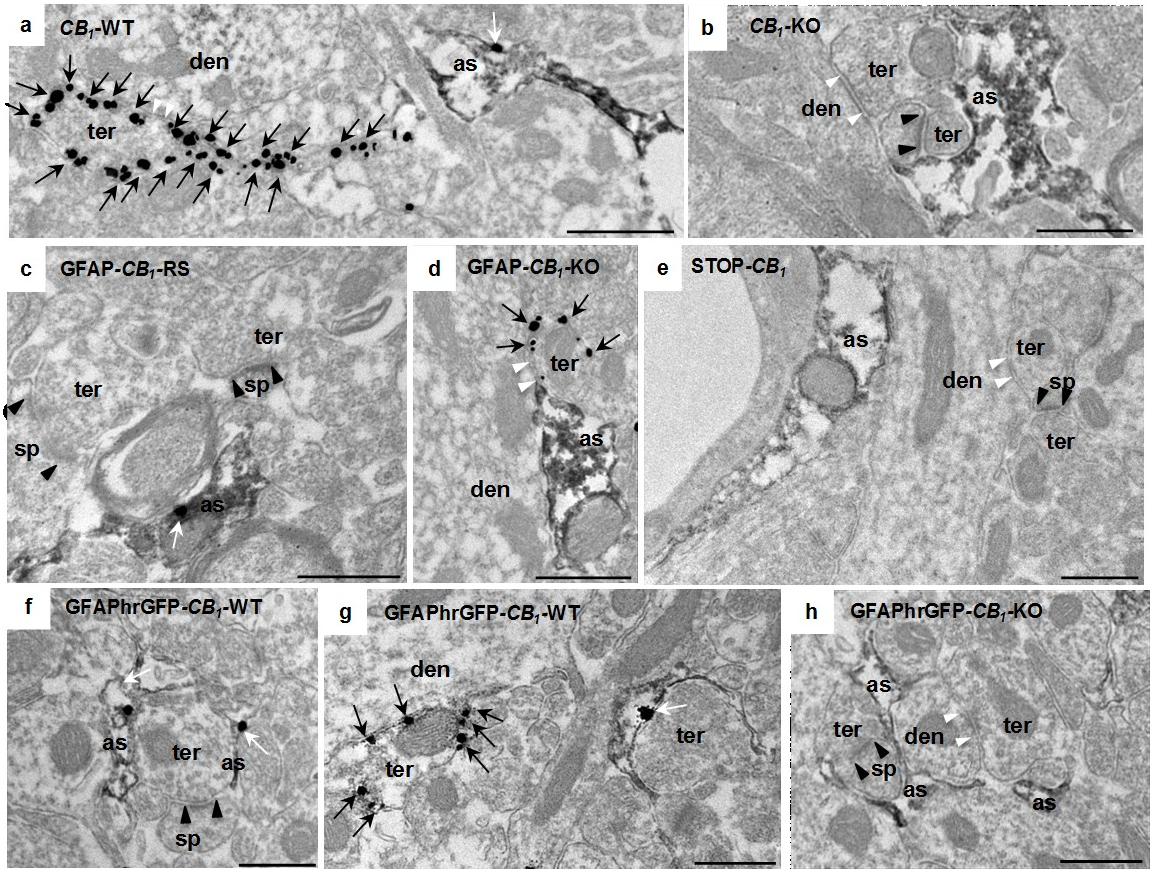

Figure 16. Subcellular CB_1 receptor localization in astrocytic processes of the hippocampal CA1 stratum radiatum. Combined preembedding immunogold and immunoperoxidase methods for electron microscopy.

In *CB1*-WT and in GFAPhrGFP-*CB1*-WT mice, CB_1 receptor immunoparticles are localized in membranes of astrocytic processes. CB_1 receptor immunoparticles are also observed on terminal membranes (**a, f, g**). CB_1 receptor immunolabeling is neither detected in *CB1*-KO nor in GFAPhrGFP-*CB1*-KO, indicating that the CB_1 receptor antibody used is highly specific (**b, h**). CB_1 receptor immunoparticles appear in astrocytic processes but not in terminals of GFAP-*CB1*-RS (**c**). In GFAP-*CB1*-KO, CB_1 receptors disappear from membranes of astrocytic processes whereas they remain in synaptic terminals (**d**). There is not CB_1 receptor immunoparticles in STOP-*CB1* mice (**e**).

Black arrowheads: excitatory synapses; white arrowheads: inhibitory synapses; black arrows: CB_1 receptor immunoparticles; white arrows: astrocytic CB_1 receptor immunoparticles. as: astrocytic processes; ter: terminal; den: dendrite; sp: dendritic spine. Scale bars: 0.5 µm.

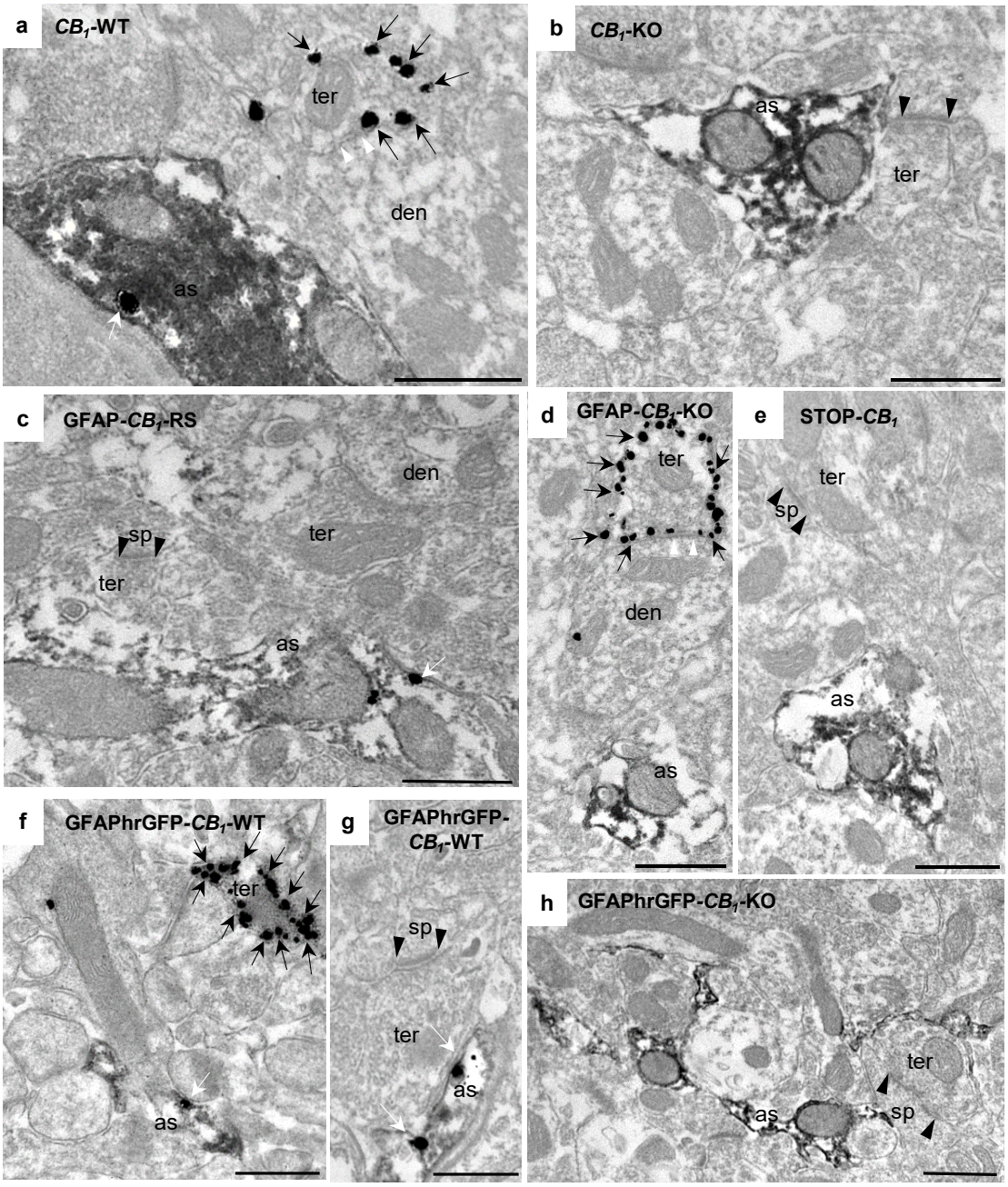

Figure 17. Subcellular CB_1 receptor localization in astrocytic processes of the dentate molecular layer. Combined preembedding immunogold and immunoperoxidase methods for electron microscopy.

In *CB1*-WT and GFAPhrGFP-*CB1*-WT mice, CB_1 receptor is localized on presynaptic terminal membranes and on membranes of astrocytic processes (**a, f, g**). The CB_1 receptor labeling pattern disappears in *CB1*-KO and in GFAPhrGFP-*CB1*-KO showing the specificity of the antibody used (**b, h**). In GFAP-*CB1*-RS, CB_1 receptor immunogold particles are on astrocytic processes and not on neuronal terminal membranes (**c**). However, in GFAP-*CB1*-KO, astrocytic processes are CB_1 receptor immunonegative but inhibitory and excitatory terminals contain the receptor (**d**). There is no CB_1 receptor immunolabeling in STOP-*CB1* (**e**).

Black arrowheads: excitatory synapses; white arrowheads: inhibitory synapses; black arrows: CB_1 receptor immunoparticles; white arrows: astrocytic CB_1 receptor immunoparticles. as: astrocytic processes; ter: terminal; den: dendrite; sp: dendritic spine. Scale bars: 0.5 µm.

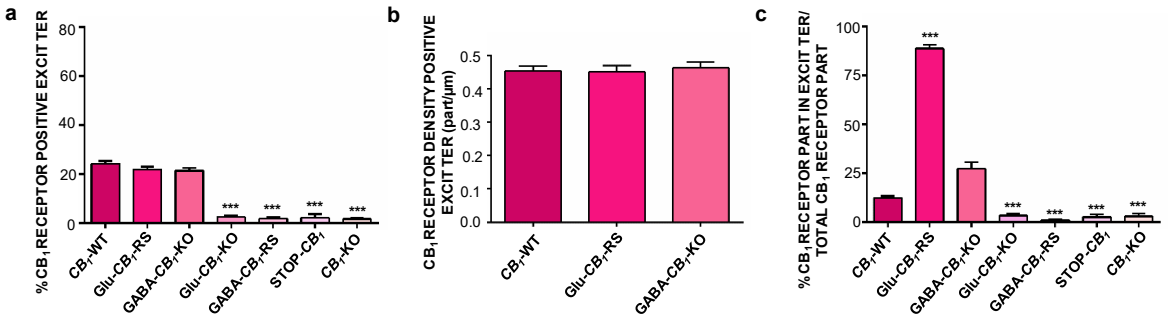

Figure 18. **Statistics of the CB_1 receptor immunopositive glutamatergic terminals in the CA1 stratum radiatum**.

No significant differences are found between *CB1*-WT (24.29% ± 1.09), Glu-*CB1*-RS (21.89% ± 1.21) and GABA-*CB1*-KO (21.37% ± 1.13). Just residual excitatory terminals with metal particles were found in Glu-*CB1*-KO (2.50% ± 0.76), GABA-*CB1*-RS (1.92% ± 0.66) STOP- *CB1* (2.20% ± 1.54) and *CB1*-KO (1.68% ± 0.62) (**a**). Graphical representation of the CB_1 receptor density (particles/µm) in CB_1 receptor positive excitatory terminals. No statistical differences are obtained between *CB1*-WT (0.45 ± 0.01), Glu-*CB1*-RS (0.45 ± 0.02) and GABA-*CB1*-KO (0.46 ± 0.02) (**b**). Proportion of CB_1 receptor in glutamatergic terminals normalized to the total CB_1 receptor signal in plasmalemma of cellular structures: 12.35% ± 1.04 of the total immunoparticles are located in glutamatergic terminals of *CB1*-WT and 27.30% ± 3.34 of GABA-*CB1*-KO. In Glu-*CB1*-RS the proportion increases to 88.78% ± 1.96 and only residual CB_1 receptor immunoparticles are found in excitatory terminals of GABA-*CB1*-RS (1.10% ± 0.30), Glu-*CB1*-KO (3.39% ± 0.96), STOP-*CB1* (3.03% ± 1.52) and *CB1*-KO (2.65% ± 1.45) (**c**). Data are expressed as mean ± Standard Error of the Mean of three different animals. Data were analyzed by means of Kruskal-Wallis Test and the Dunn's Multiple Comparison Post-hoc test. *** indicate statistically significant differences with $p < 0.001$. EXCIT, excitatory; PART, particles; TER, terminals.

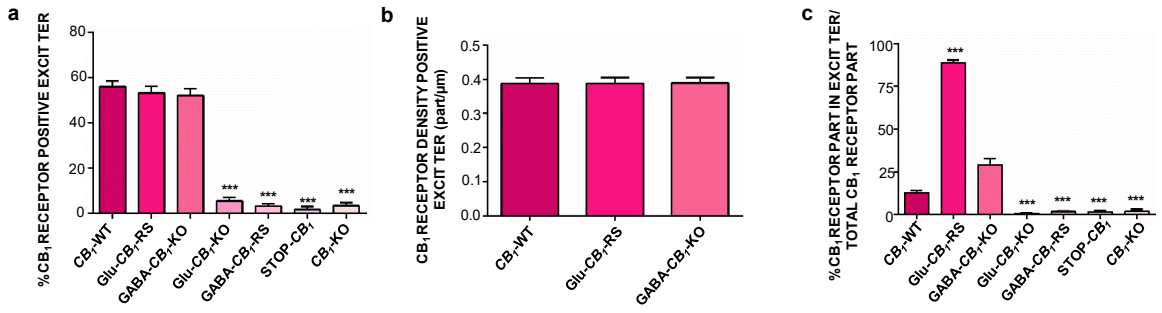

Figure 19. **Statistics of the CB_1 receptor distribution in glutamatergic terminals of the dentate inner 1/3 molecular layer**.

The percentage of CB_1 receptor immunopositive excitatory synaptic terminals is statistically similar between *CB1*-WT (55.98% ± 2.51), Glu-*CB1*-RS (53.19% ± 2.89) and GABA-*CB1*-KO (52.12% ± 3.00). The terminal labeling drastically decreases in Glu-*CB1*-KO (5.48% ± 1.70) and practically disappears in GABA-*CB1*-RS (3.19% ± 1.08), STOP-*CB1* (1.69% ± 1.36) and *CB1*-KO (3.41% ± 1.36) (**a**). Graphical representation of the CB_1 receptor density (particles/µm) in CB_1 receptor positive excitatory terminals. Density in *CB1*-WT (0.39 ±0.02), Glu-*CB1*-RS (0.39 ± 0.02) and GABA-*CB1*-KO (0.39 ± 0.02) is not statistically different (**b**). Proportion of CB_1 receptors in glutamatergic terminals normalized to the total CB_1 receptor signal in plasmalemma of cellular structures: 12.80% ± 1.39 of the total CB_1 receptor immunoparticles in *CB1*-WT, 29.22% ± 3.65 in GABA-*CB1*-KO and 88.64% ± 1.71 in Glu-*CB1*-RS are localized in excitatory terminals. Only scarce CB_1 receptor immunoparticles are in excitatory terminals of GABA-*CB1*-RS (1.78% ± 0.45), Glu-*CB1*-KO (0.65% ± 0.27), STOP-*CB1* (1.54% ± 1.10) and *CB1*-KO (1.87% ± 1.14) (**c**). Data are expressed as mean ± Standard Error of the Mean of three different animals. Data were analyzed by means of Kruskal-Wallis Test and the Dunn's Multiple Comparison Post-hoc test. *** indicate statistically significant differences with $p < 0.001$. EXCIT, excitatory; PART, particles; TER, terminals.

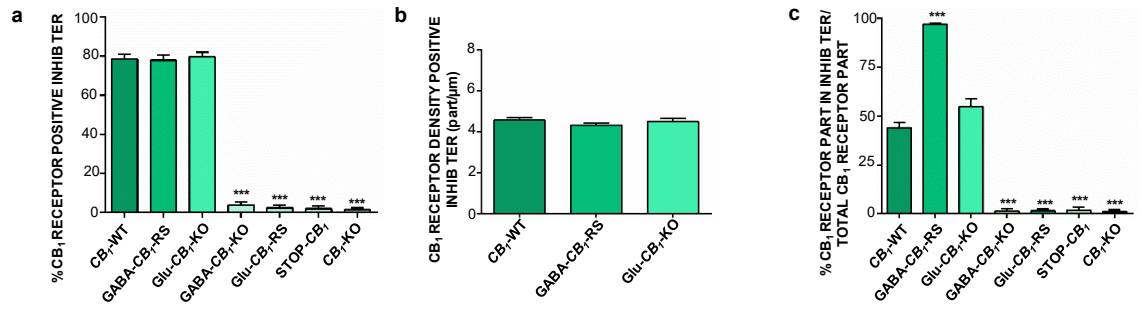

Figure 20. Statistics of the CB_1 receptor distribution in GABAergic terminals of the CA1 stratum radiatum.

Statistical analysis indicates that the percentages of CB_1 receptor immunopositive inhibitory synaptic terminals in *CB1*-WT (78.50% ± 2.44), GABA-*CB1*-RS (77.92% ± 2.63) and Glu-*CB1*-KO (79.63% ± 2.35) are not different. The values virtually disappear in GABA-*CB1*-KO (2.71% ± 1.20), Glu-*CB1*-RS (2.38% ± 1.37), STOP-*CB1* (1.95% ± 1.44) and CB_1-KO (1.53% ± 0.90) (**a**). Graphical representation of the CB_1 receptor density (particles/µm) in CB_1 receptor positive inhibitory terminals. There are no statistical differences between *CB1*-WT (4.57 ± 0.13), GABA-*CB1*-RS (4.33 ± 0.11) and Glu-*CB1*-KO (4.50 ± 0.15) (**b**). Proportion of CB_1 receptor in GABAergic terminals normalized to the total CB_1 receptor signal in plasmalemma of cellular structures: 44.06% ± 2.67 of CB_1 receptor immunoparticles in *CB1*-WT, 54.87% ± 3.94 in Glu-*CB1*-KO and 97.10% ± 0.46 in GABA-*CB1*-RS are in inhibitory terminals. Only sparse CB_1 receptor immunoparticles are in inhibitory terminals of Glu-*CB1*-RS (1.60% ± 0.92), GABA-*CB1*-KO (1.35% ± 1.35), STOP-*CB1* (1.97% ± 1.46) and *CB1*-KO (1.18% ± 0.83) (**c**). Data are expressed as mean ± Standard Error of the Mean of three different animals. Data were analyzed by means of Kruskal-Wallis Test and the Dunn's Multiple Comparison Post-hoc test. *** indicate statistically significant differences with $p < 0.001$. INHIB, inhibitory; PART, particles; TER, terminals.

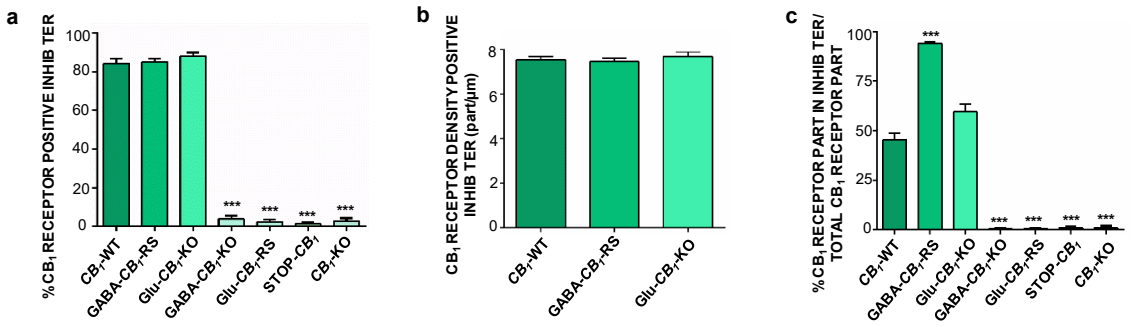

Figure 21. **Statistics of the CB_1 receptor distribution in GABAergic terminals of the dentate inner 1/3 molecular layer.**

Percentages of CB_1 receptor immunopositive inhibitory synaptic terminals do not defer statistically between *CB1*-WT (84.27% ± 2.38), GABA-*CB1*-RS (85.07% ± 1.76) and Glu-*CB1*-KO (88.02% ± 1.93). Only residual particles are detected in scarce terminals of GABA-*CB1*-KO (3.82% ± 1.68), Glu-*CB1*-RS (2.30% ± 1.32), STOP-*CB1* (1.28% ± 0.90) and *CB1*-KO (2.84% ± 1.48) (**a**). Graphical representation of the CB_1 receptor density (particles/µm) in CB_1 receptor positive inhibitory terminals. Density in *CB1*-WT (7.54 ± 0.16), GABA-*CB1*-RS (7.47 ± 0.14) and Glu-*CB1*-KO (7.69 ± 0.21) is not statistically different (**b**). Proportion of CB_1 receptor immunoparticles in GABAergic terminals normalized to the total CB_1 signal in plasmalemma of cellular structures: 45.38% ± 3.18 in *CB1*-WT, 59.45% ± 4.00 in Glu-*CB1*-KO and 93.87% ± 0.93 in GABA-*CB1*-RS are distributed in GABAergic terminals. Rare CB_1 receptor immunoparticles are in inhibitory terminals of Glu-*CB1*-RS (0.60% ± 0.43), GABA-*CB1*-KO (0.53% ± 0.53), STOP-*CB1* (0.86% ± 0.86) and *CB1*-KO (0.93% ± 0.93) (**c**). Data are expressed as mean ± Standard Error of the Mean of three different animals. Data were analyzed by means of Kruskal-Wallis Test and the Dunn's Multiple Comparison Post-hoc test. *** indicate statistically significant differences with $p < 0.001$. INHIB, inhibitory; PART, particles; TER, terminals.

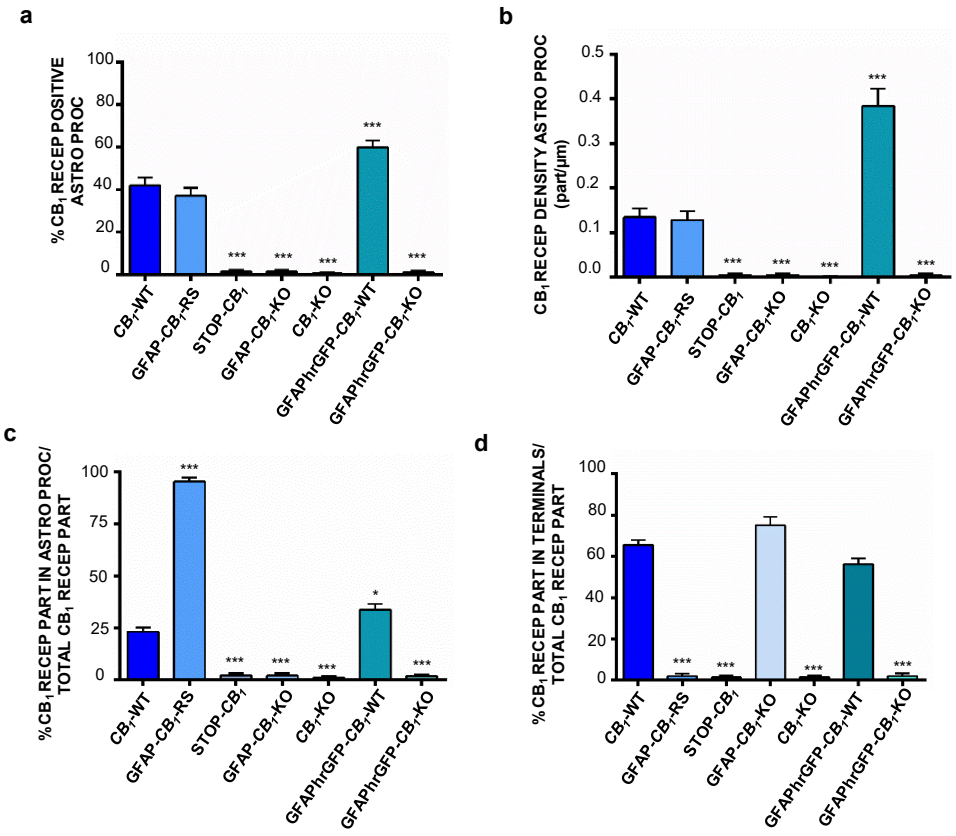

Figure 22. Statistics of the CB_1 receptor distribution in astrocytic processes of the CA1 stratum radiatum.

Percentages of CB_1 receptor immunopositive astrocytes do not show statistical differences between *CB1*-WT mice (42.06% ± 3.56) and GFAP-*CB1*-RS mice (37.12% ± 3.79). In GFAPhrGFP-*CB1*-WT, proportion increases to 59.91 % ± 3.29. Residual immunolabeling is found in GFAP-*CB1*-KO (1.46% ± 0.78), STOP-*CB1* (1.15% ± 0.67), *CB1*-KO (0.54% ± 0.39) and GFAPhrGFP-*CB1*-KO (1.60% ± 0.66) (**a**). CB_1 immunoparticle density on membranes of astrocytic processes (particles / µm) are analyzed. *CB1*-WT (0.135 ± 0.019) and GFAP-*CB1*-RS (0.128 ± 0.020) are statistically similar, whereas a significant increase is found in GFAPhrGFP-*CB1*-WT (0.384 ± 0.039). Just unspecific particles are observed in GFAP-*CB1*-KO (0.005 ± 0.003), STOP-*CB1* (0.005 ± 0.003), *CB1*-KO (0.001 ± 0.001) and GFAPhrGFP-*CB1*-KO (0.004 ± 0.002) (**b**). Proportion of CB_1 gold particles in astrocytic processes versus total CB_1 expression in plasmalemma of cellular structures: 95.45% ± 1.82 of the total CB_1 receptor immunoparticles are located in astrocytic processes of GFAP-*CB1*-RS and 23.08% ± 1.99 are in *CB1*-WT mice. In GFAPhrGFP-*CB1*-WT, the proportion increases to 33.71% ± 2.75. Only residual CB_1 immunoparticles are located in astrocytic processes of GFAP-*CB1*-KO (1.94% ± 1.27), STOP-*CB1* (1.96% ± 1.28), GFAPhrGFP-*CB1*-KO (1.62% ± 0.94) and *CB1*-KO mice (1.01% ± 0.71) (**c**). Proportion of immunogold particles localized in terminals versus total CB_1 receptor expression in plasmalemma: 75.13% ± 4.06 of the total CB_1 immunoparticles are in terminals of GFAP-*CB1*-KO and 65.52% ± 2.44 in *CB1*-WT. In GFAPhrGFP-*CB1*-WT, the proportion is 56.32% ± 2.73. Residual CB_1 receptor immunoparticles are located in astrocytic processes of GFAP-*CB1*-RS (2.02% ± 1.17), STOP-*CB1* (1.47% ± 0.84), GFAPhrGFP-*CB1*-KO (2.08% ± 1.19) and *CB1*-KO (1.51% ± 0.86) mice (**d**). Data are expressed as mean ± Standard Error of the Mean of three different animals. Data were analyzed by means of Kruskal-Wallis Test and the Dunn's Multiple Comparison Post-hoc test. *** indicate statistically significant differences with $p < 0.001$; ** indicate statistically significant differences with $p < 0.01$; * indicate statistically significant differences with $p < 0.05$.

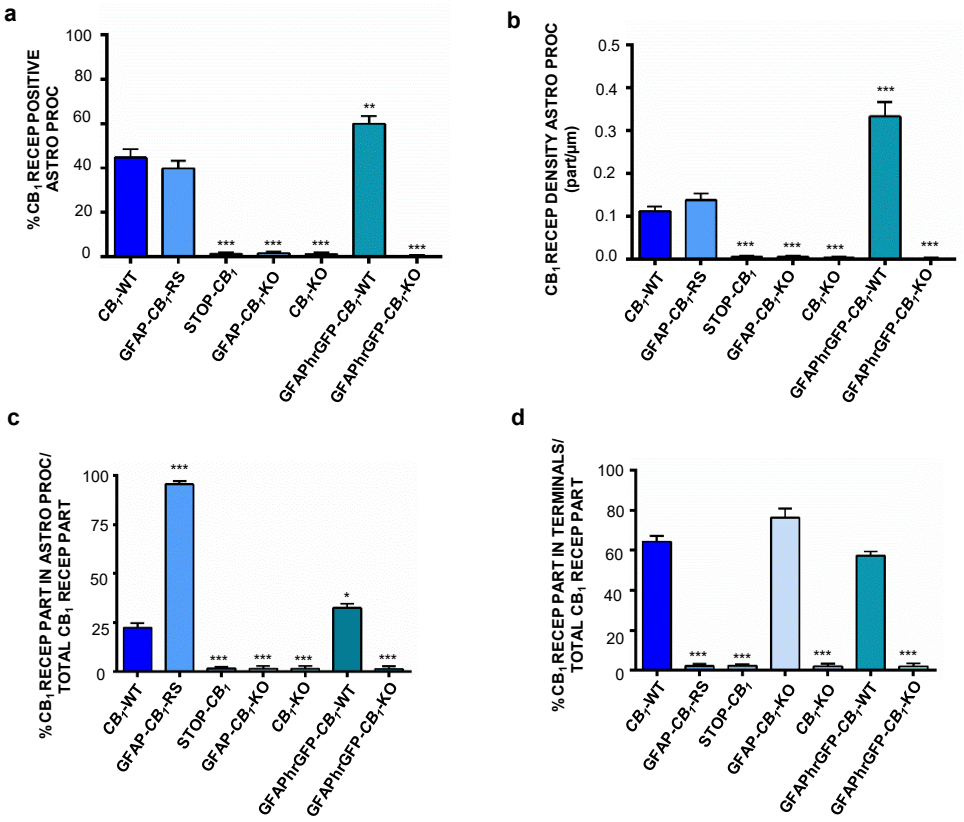

Figure 23. Statistics of the CB_1 receptor distribution in astrocytic processes of the dentate molecular layer.

Similar percentages of CB_1 receptor immunopositive astrocytic processes in*CB1*-WT (44.67% ± 3.85) and GFAP-*CB1*-RS (39.84% ± 3.50) are found. Statistical differences are obtained with GFAPhrGFP-*CB1*-WT (59.99% ± 3.37). Proportion decreases to reach just residual level in: GFAP-*CB1*-KO (1.56% ± 0.65), STOP-*CB1* (1.33% ± 0.64), GFAPhrGFP-*CB1*-KO (0.47% ± 0.36) and *CB1*-KO mice (1.19% ± 0.70) (**a**). Analysis of CB_1 receptor density (particles/µm) on astrocytic processes shows no statistical differences comparing: *CB1*-WT (0.112 ± 0.011) and GFAP-*CB1*-RS (0.138 ± 0.016) mice. However, statistical differences are found with GFAPhrGFP-*CB1*-WT (0.334 ± 0.033). Just residual particles are observed in: GFAP-*CB1*-KO (0.006 ± 0.003), STOP-*CB1* (0.006 ± 0.003), GFAPhrGFP-*CB1*-KO (0.002 ± 0.002) and *CB1*-KO (0.004 ± 0.002) (**b**). Proportion of CB_1 gold particles in astrocytic processes versus total CB_1 expression in plasmalemma is 22.40% ± 2.28 in *CB1*-WT, 95.61% ± 1.56 in GFAP-*CB1*-RS and 32.57% ± 2.09 in GFAPhrGFP-*CB1*-WT. Only non-specific CB_1 receptor immunoparticles are found in astrocytic processes of GFAP-*CB1*-KO (1.43% ± 1.43), STOP-*CB1* (1.65% ± 0.66) GFAPhrGFP-*CB1*-KO (1.37% ± 1.37) and *CB1*-KO (1.43% ± 1.43) mice (**c**). Proportion of immunogold particles localized in terminals versus total CB_1 receptor expression in plasmalemma: 76.17% ± 4.70 of the total CB_1 immunoparticles are in terminals of GFAP-*CB1*-KO, 64.27% ± 2.88 in *CB1*-WTand 57.17% ± 2.19 in GFAPhrGFP-*CB1*-WT. Residual CB_1 receptor immunoparticles are located in astrocytic processes of GFAP-*CB1*-RS (2.19% ± 1.10), STOP-*CB1* (2.36% ± 0.85), GFAPhrGFP-*CB1*-KO (2.05% ± 1.52) and *CB1*-KO (2.14% ± 1.52) mice (**d**). Data are expressed as mean ± Standard Error of the Mean of three different animals. Data were analyzed by means of Kruskal-Wallis Test and the Dunn's Multiple Comparison Post-hoc test. *** indicate statistically significant differences with $p < 0.001$; ** indicate statistically significant differences with $p < 0.01$; * indicate statistically significant differences with $p < 0.05$.

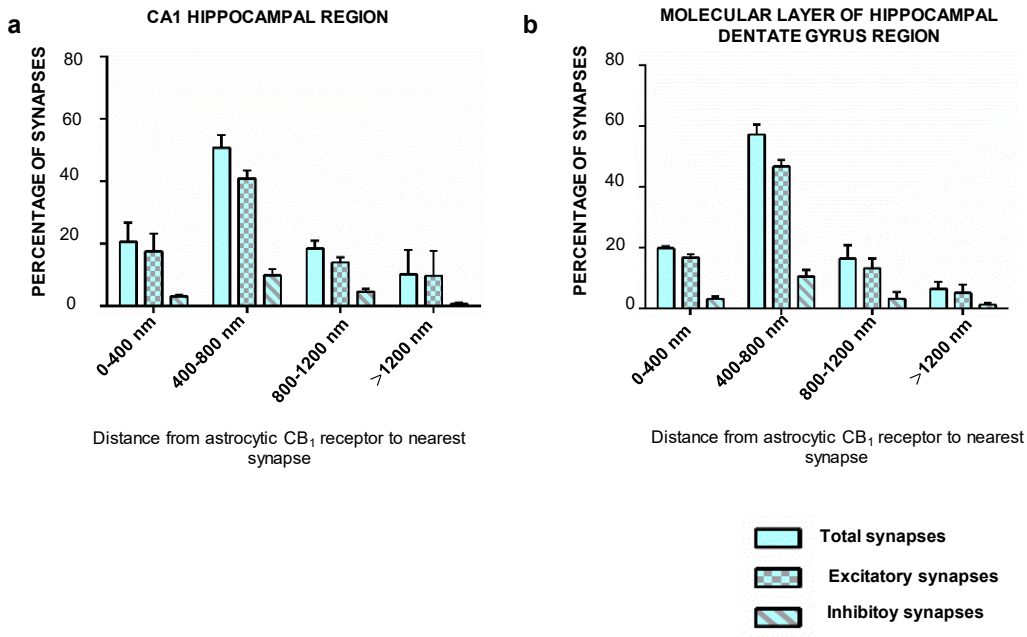

Figure 24. **Statistics of distances from the astrocytic CB_1 receptors to the nearest synapse in the hippocampus.**

Analysis of the distance from the astrocytic CB_1 receptors and the midpoint of the nearest synapse surrounded by the astrocytic processes in the GFAPhrGFP-*CB1*-WT mice. In CA1, of the total analyzed synapses (n= 159) 50.76% ± 4.10 are localized at a distance between 400-800 nm from the astrocytic CB_1 receptor immunoparticle. 40.89% ± 2.57 of them are excitatory and 9.86% ± 1.97 are inhibitory synapses. 20.60% ± 6.12 of the synapses are in a range of 0-400 nm from the astrocytic CB_1 receptor immunoparticle. Of those, 17.52% ± 5.63 are excitatory synapses and 3.08% ± 0.49 are inhibitory synapses. 18.46% ± 2.53 of the total synapses are between 800 nm and 1200 nm; 13,96% ± 1,60 are excitatory and 4.50% ± 0.95 are inhibitory synapses. Only 10.18% ± 7.81 of the synapses are found at more than 1200 nm from the astrocytic CB_1 receptor. Of those, 9.62% ± 8.01 are excitatory and only 0.56% ± 0.56 are inhibitory synapses **(a)**. In the dentate molecular layer, 57.25% ± 3.19 of the total analyzed synapses (n=166) are placed at a distance between 400-800 nm from the astrocytic CB_1 receptor particle; 46.67% ± 2.17 of them are excitatory and 10.59% ± 2.18 are inhibitory synapses. 19.83% ± 0.58 of the synapses are in a range of 0-400 nm; 16.67% ± 1.31 of them are excitatory and 3.16% ± 0.82 are inhibitory synapses. 16.42% ± 4.37 of the total synapses are located between 800-1200 nm. Of these synapses, 13.22% ± 3.19 are excitatory and 3.21% ± 2.52 are inhibitory. Only 6.48% ± 2.31 of the synapses are observed at more than 1200 nm from the astrocytic CB_1 receptor metal particle; 5.16% ± 2.72 being excitatory and 1.32% ± 0.66 inhibitory synapses **(b)**. Data are expressed as mean ± Standard Error of the Mean of three different animals.

6 DISCUSSION

6.1 THE IMPORTANCE OF CB_1 RECEPTOR MUTANTS IN THE STUDY OF CB_1 RECEPTOR

The CB_1 receptor is expressed in different brain cell types populations (Marsicano and Lutz, 1999; Tsou et al., 1999; Nyíri et al., 2005b; Monory et al., 2006; Häring et al., 2007; Scavone et al., 2010; Han et al., 2012; Metna-Laurent and Marsicano, 2015). Moreover, a wide variety of intracellular effects such as modulation of kinases, ion channels and transcription factors are triggered by the activation of CB_1 receptors (Bosier et al., 2010; Pertwee, 2015). One of the most known and important result of these intracellular events is the retrograde inhibition of transmitter release (Kano et al., 2009). Consequently, the activation of CB_1 receptors modulates the release of several neurotransmitters, such as: glutamate, GABA, glycine, acetylcholine, norepinephrine, dopamine, serotonin and cholecystokinin (Kano et al., 2009).

Anatomically, the CB_1 receptor is also widely distributed in the brain with a preferential localization in motor, limbic, reward and cortical regions (Matsuda et al., 1993; Tsou et al., 1998). Its high concentration in certain brain areas is an advantage for studying the functional role of the receptor in the neural circuits where it is abundantly localized (Katona et al., 1999; Kawamura et al., 2006; Ludányi et al., 2008; Marsicano and Kuner, 2008; Katona and Freund, 2012; De-May and Ali, 2013; Steindel et al., 2013; Hu and Mackie, 2015).

However, CB_1 receptor density is not uniform through the regions expressing the receptor which makes extremely difficult to identify low CB_1 receptor expression in cell types and/or in subcellular compartments of wild-type brains (Busquets-Garcia et al., 2015).

The hippocampus is one of the brain structures with the highest CB_1 receptor immunoreactivity (Herkenham et al., 1990; Mailleux and Vanderhaeghen, 1992; Matsuda et al., 1993; Tsou et al., 1998; Marsicano and Lutz, 1999; Egertová and Elphick, 2000; Katona et al., 2006; Kawamura et al., 2006; Ludányi et al., 2008; Katona and Freund, 2012; Steindel et al., 2013; Hu and Mackie, 2015) and where CB_1 receptors have shown to play key functional roles (Campbell et al., 1986; Heyser et al., 1993; Stella et al., 1997; Hampson and Deadwyler, 1999; Katona et al., 2000; Carlson et al., 2002; Chevaleyre and Castillo, 2003, 2004; Vanderbyl et al., 2005; Robbe et al., 2006; Akirav, 2011; Puighermanal et al., 2012; Han et al., 2012; Basavarajappa and Subbanna, 2014).

The development and use of cell type specific CB_1-receptor-knockout mice, lacking the CB_1 receptor in specific brain cell populations served to identify low CB_1 receptor expression in cellular, subcellular or intracellular compartments as well as to understand its physiological functions in those compartments (Marsicano et al., 2003; Monory et al., 2006, 2007; Puighermanal et al., 2009; Bellocchio et al., 2010; Bénard et al., 2012; Han et al., 2012; Ruehle et al., 2013; Steindel et al., 2013; Soria-Gómez et al., 2014; Busquets-Garcia et al., 2015; Martín-García et al., 2015; Oliveira da Cruz et al., 2016). For instance, in the GABA-*CB$_1$*-KO brain, a drastic decrease of the CB_1 receptor immunoreactivity was observed throughout the hippocampus but remaining a noticeable immunoreactive band in the inner third of the dentate molecular layer (Martín-García et al., 2015). On the other hand, just a very faint decrease of the CB_1 receptor immunostaining was noticed in the Glu-*CB$_1$*-KO hippocampus (Martín-García et al., 2015). Yet, there was not a full disappearance of the CB_1 receptor immunoreactivity in either condition as it occurred in *CB$_1$*-KO. The reason is because the CB_1 receptor localization is mostly,

but not exclusively, restricted to neuronal membrane compartments, as CB_1 receptors are also distributed in astrocytic processes (Bosier et al., 2013) and mitochondrial membranes of the hippocampus (Bénard et al., 2012; Hebert-Chatelain et al., 2014a; b). The light microscopic observations previously described by our group (Martín-García et al., 2015) correlate well with the present findings in the electron microscope of the subcellular CB_1 receptor localization in hippocampal glutamatergic and GABAergic axon terminals of GABA-*CB1*-KO and Glu-*CB1*-KO, respectively. This work has also shown that CB_1 receptor immunolabeling was abolished in excitatory terminals of Glu-*CB1*-KO while the proportion and density of CB_1 receptors in GABA-*CB1*-KO were maintained in the glutamatergic excitatory terminals of CA1 stratum radiatum (Takahashi and Castillo, 2006; Takács et al., 2012; Witter, 2012). On the contrary, CB_1 receptor metal particles were not observed in the hippocampal inhibitory synaptic terminals of GABA-*CB1*-KO though CB_1 receptor expression and distribution in CA1 and dentate inhibitory boutons were undistinguishable from *CB1*-WT.

Moreover, the using of GFAP-*CB1*-KO mice have already demonstrated that the activation of CB_1 receptors in CA1 astrocytes mediates the impairment of working memory elicited by acute cannabinoids through the modulation of hippocampal long term depression (Han et al., 2012). The results obtained on the proportion of CB_1 receptor immunopositive CA1 hippocampal astrocytes in in this thesis is similar to the value reported in our previous work (Han et al. in 2012). Furthermore, the expression levels of CB_1 receptor immunoparticles in terminals of GFAP-*CB1*-KO mice was comparable to *CB1*-WT indicating that GFAP-*CB1*-KO are good tools for studies based on the loss of function of astrocytic CB_1 (Han et al., 2012).

However, conditional mutant mice have limitations as a biological compensation derived from the CB_1 receptor deletion could occur. In addition, they do not allow establishing a link between the anatomical CB_1 receptor localization in some nerve cells and a certain physiological task (Ruehle et al., 2013).

6.2 CB_1 RECEPTOR EXPRESSION IN SPECIFIC BRAIN CELL TYPES OF RESCUE MUTANTS

The CB_1 receptor expression protein restoration in phenotype-specific brain cell populations can provide great insights into the sufficiency of the CB_1 receptor for specific brain functions and behaviors. Thus, it is crucial to ensure that the rescue of CB_1 receptors in particular cell types of CB_1 receptor-null mutants correlates with the endogenous CB_1 receptor expression and localization in the wild-type mouse brain. This thesis work has analyzed in detail the anatomical distribution pattern of the CB_1 receptor in the mutant mice.

6.2.1 CB_1 RECEPTOR EXPRESSION IN SPECIFIC NEURONAL CELL TYPES OF THE RESCUE MUTANT MICE

The cellular CB_1 receptor staining described here for the Glu-*CB_1*-RS and GABA-*CB_1*-RS mutants by a preembedding immunoperoxidase method for light microscopy reflects the distribution of CB_1 receptors throughout the brain (Herkenham et al., 1990; Tsou et al., 1998; Marsicano and Lutz, 1999; Egertová and Elphick, 2000; Mackie, 2005; Monory et al., 2006, 2007; Kano et al., 2009; Ruehle et al., 2013; Martín-García et al., 2015). CB_1 receptor immunoreactivity was much fainter in Glu-*CB_1*-RS than in GABA-*CB_1*-RS, as expected for the much lower CB_1 receptor expression in glutamatergic (Marsicano and Lutz, 1999; Katona et al., 2006; Kawamura et al., 2006; Monory et al., 2006, 2007; Martín-García et al., 2015;

Lu and Mackie, 2016) than in GABAergic neurons (Katona et al., 1999; Hájos et al., 2000; Nyíri et al., 2005a; Kano et al., 2009; Takács et al., 2015; Lu and Mackie, 2016). Subcellularly, CB_1 receptors were localized in glutamatergic terminals of the CA1 stratum radiatum and the inner third of the dentate molecular layer of the Glu-*CB_1*-RS, the *CB_1*-WT and the GABA-*CB_1*-KO hippocampus. Furthermore, no significant differences in the proportion of immunopositive excitatory synaptic terminals and density of CB_1 receptors were detected between Glu-*CB_1*-RS, *CB_1*-WT or GABA-*CB_1*-KO (Gutiérrez-Rodríguez et al., 2016). This pattern corresponds well with the distribution and expression of CB_1 receptors in the intrahippocampal excitatory pathways (Marsicano and Lutz, 1999; Katona et al., 2006; Kawamura et al., 2006; Monory et al., 2006; Uchigashima et al., 2011; Katona and Freund, 2012). Very importantly, the inhibitory presynaptic profiles in the Glu-*CB_1*-RS hippocampus were virtually devoid of CB_1 immunoparticles. Also, the labeling was almost nil in the *CB_1*-KO, indicating that the CB_1 receptor antibody used in this study was highly specific. Previous electron microscopy studies described that more than 80% of excitatory synapses are CB_1 receptor immunopositive in the inner third of the dentate molecular layer, compared to only 30–50% in other hippocampal layers (Katona et al., 2006; Uchigashima et al., 2011). Although these values were somehow higher than those obtained in *CB_1*-WT and Glu-*CB_1*-RS in our study, it is plausible to assume that this is probably due to the different CB_1 receptor antibodies used and/or the immunocytochemical protocols applied (Katona et al., 2006; Uchigashima et al., 2011). Besides, in these studies only anatomical features of the synapses were used to distinguish between excitatory and inhibitory synapses. In our study, the CB_1 receptor localization was determined

not only based on anatomical features but also using genetic tools (Glu-*CB$_1$*-RS mice and GABA-*CB$_1$*-RS mice) probably making a difference.

CB_1 receptors in GABA-*CB$_1$*-RS were densely localized in axon terminals of presumably cholecystokinin-containing interneurons as well as of calbindin D28k positive interneurons innervating the proximal portions of the pyramidal cell dendrites in the CA1 stratum radiatum and the dentate molecular layer (Katona et al., 1999; Marsicano and Lutz, 1999; Hájos et al., 2000; Nyíri et al., 2005; Kano et al., 2009; Katona and Freund, 2012; Lu and Mackie, 2016; Takács et al., 2015). Significantly, the excitatory presynaptic profiles in the GABA-*CB$_1$*-RS hippocampus were virtually lacking CB_1 immunoparticles. Furthermore, the proportion of the CB_1 receptor immunopositive inhibitory synaptic terminals was similar in GABA-*CB$_1$*-RS, Glu-*CB$_1$*-KO and *CB$_1$*-WT (Gutiérrez-Rodríguez et al., 2016), and the localization coincides with the CB_1 receptor distribution pattern described in rodent interneurons (Katona et al., 1999; Hájos et al., 2000; Nyíri et al., 2005a) and human hippocampus (Katona et al., 2000).

Another parameter studied here was the density of immunogold particles in the CB_1 receptor positive excitatory and inhibitory terminals. The molecular and microscopic analysis of the hippocampal CB_1 receptors in Glu-*CB$_1$*-RS and GABA-*CB$_1$*-KO, on the one hand, and GABA-*CB$_1$*-RS and Glu-*CB$_1$*-KO, on the other, confirmed that the CB_1 receptor is present at much higher density in hippocampal GABAergic than glutamatergic cells (Katona et al., 2006; Kawamura et al., 2006; Gutiérrez-Rodríguez et al., 2016). The study by Kawamura et al. (2006) revealed a CB_1 receptor density of 5.75 particles/µm in inhibitory terminals and only 0.29 particles/µm in excitatory terminals of the CA1 stratum radiatum. In the same study,

inhibitory terminals in the inner third of the dentate molecular layer had 7.14 particles/µm in contrast to 0.62 particles/µm found in excitatory terminals (Kawamura et al., 2006). The CB_1 receptor densities observed in the CB_1 receptor positive excitatory and inhibitory terminals of the mutant mice are in line with these previous hippocampal data obtained in *CB1*-WT mice, though the differences observed could be attributed to the diverse antibodies and methods used, as mentioned before. To mention that higher receptor abundancy in inhibitory synapses does not directly correlate with downstream signaling activation, as the glutamatergic CB_1 receptor is more efficiently coupled to G protein signaling than the GABAergic CB_1 receptor (Steindel et al., 2013).

6.2.2 CB_1 RECEPTOR EXPRESSION IN ASTROCYTES OF RESCUE MUTANT MICE

In this study, the subcellular CB_1 receptor labeling was also described in rescue mice where the CB_1 receptor expression has been specifically restored in astrocytes of GFAP-*CB1*-RS mice. The low levels of expression of CB_1 receptors in astrocytes can only be accurately detected using high resolution immunocytochemical techniques for electron microscopy. Hence, a preembedding immunogold and immunoperoxidase methods applied to hippocampal sections had previously shown in our laboratory to be an excellent methodological strategy for the localization of CB_1 in astrocytes (Han et al., 2012; Bosier et al., 2013). Our present results have shown the proportion of the CB_1 receptor positive astrocytic processes and the density of the receptor in the astrocytic elements (particles /µm) were not statistically significant different in *CB1*-WT and GFAP-*CB1*-RS. Moreover, the percentage of the CB_1 receptor immunopositive CA1 astrocytes obtained here is similar to the previous values reported by our group (Han et al., 2012). The

analysis of the CB_1 particles localized in astrocytic processes or terminals versus total CB_1 receptor particles in plasmalemmal structures of the GFAP-*CB_1*-RS hippocampus showed that almost all the labeling was in astrocytic processes and just only residual particles were in terminals confirming the high specify of the astrocytic CB_1 receptor genetic rescue approach carried in the mutant mice. Consequently, these rescue mice emerge as excellent models to study the contribution to brain functions of the CB_1 receptors in astrocytes. Specifically, a more comprehensive characterization of the functional consequences of the eCB signaling through the astrocytic CB_1 receptor could be achieve in the tripartite synapses using these rescue mice.

Importantly, the CB_1 receptor expression virtually disappeared in the STOP-*CB_1* mice corroborating previous findings published with these mutants (Ruehle et al., 2013; de Salas-Quiroga et al., 2015).

To sum up, the genetic rescue mouse models of the Glu-*CB_1*-RS expressed CB_1 receptors only in dorsal telencephalic glutamatergic neurons (Ruehle et al., 2013; Soria-Gómez et al., 2014; de Salas-Quiroga et al., 2015; Gutiérrez-Rodríguez et al., 2016), the GABA-*CB_1*-RS only in GABAergic neurons (de Salas-Quiroga et al., 2015; Gutiérrez-Rodríguez et al., 2016) and the GFAP-*CB_1*-RS exclusively in astrocytic processes. Furthermore, these results may suggest that the regulation of the CB_1 receptor expression in glutamatergic and GABAergic cells may be independent one from another. Moreover, astrocytic CB_1 receptor expression may be also independent from the CB_1 receptor in neurons. However, the absence of a crosstalk in the expression of CB_1 receptor between these type of cells cannot be proved with the present experimental design, since the analysis of only one point

in the mouse's life time is insufficient to assess the regulation pathway. Therefore, further analysis would be required in order to corroborate this assumption.

The demonstration in this thesis work that the hippocampus of the rescue Glu-*CB*$_1$-RS, GABA-*CB*$_1$-RS and GFAP-*CB*$_1$-RS mutant mice maintain the normal anatomical distribution and expression levels of CB_1 receptors in the cell types with restored receptors, proves the great potential of these mutants for the study of the CB_1 receptor function in specific brain cell populations. In fact, the rescue strategies have the advantage of the reestablishment and visualization of existing CB_1 receptors levels in glutamatergic neurons, GABAergic neurons and astrocytes more accurately, without the interference of additional cells expressing CB_1 receptors. This is especially important for the anatomical and functional investigation of the endocannabinoid system in cell types or brain areas with sparse CB_1 receptors. Finally, the comprehension of the exact expression and distribution of the CB_1 receptor will not only help to better understand the receptor architecture of the brain, but will also improve the conceptual framework for a more specific pharmacological intervention against complex brain diseases in regions where balanced CB_1 receptors are crucial for brain function.

6.3 CB_1 RECEPTOR EXPRESSION IN GFAPhrGFP-*CB*$_1$-WT MUTANT MICE

Additionally, mutant mice target to express hrGFP into astroglial cells were used in this thesis. In this animal model, the percentage and density (particles/µm) of astrocytic elements expressing CB_1 receptor were higher and more statistically significant when compared with the GFAP-*CB*$_1$-RS mutants using GFAP as a

marker for astrocytes. These results suggest that the expression of CB_1 receptors on astrocytes could actually be higher than in previous observations reported using GFAP as a marker for the identification of the astrocytes (Han et al., 2012; Bosier et al., 2013). A plausible explanation could be based on the different molecular nature of the GFAP and hr-GFP proteins. GFAP is a cytoskeletal protein which is assembled in intermediate filament packet (Inagaki et al., 1994; Eng et al., 2000; Hol and Pekny, 2015), then GFAP immunostaining only shows the main radial processes of the astrocyte. However, hr-GFP is a diffusible protein which fills all the cytoplasmic regions, including the fine processes of astrocytes that are normally lacking GFAP (Nolte et al., 2001), hence, a better detection of astrocytic processes can be accomplished.

6.3.1 TRIPARTITE SYNAPSE: ANATOMICAL INTERPLAY BETWEEN CB_1 RECEPTORS IN ASTROCYTES AND THE NEARBY SYNAPSES

Taking advantage of the better detection of CB_1 receptors in astrocytes of the GFAPhrGFP-*CB*$_1$-WT mouse, we also examined the distance between the astrocytic CB_1 receptor and the nearest synapse in order to put the CB_1 receptors in astrocytes in the anatomical context of the functional tripartite synapse (Navarrete and Araque, 2008, 2010; Navarrete et al., 2013, 2014; Gómez-Gonzalo et al., 2014). It was demonstrated that the endocannabinoids coming from a postsynaptic neuron activate astrocytic CB_1 receptors leading to an increase in the intracellular calcium that triggers a release of astrocytic glutamate, which stimulates a neurotransmitter release in heteroneuronal synapses (Navarrete and Araque, 2008, 2010; Navarrete et al., 2013, 2014; Gómez-Gonzalo et al., 2014).

Glial cells constitute the most abundant cellular population in the central nervous system. Amongst glial cell types, astrocytes are excellent players in brain information processing (Volterra and Meldolesi, 2005), due to the bidirectional communication established with neurons (Araque et al., 2001; Bezzi and Volterra, 2011) through intricate morphological and biochemical interactions. The morphology of astrocytes is particularly complex, suggesting that their structures have important functional roles in brain functions. In rodents, astrocytes are distributed covering non-overlapping domains in the cerebral cortex, where they contact tens of thousands of synapses (Halassa et al., 2007). Astrocytes are in close apposition to the synaptic structures, forming tripartite synapses, and play important roles in maintaining and regulating synaptic physiology (Perez-Alvarez et al., 2014). Functionally, endocannabinoids, through CB_1, promote astroglial differentiation and mediate neuron-astrocyte communication regulating synaptic transmission (Aguado et al., 2006; Navarrete and Araque, 2008, 2010). Furthermore, our laboratories (Han et al., 2012) showed that the impairment of spatial working memory and *in vivo* long-term depression at hippocampal CA3-CA1 synapses, induced by an acute exposure of exogenous cannabinoids, is fully abolished in conditional mutant mice lacking CB_1 receptors in brain astroglial cells but is conserved in mice lacking CB_1 receptors in glutamatergic or GABAergic neurons. Blockade of neuronal glutamate N-methyl-D-aspartate receptors (NMDAR) and of synaptic trafficking of glutamate α-amino-3-hydroxy-5-methyl-isoxazole propionic acid receptors (AMPAR) also abolished cannabinoid effects on spatial working memory and long-term depression induction and expression (Han et al., 2012).

In addition, CB_1 activation in astrocytes is involved in energy supply to the brain. Our findings have revealed that genetic and pharmacological manipulations of the CB_1 receptor expression and activity in cultured cortical and hypothalamic astrocytes demonstrated that cannabinoid signaling controls the levels of leptin receptors expression (Bosier et al., 2013). Lack of CB_1 receptors also markedly impaired leptin-mediated activation of signal transducers and activators of transcription 3 and 5 (STAT3 and STAT5) in astrocytes. In particular, CB_1 deletion determined a basal over activation of STAT5, thereby leading to the downregulation of leptin receptors expression, and leptin failed to regulate STAT5-dependent glycogen storage in the absence of CB_1 receptors in astrocytes (Bosier et al., 2013).

Our present results showed that the most common distance between astrocytic CB_1 receptors and the nearest synapses is in a rank of 400-800 nm. Moreover, most of those synapses were found to be excitatory. Thus, it is tempting to suggest that this distance would represent the distance travelled by the endocannabinoid molecules from the postsynaptic neuron to the CB_1 receptor localized in the astrocyte. According to this interpretation, once inside the astrocyte, the endocannabinoid would activate the astrocytic CB_1 receptor, hence triggering the increase of calcium and stimulate the release of neurotransmitter that modulates synaptic transmission and plasticity. Finally, the fixed anatomical distribution pattern of the astrocytic CB_1 receptors relative to the nearest synapse both in the CA1 stratum radiatum and in the dentate molecular layer suggests the existence of a molecular architecture underlying the functional activity of the astrocytic CB_1 receptors at the tripartite synapse.

7 CONCLUSIONS

The conclusions of the Thesis work are the following:

1. The CB_1 receptor in glutamatergic neurons of the Glu-*CB_1*-RS mouse hippocampus maintains the same levels of expression and localization of the *CB_1*-WT mouse hippocampus.
2. The CB_1 receptor in GABAergic neurons of the GABA-*CB_1*-RS mouse hippocampus maintains the same levels of expression and localization of the *CB_1*-WT mouse hippocampus.
3. The CB_1 receptor in astrocytes of the GFAP-*CB_1*-RS mouse hippocampus maintains the same levels of expression and localization of the *CB_1*-WT mouse hippocampus.
4. The detection of CB_1 receptors in astrocytes of the GFAPhrGFP-*CB_1*-WT mouse hippocampus is significantly higher than in *CB_1*-WT mouse hippocampus with GFAP as an astrocytic marker.
5. The most common distance between the astrocytic CB_1 receptors and the nearest synapses in the hippocampus, is between 400-800 nm.
6. The majority of the CA1 and dentate molecular layer synapses surrounded by CB_1 receptor immunopositive astrocytes in the 400-800 nm range are of excitatory nature.
7. The CB_1 receptor rescue mutant mice characterized in this Doctoral Thesis have proven: 1) to express CB_1 receptors in specific brain cell types; 2) the re-expression is limited to the particular neuronal populations or to astrocytes; 3) the endogenous levels of CB_1 receptors are maintained in the brain cell types re-expressing the receptor.

8. Altogether, the studied CB_1 receptor rescue mutant mice are excellent tools for functional and translational investigations on the role of the CB_1 receptors in the normal and diseased brain.

8 ABREVIATIONS

- 2-AG: 2-arachidonoylglycerol.
- AA: Arachidonic acid.
- ABHD12: α/β-hydrolase domain containing 12.
- ABHD6: α/β-hydrolase domain containing 6.
- AC: Adenylate cyclase.
- AEA: N-arachidonoylethanolamine or anandamide.
- AMPAR: α-amino-3-hydroxy-5-methyl-isoxazole propionic acid receptor.
- Amyg: Amygdala.
- AON: Anterior olfactory nucleus.
- as: Astrocyte.
- Astro: Astrocytic.
- CA: Cornu ammonis or Ammon´s horn.
- CA1: Region 1 of Cornu Ammonis.
- CA2: Region 2 of Cornu Ammonis.
- CA3: Region 3 of Cornu Ammonis.
- Cb: Cerebellar cortex.
- CB_1: Cannabionid type I receptor
- *CB_1*-KO: Cannabinoid type-1 receptor knock-out mouse.
- *CB_1*-WT: Cannabinoid type-1 receptor wild type mouse.
- *CB_2*: Cannabionid type 2 receptor.
- CNS: Central Nervous System.
- CPu: Caudate putamen.
- Cx: Cortex.
- DAB: Diaminobezidine.
- den: Dendrite.
- DG: Dentate gyrus.
- DG: Diacylglycerol.
- DGL: Diacylglycerol lipase.
- DSE: Depolarization-induced supression of excitation.
- DSI: Depolarization-induced suppression of inhibition.
- eCB-LTD: Endocannabinoid-mediated long-term depression.
- eCBs: Endocannabinoids.
- eCB-STD: Endocannabinoid-mediated short-term depression.
- EP: Entopeduncular nucleus.
- EXCIT: Excitatory.
- FAAH: Fatty acid amide hydrolase.
- GABA: Gamma-Aminobutyric acid.
- GABA-*CB_1*-KO: GABAergic neurons cannabinoid type-1 receptor knock-out mouse.
- GABA-*CB_1*-RS: GABAergic neurons cannabinoid type-1 receptor rescue mouse
- GFAP: Glial Fibrillary Acidic Protein.
- GFAP-*CB_1*-KO: Astrocyte cannabinoid type-1 receptor knock-out mouse
- GFAP-*CB_1*-RS: Astrocyte cannabinoid type-1 receptor rescue mouse
- GFAPhrGFP-*CB_1*-KO: *CB_1*-KO mouse that express hrGFP in astrocytes.

- GFAPhrGFP-*CB$_1$*-WT: *CB$_1$*-WT mouse that express hrGFP in astrocytes.
- GFP: Green Fluorescence Protein.
- Glu-*CB$_1$*-KO: Dorsal telencephalic glutamatergic neurons cannabinoid type-1 receptor knock-out mouse.
- Glu-*CB$_1$*-RS: Dorsal telencephalic neurons cannabinoid type-1 receptor rescue mouse.
- GP: Globus pallidus.
- GPCRs: G protein coupled receptors.
- GrDG: Granular dentate gyrus.
- Hi: Hippocampus.
- INHIB: Inhibitory.
- LEA: Lateral entorhinal cortex.
- LMol: Lacunosum moleculare,
- LTD: Long-term depression.
- LTP: Long-term potentiation.
- M1: Primary motor cortex.
- MAGL: Monoacylglicerol lipase.
- MEA: Medial Entorhinal Cortex.
- mGluR: Metabotropic glutamate receptors.
- Mid: Midbrain.
- MO: Medulla oblongata.
- MoDG: Molecular dentate gyrus.
- NAc: Nucleus accumbens.
- NAPE: N-arachidonoyl phosphatidylethanolamine.
- NAPE-PLD: N-acyl phosphatidylethanolamine especific phospholipase D.
- NAT: N-acyltransferase.
- NMDAR: N-Methyl-D-aspartate receptor.
- NOS: Nitric oxide synthase.
- OEA: Oleoylethanolamine.
- Or: Stratum oriens.
- OT: Olfactory tubercle.
- PART: Particles.
- PaS: Parasubiculum.
- PEA: Palmitoylethanolamine.
- PFCx: Prefrontal cortex.
- Pir: Piriform cortex.
- PLC: Phospholipase C.
- Po: Pons.
- PoDG: Polymorph dentate gyrus.
- PPAR: Peroxisome Proliferator-Activated Receptor.
- PROC: Processes.
- PrS: Presubiculum.
- Py: Pyramidal cell hippocampus.
- Rad: Stratum radiatum.

- RECEP: Receptor.
- S1: Primary somatosensory cortex.
- SLu: Stratum lucidum.
- SNR: Substantia nigra pars reticulata.
- sp: Dendritic spine.
- STAT: Signal transducer and activator of transcription.
- STOP-*CB_1*: mouse carrying a loxP-flanked stop cassette inserted in the 5'UTR upstream of the CB1 receptor translational start codon.
- Str: Striatum.
- Sub: The subiculum.
- TER: Terminals.
- Th: Thalamus.
- TRPA1: Transient Receptor Potential Ankyrin 1.
- TRPV1: Transient Receptor Potential Vanilloid 1.
- V1: Primary visual cortex.
- VIP: Vasoactive intestinal polypeptide.
- VP: Ventral pallidum.
- WT: Wild type.
- Δ9-THC or THC: Delta (9) - tetrahydrocannabinol.

9 BIBLIOGRAPHY

Aguado T, Monory K, Palazuelos J, Stella N, Cravatt B, Lutz B, Marsicano G, Kokaia Z, Guzmán M, Galve-Roperh I. 2005. The endocannabinoid system drives neural progenitor proliferation. FASEB J 19:1704–6.

Aguado T, Palazuelos J, Monory K, Stella N, Cravatt B, Lutz B, Marsicano G, Kokaia Z, Guzmán M, Galve-Roperh I. 2006. The endocannabinoid system promotes astroglial differentiation by acting on neural progenitor cells. J Neurosci 26:1551–61.

Aika Y, Ren JQ, Kosaka K, Kosaka T. 1994. Quantitative analysis of GABA-like-immunoreactive and parvalbumin-containing neurons in the CA1 region of the rat hippocampus using a stereological method, the disector. Exp brain Res 99:267–76.

Akirav I. 2011. The role of cannabinoids in modulating emotional and non-emotional memory processes in the hippocampus. Front Behav Neurosci 5:34.

Alhouayek M, Masquelier J, Muccioli GG. 2014. Controlling 2-arachidonoylglycerol metabolism as an anti-inflammatory strategy. Drug Discov Today 19:295–304.

Amaral DG, Dolorfo C, Alvarez-Royo P. 1991. Organization of CA1 projections to the subiculum: a PHA-L analysis in the rat. Hippocampus 1:415–35.

Amaral DG, Ishizuka N, Claiborne B. 1990. Neurons, numbers and the hippocampal network. Prog Brain Res 83:1–11.

Amaral DG. 1978. A Golgi study of cell types in the hilar region of the hippocampus in the rat. J Comp Neurol 182:851–914.

Ameri A. 1999. The effects of cannabinoids on the brain. Prog Neurobiol 58:315–48.

Araque A, Carmignoto G, Haydon PG. 2001. Dynamic Signaling Between Astrocytes and Neurons. Annu Rev Physiol 63:795–813.

Araque A, Parpura V, Sanzgiri RP, Haydon PG. 1999. Tripartite synapses: glia, the unacknowledged partner. Trends Neurosci 22:208–15.

Bakst I, Avendano C, Morrison JH, Amaral DG. 1986. An experimental analysis of the origins of somatostatin-like immunoreactivity in the dentate gyrus of the rat. J Neurosci 6:1452–62.

Balthasar N, Dalgaard LT, Lee CE, Yu J, Funahashi H, Williams T, Ferreira M, Tang V, McGovern RA, Kenny CD, Christiansen LM, Edelstein E, Choi B, Boss O, Aschkenasi C, Zhang C, Mountjoy K, Kishi T, Elmquist JK, Lowell BB. 2005. Divergence of melanocortin pathways in the control of food intake and energy expenditure. Cell 123:493–505.

Bartholomä A, Nave KA. 1994. NEX-1: a novel brain-specific helix-loop-helix protein with autoregulation and sustained expression in mature cortical neurons. Mech Dev 48:217–28.

Basavarajappa BS, Subbanna S. 2014. CB1 receptor-mediated signaling underlies the hippocampal synaptic, learning, and memory deficits following treatment with JWH-081, a new component of spice/K2 preparations. Hippocampus

24:178–88.

Bélanger M, Magistretti PJ. 2009. The role of astroglia in neuroprotection. Dialogues Clin Neurosci 11:281–95.

Bellocchio L, Lafenêtre P, Cannich A, Cota D, Puente N, Grandes P, Chaouloff F, Piazza PV, Marsicano G. 2010. Bimodal control of stimulated food intake by the endocannabinoid system. Nat Neurosci 13:281–3.

Bénard G, Massa F, Puente N, Lourenço J, Bellocchio L, Soria-Gómez E, Matias I, Delamarre A, Metna-Laurent M, Cannich A, Hebert-Chatelain E, Mulle C, Ortega-Gutiérrez S, Martín-Fontecha M, Klugmann M, Guggenhuber S, Lutz B, Gertsch J, Chaouloff F, López-Rodríguez ML, Grandes P, Rossignol R, Marsicano G. 2012. Mitochondrial CB_1 receptors regulate neuronal energy metabolism. Nat Neurosci 15:558–64.

Benito C, Romero JP, Tolón RM, Clemente D, Docagne F, Hillard CJ, Guaza C, Romero J. 2007. Cannabinoid CB1 and CB2 receptors and fatty acid amide hydrolase are specific markers of plaque cell subtypes in human multiple sclerosis. J Neurosci 27:2396–402.

Bezzi P, Volterra A. 2011. Astrocytes: Powering Memory. Cell 144:644–45.

Blankman JL, Simon GM, Cravatt BF. 2007. A comprehensive profile of brain enzymes that hydrolyze the endocannabinoid 2-arachidonoylglycerol. Chem Biol 14:1347–56.

Blasco-Ibáñez JM, Freund TF. 1997. Distribution, ultrastructure, and connectivity of calretinin-immunoreactive mossy cells of the mouse dentate gyrus. Hippocampus 7:307–20.

Block RI, Farinpour R, Braverman K. 1992. Acute effects of marijuana on cognition: relationships to chronic effects and smoking techniques. Pharmacol Biochem Behav 43:907–17.

Bosier B, Bellocchio L, Metna-Laurent M, Soria-Gomez E, Matias I, Hebert-Chatelain E, Cannich A, Maitre M, Leste-Lasserre T, Cardinal P, Mendizabal-Zubiaga J, Canduela MJ, Reguero L, Hermans E, Grandes P, Cota D, Marsicano G. 2013. Astroglial CB1 cannabinoid receptors regulate leptin signaling in mouse brain astrocytes. Mol Metab 2:393–404.

Bosier B, Muccioli GG, Hermans E, Lambert DM. 2010. Functionally selective cannabinoid receptor signaling: therapeutic implications and opportunities. Biochem Pharmacol 80:1–12.

Bouaboula M, Bourrie B, Rinaldi-Carmona M, Shire D, Fur GL, Casellas P. 1995a. Stimulation of Cannabinoid Receptor CB1 Induces krox-24 Expression in Human Astrocytoma Cells. J Biol Chem 270:13973–80.

Bouaboula M, Poinot-Chazel C, Bourrié B, Canat X, Calandra B, Rinaldi-Carmona M, Le Fur G, Casellas P. 1995b. Activation of mitogen-activated protein kinases by stimulation of the central cannabinoid receptor CB1. Biochem 312(Pt 2): 637–41.

Buckmaster PS, Strowbridge BW, Schwartzkroin PA. 1993. A comparison of rat hippocampal mossy cells and CA3c pyramidal cells. J Neurophysiol 70:1281–

99.

Busquets-Garcia A, Desprez T, Metna-Laurent M, Bellocchio L, Marsicano G, Soria-Gomez E. 2015. Dissecting the cannabinergic control of behavior: The where matters. Bioessays 37:1215–25.

Cabral GA, Ferreira GA, Jamerson MJ. 2015. Endocannabinoids and the Immune System in Health and Disease. Endocannabinoids, Handb Exp Pharmacol. Springer International Publishing. 185-211

Cadas H, Gaillet S, Beltramo M, Venance L, Piomelli D. 1996. Biosynthesis of an endogenous cannabinoid precursor in neurons and its control by calcium and cAMP. JNeurosci 16:3934–42.

Campbell KA, Foster TC, Hampson RE, Deadwyler SA. 1986. delta 9-Tetrahydrocannabinol differentially affects sensory-evoked potentials in the rat dentate gyrus. J Pharmacol Exp Ther 239:936–40.

Carlson G, Wang Y, Alger BE. 2002. Endocannabinoids facilitate the induction of LTP in the hippocampus. Nat Neurosci 5:723–4.

Castillo PE, Younts TJ, Chávez AE, Hashimotodani Y. 2012. Endocannabinoid signaling and synaptic function. Neuron 76:70–81.

Castillo PE. 2012. Presynaptic LTP and LTD of excitatory and inhibitory synapses. Cold Spring Harb Perspect Biol 1;4(2).

Celio MR. 1990. Calbindin D-28k and parvalbumin in the rat nervous system. Neuroscience 35:375–475.

Cenquizca LA, Swanson LW. 2007. Spatial organization of direct hippocampal field CA1 axonal projections to the rest of the cerebral cortex. Brain Res Rev 56:1–26.

Chait LD, Perry JL. 1994. Acute and residual effects of alcohol and marijuana, alone and in combination, on mood and performance. Psychopharmacology (Berl) 115:340–9.

Chalfie M. 1995. GREEN FLUORESCENT PROTEIN. Photochem Photobiol 62:651–6.

Chevaleyre V, Castillo PE. 2003. Heterosynaptic LTD of hippocampal GABAergic synapses: a novel role of endocannabinoids in regulating excitability. Neuron 38:461–72.

Chevaleyre V, Castillo PE. 2004. Endocannabinoid-mediated metaplasticity in the hippocampus. Neuron 43:871–81.

Chevaleyre V, Takahashi KA, Castillo PE. 2006. Endocannabinoid-mediated synaptic plasticity in the CNS. Annu Rev Neurosci 29:37–76.

Chiarlone A, Bellocchio L, Blázquez C, Resel E, Soria-Gómez E, Cannich A, Ferrero JJ, Sagredo O, Benito C, Romero J, Sánchez-Prieto J, Lutz B, Fernández-Ruiz J, Galve-Roperh I, Guzmán M. 2014. A restricted population of CB1 cannabinoid receptors with neuroprotective activity. Proc Natl Acad Sci U S A 111 (22):8257-62

Coiret G, Ster J, Grewe B, Wendling F, Helmchen F, Gerber U, Benquet P. 2012. Neuron to astrocyte communication via cannabinoid receptors is necessary for sustained epileptiform activity in rat hippocampus. PLoS One 7:e37320.

Costa B, Comelli F, Bettoni I, Colleoni M, Giagnoni G. 2008. The endogenous fatty acid amide, palmitoylethanolamide, has anti-allodynic and anti-hyperalgesic effects in a murine model of neuropathic pain: involvement of CB1, TRPV1 and PPARgamma receptors and neurotrophic factors. Pain 139:541–50.

Court JM. 1998. Cannabis and brain function. J Paediatr Child Health 34:1–5.

De-May CL, Ali AB. 2013. Cell type-specific regulation of inhibition via cannabinoid type 1 receptors in rat neocortex. J Neurophysiol 109:216–24.

Derkinderen P, Toutant M, Burgaya F, Le Bert M, Siciliano JC, de Franciscis V, Gelman M, Girault JA. 1996. Regulation of a neuronal form of focal adhesion kinase by anandamide. Science 273:1719–22.

Desmond NL, Levy WB. 1982. A quantitative anatomical study of the granule cell dendritic fields of the rat dentate gyrus using a novel probabilistic method. J Comp Neurol 212:131–45.

Desmond NL, Levy WB. 1985. Granule cell dendritic spine density in the rat hippocampus varies with spine shape and location. Neurosci Lett 54:219–24.

Devane WA, Dysarz FA, Johnson MR, Melvin LS, Howlett AC. 1988. Determination and characterization of a cannabinoid receptor in rat brain. Mol Pharmacol 34:605–13.

Devane WA, Hanus L, Breuer A, Pertwee RG, Stevenson LA, Griffin G, Gibson D, Mandelbaum A, Etinger A, Mechoulam R. 1992. Isolation and structure of a brain constituent that binds to the cannabinoid receptor. Science 258:1946–9.

Dinh TP, Carpenter D, Leslie FM, Freund TF, Katona I, Sensi SL, Kathuria S, Piomelli D. 2002. Brain monoglyceride lipase participating in endocannabinoid inactivation. Proc Natl Acad Sci U S A 99:10819–24.

Domenici MR, Azad SC, Marsicano G, Schierloh A, Wotjak CT, Dodt H-U, Zieglgänsberger W, Lutz B, Rammes G. 2006. Cannabinoid receptor type 1 located on presynaptic terminals of principal neurons in the forebrain controls glutamatergic synaptic transmission. J Neurosci 26:5794–9.

Dong H-W, Swanson LW, Chen L, Fanselow MS, Toga AW. 2009. Genomic–anatomic evidence for distinct functional domains in hippocampal field CA1. Proc Natl Acad Sci U S A 106:11794–9.

Egertová M, Cravatt B., Elphick M. 2003. Comparative analysis of fatty acid amide hydrolase and cb1 cannabinoid receptor expression in the mouse brain: evidence of a widespread role for fatty acid amide hydrolase in regulation of endocannabinoid signaling. Neuroscience 119:481–96.

Egertová M, Elphick MR. 2000. Localisation of cannabinoid receptors in the rat brain using antibodies to the intracellular C-terminal tail of CB. J Comp Neurol 422:159–71.

Egertová M, Giang DK, Cravatt BF, Elphick MR. 1998. A new perspective on

cannabinoid signaling: complementary localization of fatty acid amide hydrolase and the CB1 receptor in rat brain. Proc Biol Sci 265:2081–5.

Elphick MR, Egertová M. 2005. The phylogenetic distribution and evolutionary origins of endocannabinoid signaling. Handb Exp Pharmacol. Springer Berlin Heidelberg 283-97

Eng LF, Ghirnikar RS, Lee YL. 2000. Glial Fibrillary Acidic Protein: GFAP-Thirty-One Years (1969–2000). Neurochem Res 25:1439–51.

Eng LF. 1985. Glial fibrillary acidic protein (GFAP): the major protein of glial intermediate filaments in differentiated astrocytes. J Neuroimmunol 8:203–14.

Fanselow M, Dong H-W. 2010. Are the Dorsal and Ventral Hippocampus functionally distinct structures. Neuron 65:1–25.

Fernández-Ruiz J, Romero J, Ramos JA. 2015. Endocannabinoids and Neurodegenerative Disorders: Parkinson's Disease, Huntington's Chorea, Alzheimer's Disease, and Others. Handb Exp Pharmacol. Springer International Publishing. 231:233–59

Fernández-Ruiz J. 2010. The endocannabinoid system as a target for the treatment of motor dysfunction. Br J Pharmacol 156:1029–40.

Finch DM, Nowlin NL, Babb TL. 1983. Demonstration of axonal projections of neurons in the rat hippocampus and subiculum by intracellular injection of HRP. Brain Res 271:201–16.

De Francesco PN, Valdivia S, Cabral A, Reynaldo M, Raingo J, Sakata I, Osborne-Lawrence S, Zigman JM, Perelló M. 2015. Neuroanatomical and functional characterization of CRF neurons of the amygdala using a novel transgenic mouse model. Neuroscience 289:153–65.

Franklin KBJ, Paxinos G. 2008. The mouse brain in stereotaxic coordinates. Elsevier.

Freund TF, Katona I, Piomelli D. 2003. Role of endogenous cannabinoids in synaptic signaling. Physiol Rev 83:1017–66.

Fride E, Mechoulam R. 1993. Pharmacological activity of the cannabinoid receptor agonist, anandamide, a brain constituent. Eur J Pharmacol 231:313–4.

Frotscher M, Seress L, Schwerdtfeger WK, Buhl E. 1991. The mossy cells of the fascia dentata: a comparative study of their fine structure and synaptic connections in rodents and primates. J Comp Neurol 312:145–63.

Frotscher M, Soriano E, Misgeld U. 1994. Divergence of hippocampal mossy fibers. Synapse 16:148–60.

Fu J, Gaetani S, Oveisi F, Lo Verme J, Serrano A, Rodríguez De Fonseca F, Rosengarth A, Luecke H, Di Giacomo B, Tarzia G, Piomelli D. 2003. Oleylethanolamide regulates feeding and body weight through activation of the nuclear receptor PPAR-alpha. Nature 425:90–3.

Fujise N, Kosaka T. 1999. Mossy cells in the mouse dentate gyrus: identification in the dorsal hilus and their distribution along the dorsoventral axis. Brain Res

816:500–11.

Galve-Roperh I, Chiurchiù V, Díaz-Alonso J, Bari M, Guzmán M, Maccarrone M. 2013. Cannabinoid receptor signaling in progenitor/stem cell proliferation and differentiation. Prog Lipid Res 52:633–50.

Gao Y, Vasilyev D V, Goncalves MB, Howell F V, Hobbs C, Reisenberg M, Shen R, Zhang M-Y, Strassle BW, Lu P, Mark L, Piesla MJ, Deng K, Kouranova E V, Ring RH, Whiteside GT, Bates B, Walsh FS, Williams G, Pangalos MN, Samad TA, Doherty P. 2010. Iiu. J Neurosci 30:2017–24.

Gaoni Y, Mechoulam R. 1964. Isolation, structure and partial synthesis of an active constituent of hashish. J Am Chem Soc 86:1646–47.

Garcia-Ovejero D, Arevalo-Martin A, Petrosino S, Docagne F, Hagen C, Bisogno T, Watanabe M, Guaza C, Di Marzo V, Molina-Holgado E. 2009. The endocannabinoid system is modulated in response to spinal cord injury in rats. Neurobiol Dis 33:57–71.

Gifford AN, Samiian L, Gatley SJ, Ashby CR. 1997a. Examination of the effect of the cannabinoid receptor agonist, CP 55,940, on electrically evoked transmitter release from rat brain slices. Eur J Pharmacol 324:187–92.

Gifford AN, Tang Y, Gatley SJ, Volkow ND, Lan R, Makriyannis A. 1997b. Effect of the cannabinoid receptor SPECT agent, AM 281, on hippocampal acetylcholine release from rat brain slices. Neurosci Lett 238:84–6.

Gomez O, Arevalo-Martin A, Garcia-Ovejero D, Ortega-Gutierrez S, Cisneros JA, Almazan G, Sánchez-Rodriguez MA, Molina-Holgado F, Molina-Holgado E. 2010. The constitutive production of the endocannabinoid 2-arachidonoylglycerol participates in oligodendrocyte differentiation. Glia 58:1913–27.

Gómez-Gonzalo M, Navarrete M, Perea G, Covelo A, Martín-Fernández M, Shigemoto R, Luján R, Araque A. 2014. Endocannabinoids Induce Lateral Long-Term Potentiation of Transmitter Release by Stimulation of Gliotransmission. Cereb Cortex 25(10):3699-712.

Gulyás AI, Megías M, Emri Z, Freund TF. 1999. Total number and ratio of excitatory and inhibitory synapses converging onto single interneurons of different types in the CA1 area of the rat hippocampus. J Neurosci 19:10082–97.

Gulyás AI, Miettinen R, Jacobowitz DM, Freund TF. 1992. Calretinin is present in non-pyramidal cells of the rat hippocampus--I. A new type of neuron specifically associated with the mossy fibre system. Neuroscience 48:1–27.

Gulyás AI, Tóth K, Dános P, Freund TF. 1991. Subpopulations of GABAergic neurons containing parvalbumin, calbindin D28k, and cholecystokinin in the rat hippocampus. J Comp Neurol 312:371–8.

Gutiérrez-Rodríguez A, Puente N, Elezgarai I, Ruehle S, Lutz B, Reguero L, Gerrikagoitia I, Marsicano G, Grandes P. 2016. Anatomical characterization of the cannabinoid cb 1 receptor in cell type-specific mutant mouse rescue models. J Comp Neurol. 10.1002/cne.24066

Guzmán M, Sánchez C, Galve-Roperh I. 2001. Control of the cell survival/death

decision by cannabinoids. J Mol Med 78:613–25.

Hadaczek P, Forsayeth J, Mirek H, Munson K, Bringas J, Pivirotto P, McBride JL, Davidson BL, Bankiewicz KS. 2009. Transduction of nonhuman primate brain with adeno-associated virus serotype 1: vector trafficking and immune response. Hum Gene Ther 20:225–37.

Hájos N, Katona I, Naiem SS, MacKie K, Ledent C, Mody I, Freund TF. 2000. Cannabinoids inhibit hippocampal GABAergic transmission and network oscillations. Eur J Neurosci 12:3239–49.

Halassa MM, Fellin T, Takano H, Dong J-H, Haydon PG. 2007. Synaptic islands defined by the territory of a single astrocyte. J Neurosci 27:6473–7.

Halasy K, Somogyi P. 1993. Subdivisions in the multiple GABAergic innervation of granule cells in the dentate gyrus of the rat hippocampus. Eur J Neurosci 5:411–29.

Hampson RE, Deadwyler SA. 1999. Cannabinoids, hippocampal function and memory. Life Sci 65:715–23.

Han J, Kesner P, Metna-Laurent M, Duan T, Xu L, Georges F, Koehl M, Abrous DN, Mendizabal-Zubiaga J, Grandes P, Liu Q, Bai G, Wang W, Xiong L, Ren W, Marsicano G, Zhang X. 2012. Acute cannabinoids impair working memory through astroglial CB1 receptor modulation of hippocampal LTD. Cell 148:1039–50.

Häring M, Marsicano G, Lutz B, Monory K. 2007. Identification of the cannabinoid receptor type 1 in serotonergic cells of raphe nuclei in mice. Neuroscience 146:1212–9. Hashimotodani Y, Ohno-Shosaku T, Tsubokawa H, Ogata H, Emoto K, Maejima T, Araishi K, Shin H-S, Kano M. 2005. Phospholipase Cbeta serves as a coincidence detector through its Ca2+ dependency for triggering retrograde endocannabinoid signal. Neuron 45:257–68.

Haydon PG, Carmignoto G. 2006. Astrocyte control of synaptic transmission and neurovascular coupling. Physiol Rev 86:1009–31.

Hazlett JC, Farkas N. 1978. Short axon molecular layer neurons in the opossum fascia dentata: a Golgi study. Brain Res 143:355–60.

Hebert-Chatelain E, Reguero L, Puente N, Lutz B, Chaouloff F, Rossignol R, Piazza P-V, Benard G, Grandes P, Marsicano G. 2014a. Studying mitochondrial CB1 receptors: Yes we can. Mol Metab 3:339.

Hebert-Chatelain E, Reguero L, Puente N, Lutz B, Chaouloff F, Rossignol R, Piazza P-V, Benard G, Grandes P, Marsicano G. 2014b. Cannabinoid control of brain bioenergetics: Exploring the subcellular localization of the CB1 receptor. Mol Metab 3:495–504.

Heishman SJ, Arasteh K, Stitzer ML. 1997. Comparative effects of alcohol and marijuana on mood, memory, and performance. Pharmacol Biochem Behav 58:93–101.

Herkenham M, Groen BG, Lynn AB, De Costa BR, Richfield EK. 1991. Neuronal localization of cannabinoid receptors and second messengers in mutant mouse cerebellum. Brain Res 552:301–10.

Herkenham M, Lynn AB, Little MD, Johnson MR, Melvin LS, de Costa BR, Rice KC. 1990. Cannabinoid receptor localization in brain. Proc Natl Acad Sci U S A 87:1932–6.

Heyser CJ, Hampson RE, Deadwyler SA. 1993. Effects of delta-9-tetrahydrocannabinol on delayed match to sample performance in rats: alterations in short-term memory associated with changes in task specific firing of hippocampal cells. J Pharmacol Exp Ther 264:294–307.

Hirrlinger PG, Scheller A, Braun C, Hirrlinger J, Kirchhoff F. 2006. Temporal Control of Gene Recombination in Astrocytes by Transgenic Expression of the Tamoxifen-Inducible DNA Recombinase Variant CreERT2. Glia 54(1):11-20.

Hol EM, Pekny M. 2015. Glial fibrillary acidic protein (GFAP) and the astrocyte intermediate filament system in diseases of the central nervous system. Curr Opin Cell Biol 32:121–30.

Howlett AC, Barth F, Bonner TI, Cabral G, Casellas P, Devane WA, Felder CC, Herkenham M, Mackie K, Martin BR, Mechoulam R, Pertwee RG. 2002. International Union of Pharmacology. XXVII. Classification of Cannabinoid Receptors. Pharmacol Rev 54:161–202.

Howlett AC, Bidaut-Russell M, Devane WA, Melvin LS, Johnson MR, Herkenham M. 1990. The cannabinoid receptor: biochemical, anatomical and behavioral characterization. Trends Neurosci 13:420–3.

Hu SS-J, Mackie K. 2015. Distribution of the Endocannabinoid System in the Central Nervous System. Handb Exp Pharmacol, Endocannabinoids. Springer International Publishing 231:59-93

Inagaki M, IMakamura Y, Takeda M, Nishimura T, Inagaki N. 1994. Glial Fibrillary Acidic Protein: Dynamic Property and Regulation by Phosphorylation. Brain Pathol 4:239–43.

Jinno S, Kosaka T. 2000. Colocalization of parvalbumin and somatostatin-like immunoreactivity in the mouse hippocampus: quantitative analysis with optical dissector. J Comp Neurol 428:377–88.

Jinno S, Kosaka T. 2006. Cellular architecture of the mouse hippocampus: a quantitative aspect of chemically defined GABAergic neurons with stereology. Neurosci Res 56:229–45.

Jonquieres G von, Mersmann N, Klugmann CB, Harasta AE, Lutz B, Teahan O, Housley GD, Fro¨hlich D, Kra¨mer-Albers E-M, Klugmann M. 2013. Glial Promoter Selectivity following AAV-Delivery to the Immature Brain. PLoS One 8:e65646

Kamprath K, Plendl W, Marsicano G, Deussing JM, Wurst W, Lutz B, Wotjak CT. 2009. Endocannabinoids mediate acute fear adaptation via glutamatergic neurons independently of corticotropin-releasing hormone signaling. Genes Brain Behav 8:203–11.

Kano M, Ohno-Shosaku T, Hashimotodani Y, Uchigashima M, Watanabe M. 2009. Endocannabinoid-mediated control of synaptic transmission. Physiol Rev 89:309–80.

Kano M. 2014. Control of synaptic function by endocannabinoid-mediated retrograde signaling. Proc Jpn Acad Ser B Phys Biol Sci 90:235–50.

Katona I, Freund TF. 2012. Multiple functions of endocannabinoid signaling in the brain. Annu Rev Neurosci 35:529–58

Katona I, Sperlágh B, Maglóczky Z, Sántha E, Köfalvi A, Czirják S, Mackie K, Vizi E. S, Freund TF. 2000. GABAergic interneurons are the targets of cannabinoid actions in the human hippocampus. Neuroscience 100:797–804.

Katona I, Sperlágh B, Sík A, Käfalvi A, Vizi ES, Mackie K, Freund TF, Sperlagh B, Sik A, Kafalvi A. 1999. Presynaptically Located CB1 Cannabinoid Receptors Regulate GABA Release from Axon Terminals of Specific Hippocampal Interneurons. J Neurosci 19:4544–58.

Katona I, Urbán GM, Wallace M, Ledent C, Jung K-M, Piomelli D, Mackie K, Freund TF. 2006. Molecular composition of the endocannabinoid system at glutamatergic synapses. J Neurosci 26:5628–37.

Katona I. 2015. Cannabis and Endocannabinoid Signaling in Epilepsy. Handb Exp Pharmacol. Springer International Publishing 231:285-316

Kawamura Y, Fukaya M, Maejima T, Yoshida T, Miura E, Watanabe M, Ohno-Shosaku T, Kano M. 2006. The CB1 cannabinoid receptor is the major cannabinoid receptor at excitatory presynaptic sites in the hippocampus and cerebellum. J Neurosci 26:2991–3001.

Kerr N, Holmes FE, Hobson S-A, Vanderplank P, Leard A, Balthasar N, Wynick D. 2015. The generation of knock-in mice expressing fluorescently tagged galanin receptors 1 and 2. Mol Cell Neurosci 68:258–71.

Klausberger T, Somogyi P. 2008. Neuronal diversity and temporal dynamics: the unity of hippocampal circuit operations. Science 321:53–7.

Kleppisch T, Wolfsgruber W, Feil S, Allmann R, Wotjak CT, Goebbels S, Nave K-A, Hofmann F, Feil R. 2003. Hippocampal cGMP-dependent protein kinase I supports an age- and protein synthesis-dependent component of long-term potentiation but is not essential for spatial reference and contextual memory. J Neurosci 23:6005–12.

Koch M, Varela L, Kim JG, Kim JD, Hernández-Nuño F, Simonds SE, Castorena CM, Vianna CR, Elmquist JK, Morozov YM, Rakic P, Bechmann I, Cowley MA, Szigeti-Buck K, Dietrich MO, Gao X-B, Diano S, Horvath TL. 2015. Hypothalamic POMC neurons promote cannabinoid-induced feeding. Nature 519:45–50.

Kosaka T. 1983. Axon initial segments of the granule cell in the rat dentate gyrus: synaptic contacts on bundles of axon initial segments. Brain Res 274:129–34.

Kreitzer AC, Regehr WG. 2001. Retrograde Inhibition of Presynaptic Calcium Influx by Endogenous Cannabinoids at Excitatory Synapses onto Purkinje Cells. Neuron 29:717–27.

Laurberg S. 1979. Commissural and intrinsic connections of the rat hippocampus. J Comp Neurol 184:685–708.

Lee TTY, Hill MN, Lee FS. 2015. Developmental regulation of fear learning and anxiety behavior by endocannabinoids. Genes, Brain Behav:108–24.

Li XG, Somogyi P, Ylinen A, Buzsaki G. 1994. The hippocampal CA3 network: An in vivo intracellular labeling study. J Comp Neurol 339:181–208.

Liu J, Wang L, Harvey-White J, Osei-Hyiaman D, Razdan R, Gong Q, Chan AC, Zhou Z, Huang BX, Kim H-Y, Kunos G. 2006. A biosynthetic pathway for anandamide. Proc Natl Acad Sci U S A 103:13345–50.

Lorente De Nó R. 1934. Studies on the structure of the cerebral cortex. II. Continuation of the study of the ammonic system. J für Psychol und Neurol 46:113–77.

Lu H-C, Mackie K. 2016. An Introduction to the Endogenous Cannabinoid System. Biol Psychiatry 79(7):516-25.

Ludányi A, Eross L, Czirják S, Vajda J, Halász P, Watanabe M, Palkovits M, Maglóczky Z, Freund TF, Katona I. 2008. Downregulation of the CB1 cannabinoid receptor and related molecular elements of the endocannabinoid system in epileptic human hippocampus. J Neurosci 28:2976–90.

Maccarrone M, Rossi S, Bari M, De Chiara V, Fezza F, Musella A, Gasperi V, Prosperetti C, Bernardi G, Finazzi-Agrò A, Cravatt BF, Centonze D. 2008. Anandamide inhibits metabolism and physiological actions of 2-arachidonoylglycerol in the striatum. Nat Neurosci 11:152–9.

Mackie K. 2005. Distribution of cannabinoid receptors in the central and peripheral nervous system. Handb Exp Pharmacol. Springer Berlin Heidelberg (168):299-325.

Magistretti PJ, Pellerin L. 1999. Cellular mechanisms of brain energy metabolism and their relevance to functional brain imaging. Philos Trans R Soc Lond B Biol Sci 354:1155–63.

Mailleux P, Vanderhaeghen J-J. 1992. Distribution of neuronal cannabinoid receptor in the adult rat brain: A comparative receptor binding radioautography and in situ hybridization histochemistry. Neuroscience 48:655–68.

Marsicano G, Goodenough S, Monory K, Hermann H, Eder M, Cannich A, Azad SC, Cascio MG, Gutiérrez SO, van der Stelt M, López-Rodriguez ML, Casanova E, Schütz G, Zieglgänsberger W, Di Marzo V, Behl C, Lutz B. 2003. CB1 cannabinoid receptors and on-demand defense against excitotoxicity. Science 302:84–8.

Marsicano G, Kuner R. 2008. Anatomical Distribution of Receptors, Ligands and Enzymes in the Brain and in the Spinal Cord: Circuitries and Neurochemistry. Cannabinoids and the Brain. Springer

Marsicano G, Lutz B. 1999. Expression of the cannabinoid receptor CB1 in distinct neuronal subpopulations in the adult mouse forebrain. Eur J Neurosci 11:4213–25.

Marsicano G, Lutz B. 2006. Neuromodulatory functions of the endocannabinoid system. J Endocrinol Invest 29:27–46.

Marsicano G, Wotjak CT, Azad SC, Bisogno T, Rammes G, Cascio MG, Hermann H, Tang J, Hofmann C, Zieglgänsberger W, Di Marzo V, Lutz B. 2002. The endogenous cannabinoid system controls extinction of aversive memories. Nature 418:530–4.

Martín-García E, Bourgoin L, Cathala A, Kasanetz F, Mondesir M, Gutiérrez-Rodriguez A, Reguero L, Fiancette J-F, Grandes P, Spampinato U, Maldonado R, Piazza PV, Marsicano G, Deroche-Gamonet V. 2015. Differential Control of Cocaine Self-Administration by GABAergic and Glutamatergic CB1 Cannabinoid Receptors. Neuropsychopharmacology 10.1038/npp.2015.351.

Di Marzo V, Melck D, Orlando P, Bisogno T, Zagoory O, Bifulco M, Vogel Z, De Petrocellis L. 2001. Palmitoylethanolamide inhibits the expression of fatty acid amide hydrolase and enhances the anti-proliferative effect of anandamide in human breast cancer cells. Biochem J 358:249–55.

Mato S, Alberdi E, Ledent C, Watanabe M, Matute C. 2009. CB1 cannabinoid receptor-dependent and -independent inhibition of depolarization-induced calcium influx in oligodendrocytes. Glia 57:295–306.

Matsuda LA, Bonner TI, Lolait SJ. 1993. Localization of cannabinoid receptor mRNA in rat brain. J Comp Neurol 327:535–50.

Mechoulam R, Ben-Shabat S, Hanus L, Ligumsky M, Kaminski NE, Schatz AR, Gopher A, Almog S, Martin BR, Compton DR, Pertwee RG, Griffin G, Bayewitch M, Barg J, Vogel Z. 1995. Identification of an endogenous 2-monoglyceride, present in canine gut, that binds to cannabinoid receptors. Biochem Pharmacol 50:83–90.

Mechoulam R, Parker L a. 2011. The Endocannabinoid System and the Brain. Annu Rev Psychol 64:120717165617008.

Meng X-D, Wei D, Li J, Kang J-J, Wu C, Ma L, Yang F, Zhu G-M, Ou-Yang T-P, Liu Y-Y, Jiang W. 2014. Astrocytic expression of cannabinoid type 1 receptor in rat and human sclerotic hippocampi. Int J Clin Exp Pathol 7:2825–37.

Metna-Laurent M, Marsicano G. 2015. Rising stars: Modulation of brain functions by astroglial type-1 cannabinoid receptors. Glia 63:353–64.

Meyer AH, Katona I, Blatow M, Rozov A, Monyer H. 2002. In vivo labeling of parvalbumin-positive interneurons and analysis of electrical coupling in identified neurons. J Neurosci 22:7055–64.

Miettinen R, Gulyás AI, Baimbridge KG, Jacobowitz DM, Freund TF. 1992. Calretinin is present in non-pyramidal cells of the rat hippocampus—II. Co-existence with other calcium binding proteins and gaba. Neuroscience 48:29–43.

Moldrich G, Wenger T. 2000. Localization of the CB1 cannabinoid receptor in the rat brain. An immunohistochemical study. Peptides 21:1735–42.

Molina-Holgado E, Vela JM, Arevalo-Martin A, Almazan G, Molina-Holgado F, Borrell J, Guaza C. 2002a. Cannabinoids Promote Oligodendrocyte Progenitor Survival: Involvement of Cannabinoid Receptors and

Phosphatidylinositol-3 Kinase/Akt Signaling. J Neurosci 22:9742–53.

Molina-Holgado F, Molina-Holgado E, Guaza C, Rothwell NJ. 2002b. Role of CB1 and CB2 receptors in the inhibitory effects of cannabinoids on lipopolysaccharide-induced nitric oxide release in astrocyte cultures. J Neurosci Res 67:829–36.

Monory K, Blaudzun H, Massa F, Kaiser N, Lemberger T, Schütz G, Wotjak CT, Lutz B, Marsicano G. 2007. Genetic dissection of behavioural and autonomic effects of Delta(9)-tetrahydrocannabinol in mice. PLoS Biol 5:e269.

Monory K, Massa F, Egertová M, Eder M, Blaudzun H, Westenbroek R, Kelsch W, Jacob W, Marsch R, Ekker M, Long J, Rubenstein JL, Goebbels S, Nave K-A, During M, Klugmann M, Wölfel B, Dodt H-U, Zieglgänsberger W, Wotjak CT, Mackie K, Elphick MR, Marsicano G, Lutz B. 2006. The endocannabinoid system controls key epileptogenic circuits in the hippocampus. Neuron 51:455–66.

Monory K, Polack M, Remus A, Lutz B, Korte M. 2015. Cannabinoid CB1 receptor calibrates excitatory synaptic balance in the mouse hippocampus. J Neurosci 35:3842–50.

Morrison JH, Benoit R, Magistretti PJ, Bloom FE. 1983. Immunohistochemical distribution of pro-somatostatin-related peptides in cerebral cortex. Brain Res 262:344–51.

Munro S, Thomas KL, Abu-Shaar M. 1993. Molecular characterization of a peripheral receptor for cannabinoids. Nature 365:61–5.

Navarrete M, Araque A. 2008. Endocannabinoids mediate neuron-astrocyte communication. Neuron 57:883–93.

Navarrete M, Araque A. 2010. Endocannabinoids potentiate synaptic transmission through stimulation of astrocytes. Neuron 68:113–26.

Navarrete M, Díez A, Araque A. 2014. Astrocytes in endocannabinoid signaling. Philos Trans R Soc Lond B Biol Sci 369:20130599.

Navarrete M, Perea G, Maglio L, Pastor J, García de Sola R, Araque A. 2013. Astrocyte calcium signal and gliotransmission in human brain tissue. Cereb Cortex 23:1240–6.

Navarro-Galve B, Villa A, Bueno C, Thompson L, Johansen J, Martínez-Serrano A. 2005. Gene marking of human neural stem/precursor cells using green fluorescent proteins. J Gene Med 7:18–29.

Nolte C, Matyash M, Pivneva T, Schipke CG, Ohlemeyer C, Hanisch UK, Kirchhoff F, Kettenmann H. 2001. GFAP promoter-controlled EGFP-expressing transgenic mice: a tool to visualize astrocytes and astrogliosis in living brain tissue. Glia 33:72–86.

Nyíri G, Cserép C, Szabadits E, Mackie K, Freund TF. 2005a. CB1 cannabinoid receptors are enriched in the perisynaptic annulus and on preterminal segments of hippocampal GABAergic axons. Neuroscience 136:811–22.

Nyíri G, Szabadits E, Cserép C, Mackie K, Shigemoto R, Freund TF. 2005b.

GABAB and CB1 cannabinoid receptor expression identifies two types of septal cholinergic neurons. Eur J Neurosci 21:3034–42.

Ohno-Shosaku T, Kano M. 2014. Endocannabinoid-mediated retrograde modulation of synaptic transmission. Curr Opin Neurobiol 29:1–8.

Ohno-Shosaku T, Maejima T, Kano M. 2001. Endogenous Cannabinoids Mediate Retrograde Signals from Depolarized Postsynaptic Neurons to Presynaptic Terminals. Neuron 29:729–38.

Okamoto Y, Morishita J, Tsuboi K, Tonai T, Ueda N. 2004. Molecular characterization of a phospholipase D generating anandamide and its congeners. J Biol Chem 279:5298–305.

Oliveira da Cruz JF, Robin LM, Drago F, Marsicano G, Metna-Laurent M. 2016. Astroglial type-1 cannabinoid receptor (CB1): A new player in the tripartite synapse. Neuroscience.343: 35-42

Ortega-Gutiérrez S, Molina-Holgado E, Guaza C. 2005. Effect of anandamide uptake inhibition in the production of nitric oxide and in the release of cytokines in astrocyte cultures. Glia 52:163–8.

Perea G, Navarrete M, Araque A. 2009. Tripartite synapses: astrocytes process and control synaptic information. Trends Neurosci 32:421–31.

Perez-Alvarez A, Navarrete M, Covelo A, Martin ED, Araque A. 2014. Structural and functional plasticity of astrocyte processes and dendritic spine interactions. J Neurosci 34:12738–44.

Pertwee RG, Howlett a C, Abood ME, Alexander SPH, Marzo V Di, Elphick MR, Greasley PJ, Hansen HS, Kunos G. 2010. International Union of Basic and Clinical Pharmacology . LXXIX . Cannabinoid Receptors and Their Ligands : Beyond CB 1 and CB 2. Pharmacol Rev 62:588–631.

Pertwee RG. 1997. Pharmacology of cannabinoid CB1 and CB2 receptors. Pharmacol Ther 74:129–80.

Pertwee RG. 2000. Cannabinoid receptor ligands: clinical and neuropharmacological considerations, relevant to future drug discovery and development. Expert Opin Investig Drugs 9:1553–71.

Pertwee RG. 2001. Cannabinoid receptors and pain. Prog Neurobiol 63:569–611.

Pertwee RG. 2009. Emerging strategies for exploiting cannabinoid receptor agonists as medicines. Br J Pharmacol 156:397–411.

Pertwee RG. 2015. Endocannabinoids and Their Pharmacological Actions. In: Pertwee GR, editor. Endocannabinoids. Cham: Springer International Publishing. p 1–37.

De Petrocellis L, Cascio MG, Di Marzo V. 2004. The endocannabinoid system: a general view and latest additions. Br J Pharmacol 141:765–74.

De Petrocellis L, Di Marzo V. 2009a. An introduction to the endocannabinoid system: from the early to the latest concepts. Best Pract Res Clin Endocrinol Metab 23:1–15.

De Petrocellis L, Di Marzo V. 2009b. Role of endocannabinoids and endovanilloids in Ca2+ signaling. Cell Calcium 45:611–24.

De Petrocellis L, Vellani V, Schiano-Moriello A, Marini P, Magherini PC, Orlando P, Di Marzo V. 2008. Plant-derived cannabinoids modulate the activity of transient receptor potential channels of ankyrin type-1 and melastatin type-8. J Pharmacol Exp Ther 325:1007–15.

Piomelli D. 2003. The molecular logic of endocannabinoid signaling. Nat Rev Neurosci 4:873–84.

Piomelli D. 2014. More surprises lying ahead. The endocannabinoids keep us guessing. Neuropharmacology 76 Pt B:228–34

Puente N, Cui Y, Lassalle O, Lafourcade M, Georges F, Venance L, Grandes P, Manzoni OJ. 2011. Polymodal activation of the endocannabinoid system in the extended amygdala. Nat Neurosci 14:1542–7.

Puighermanal E, Busquets-Garcia A, Maldonado R, Ozaita A. 2012. Cellular and intracellular mechanisms involved in the cognitive impairment of cannabinoids. Philos Trans R Soc Lond B Biol Sci 367:3254–63.

Puighermanal E, Marsicano G, Busquets-Garcia A, Lutz B, Maldonado R, Ozaita A. 2009. Cannabinoid modulation of hippocampal long-term memory is mediated by mTOR signaling. Nat Neurosci 12:1552-8

Ramos J, Cruz VL, Martínez-Salazar J, Campillo NE, Páez JA. 2011. Dissimilar interaction of CB1/CB2 with lipid bilayers as revealed by molecular dynamics simulation. Phys Chem Chem Phys 13:3660–8.

Reguero L, Puente N, Elezgarai I, Mendizabal-Zubiaga J, Canduela MJ, Buceta I, Ramos A, Suárez J, Rodríguez de Fonseca F, Marsicano G, Grandes P. 2011. GABAergic and cortical and subcortical glutamatergic axon terminals contain CB1 cannabinoid receptors in the ventromedial nucleus of the hypothalamus. PLoS One 6:e26167.

Ribak CE, Seress L, Amaral DG. 1985. The development, ultrastructure and synaptic connections of the mossy cells of the dentate gyrus. J Neurocytol 14:835–57.

Ribak CE, Seress L. 1983. Five types of basket cell in the hippocampal dentate gyrus: a combined Golgi and electron microscopic study. J Neurocytol 12:577–97.

Ribak CE, Vaughn JE, Saito K. 1978. Immunocytochemical localization of glutamic acid decarboxylase in neuronal somata following colchicine inhibition of axonal transport. Brain Res 140:315–32.

Robbe D, Kopf M, Remaury A, Bockaert J, Manzoni OJ. 2002. Endogenous cannabinoids mediate long-term synaptic depression in the nucleus accumbens. Proc Natl Acad Sci U S A 99:8384–8.

Robbe D, Montgomery SM, Thome A, Rueda-Orozco PE, McNaughton BL, Buzsaki G. 2006. Cannabinoids reveal importance of spike timing coordination in hippocampal function. Nat Neurosci 9:1526–33.

Rodriguez JJ, Mackie K, Pickel VM. 2001. Ultrastructural Localization of the CB1 Cannabinoid Receptor in micro-Opioid Receptor Patches of the Rat Caudate Putamen Nucleus. J Neurosci 21:823–33.

Rossi S, Motta C, Musella A, Centonze D. 2015. The interplay between inflammatory cytokines and the endocannabinoid system in the regulation of synaptic transmission. Neuropharmacology 96:105–12.

Ruehle S, Remmers F, Romo-Parra H, Massa F, Wickert M, Wörtge S, Häring M, Kaiser N, Marsicano G, Pape H-C, Lutz B. 2013. Cannabinoid CB1 receptor in dorsal telencephalic glutamatergic neurons: distinctive sufficiency for hippocampus-dependent and amygdala-dependent synaptic and behavioral functions. J Neurosci 33:10264–77.

Ryberg E, Larsson N, Sjögren S, Hjorth S, Hermansson N-O, Leonova J, Elebring T, Nilsson K, Drmota T, Greasley PJ. 2007. The orphan receptor GPR55 is a novel cannabinoid receptor. Br J Pharmacol 152:1092–101.

Sagan S, Venance L, Torrens Y, Cordier J, Glowinski J, Giaume C. 1999. Anandamide and WIN 55212-2 inhibit cyclic AMP formation through G-protein-coupled receptors distinct from CB1 cannabinoid receptors in cultured astrocytes. Eur J Neurosci 11:691–9.

Sakata I, Nakano Y, Osborne-Lawrence S, Rovinsky SA, Lee CE, Perello M, Anderson JG, Coppari R, Xiao G, Lowell BB, Elmquist JK, Zigman JM. 2009. Characterization of a novel ghrelin cell reporter mouse. Regul Pept 155:91–8.

de Salas-Quiroga A, Díaz-Alonso J, García-Rincón D, Remmers F, Vega D, Gómez-Cañas M, Lutz B, Guzmán M, Galve-Roperh I. 2015. Prenatal exposure to cannabinoids evokes long-lasting functional alterations by targeting CB1 receptors on developing cortical neurons. Proc Natl Acad Sci U S A 112:13693–8.

Sánchez C, Galve-Roperh I, Canova C, Brachet P, Guzmán M. 1998. Δ 9 -Tetrahydrocannabinol induces apoptosis in C6 glioma cells. FEBS Lett 436:6–10.

Scavone JL, Mackie K, Van Bockstaele EJ. 2010. Characterization of cannabinoid-1 receptors in the locus coeruleus: Relationship with mu-opioid receptors. Brain Res 1312:18–31.

Scharfman HE. 2007. The CA3 “backprojection” to the dentate gyrus. Prog Brain Res 163:627–37.

Schlicker E, Timm J, Zentner J, Göthert M. 1997. Cannabinoid CB1 receptor-mediated inhibition of noradrenaline release in the human and guinea-pig hippocampus. Naunyn Schmiedebergs Arch Pharmacol 356:583–9.

Schwab MH, Bartholomae A, Heimrich B, Feldmeyer D, Druffel-Augustin S, Goebbels S, Naya FJ, Zhao S, Frotscher M, Tsai M-J, Nave K-A. 2000. Neuronal Basic Helix-Loop-Helix Proteins (NEX and BETA2/Neuro D) Regulate Terminal Granule Cell Differentiation in the Hippocampus. J Neurosci 20:3714–24.

Shen M, Piser TM, Seybold VS, Thayer SA. 1996. Cannabinoid receptor agonists inhibit glutamatergic synaptic transmission in rat hippocampal cultures. J Neurosci 16:4322–34.

Sheng WS, Hu S, Min X, Cabral GA, Lokensgard JR, Peterson PK. 2005. Synthetic cannabinoid WIN55,212-2 inhibits generation of inflammatory mediators by IL-1beta-stimulated human astrocytes. Glia 49:211–9.

Shimomura O, Johnson FH, Saiga Y. 1962. Extraction, Purification and Properties of Aequorin, a Bioluminescent Protein from the Luminous Hydromedusan,Aequorea. J Cell Comp Physiol 59:223–39.

Siddiqui AH, Joseph SA. 2005. CA3 axonal sprouting in kainate-induced chronic epilepsy. Brain Res 1066:129–46.

Sik A, Tamamaki N, Freund TF. 1993. Complete Axon Arborization of a Single CA3 Pyramidal Cell in the Rat Hippocampus, and its Relationship With Postsynaptic Parvalbumin-containing Interneurons. Eur J Neurosci 5:1719–28.

Sloviter RS, Nilaver G. 1987. Immunocytochemical localization of GABA-, cholecystokinin-, vasoactive intestinal polypeptide-, and somatostatin-like immunoreactivity in the area dentata and hippocampus of the rat. J Comp Neurol 256:42–60.

Sloviter RS. 1989. Calcium-binding protein (calbindin-D28k) and parvalbumin immunocytochemistry: localization in the rat hippocampus with specific reference to the selective vulnerability of hippocampal neurons to seizure activity. J Comp Neurol 280:183–96.

Somogyi P, Freund TF, Hodgson AJ, Somogyi J, Beroukas D, Chubb IW. 1985. Identified axo-axonic cells are immunoreactive for GABA in the hippocampus and visual cortex of the cat. Brain Res 332:143–9.

Somogyi P, Hodgson A, Smith A, Nunzi M, Gorio a, Wu J-Y. 1984. Different Populations Cortex and Hippocampus of Gabaergic Neurons in the Somatostatin- Visual or and. J Neurosci:2590–603.

Soria-Gómez E, Bellocchio L, Reguero L, Lepousez G, Martin C, Bendahmane M, Ruehle S, Remmers F, Desprez T, Matias I, Wiesner T, Cannich A, Nissant A, Wadleigh A, Pape H-C, Chiarlone AP, Quarta C, Verrier D, Vincent P, Massa F, Lutz B, Guzmán M, Gurden H, Ferreira G, Lledo P-M, Grandes P, Marsicano G. 2014. The endocannabinoid system controls food intake via olfactory processes. Nat Neurosci 17:407–15.

Soria-Gómez E, Busquets-Garcia A, Hu F, Mehidi A, Cannich A, Roux L, Louit I, Alonso L, Wiesner T, Georges F, Verrier D, Vincent P, Ferreira G, Luo M, Marsicano G. 2015. Habenular CB1 Receptors Control the Expression of Aversive Memories. Neuron 88:306–13.

Soriano E, Frotscher M. 1989. A GABAergic axo-axonic cell in the fascia dentata controls the main excitatory hippocampal pathway. Brain Res 503:170–4.

Stanfield BB, Cowan WM. 1979. The development of the hippocampus and dentate gyrus in normal and reeler mice. J Comp Neurol 185:423–59.

Steindel F, Lerner R, Häring M, Ruehle S, Marsicano G, Lutz B, Monory K. 2013. Neuron-type specific cannabinoid-mediated G protein signaling in mouse hippocampus. J Neurochem 124:1–13.

Stella N, Schweitzer P, Piomelli D. 1997. A second endogenous cannabinoid that modulates long-term potentiation. Nature 388:773–8.

Stella N. 2010. Cannabinoid and cannabinoid-like receptors in microglia, astrocytes, and astrocytomas. Glia 58:1017–30.

Straiker A, Hu SS-J, Long JZ, Arnold A, Wager-Miller J, Cravatt BF, Mackie K. 2009. Monoacylglycerol lipase limits the duration of endocannabinoid-mediated depolarization-induced suppression of excitation in autaptic hippocampal neurons. Mol Pharmacol 76:1220–7.

van Strien NM, Cappaert NLM, Witter MP. 2009. The anatomy of memory: an interactive overview of the parahippocampal-hippocampal network. Nat Rev Neurosci 10:272–82.

Stuhmer T. 2002. Expression from a Dlx Gene Enhancer Marks Adult Mouse Cortical GABAergic Neurons. Cereb Cortex 12:75–85.

Suárez J, Romero-Zerbo SY, Rivera P, Bermúdez-Silva FJ, Pérez J, De Fonseca FR, Fernández-Llebrez P. 2010. Endocannabinoid system in the adult rat circumventricular areas: an immunohistochemical study. J Comp Neurol 518:3065–85.

Sugiura T, Kodaka T, Kondo S, Tonegawa T, Nakane S, Kishimoto S, Yamashita A, Waku K. 1997. Inhibition by 2-arachidonoylglycerol, a novel type of possible neuromodulator, of the depolarization-induced increase in intracellular free calcium in neuroblastoma x glioma hybrid NG108-15 cells. Biochem Biophys Res Commun 233:207–10.

Sun Y, Alexander SPH, Kendall DA, Bennett AJ. 2006. Cannabinoids and PPARalpha signaling. Biochem Soc Trans 34:1095–7.

Swanson LW, Mogenson GJ, Simerly RB, Wu M. 1987. Anatomical and electrophysiological evidence for a projection from the medial preoptic area to the “mesencephalic and subthalamic locomotor regions” in the rat. Brain Res 405:108–122.

Takács VT, Klausberger T, Somogyi P, Freund TF, Gulyás AI. 2012. Extrinsic and local glutamatergic inputs of the rat hippocampal CA1 area differentially innervate pyramidal cells and interneurons. Hippocampus 22:1379–91.

Takács VT, Szőnyi A, Freund TF, Nyiri G, Gulyás AI. 2015. Quantitative ultrastructural analysis of basket and axo-axonic cell terminals in the mouse hippocampus. Brain Struct Funct 220:919–40.

Takahashi KA, Castillo PE. 2006. The CB1 cannabinoid receptor mediates glutamatergic synaptic suppression in the hippocampus. Neuroscience 139:795–802.

Tanimura A, Yamazaki M, Hashimotodani Y, Uchigashima M, Kawata S, Abe M, Kita Y, Hashimoto K, Shimizu T, Watanabe M, Sakimura K, Kano M. 2010. The endocannabinoid 2-arachidonoylglycerol produced by diacylglycerol

lipase alpha mediates retrograde suppression of synaptic transmission. Neuron 65:320–7.

Thabuis C, Tissot-Favre D, Bezelgues J-B, Martin J-C, Cruz-Hernandez C, Dionisi F, Destaillats F. 2008. Biological functions and metabolism of oleoylethanolamide. Lipids 43:887–94.

Tóth A, Blumberg PM, Boczán J. 2009. Anandamide and the vanilloid receptor (TRPV1). Vitam Horm 81:389–419.

Tóth K, Freund TF. 1992. Calbindin D28k-containing nonpyramidal cells in the rat hippocampus: Their immunoreactivity for GABA and projection to the medial septum. Neuroscience 49:793–805.

Tsou K, Brown S, Sañudo-Peña M., Mackie K, Walker J. 1998. Immunohistochemical distribution of cannabinoid CB1 receptors in the rat central nervous system. Neuroscience 83:393–411.

Tsou K, Mackie K, Sañudo-Peña MC, Walker JM. 1999. Cannabinoid CB1 receptors are localized primarily on cholecystokinin-containing GABAergic interneurons in the rat hippocampal formation. Neuroscience 93:969–75.

Uchigashima M, Yamazaki M, Yamasaki M, Tanimura A, Sakimura K, Kano M, Watanabe M. 2011. Molecular and morphological configuration for 2-arachidonoylglycerol-mediated retrograde signaling at mossy cell-granule cell synapses in the dentate gyrus. J Neurosci 31:7700–14.

Ueda N. 2002. Endocannabinoid hydrolases. Prostaglandins Other Lipid Mediat 68-69:521–34.

Vanderbyl SL, Sullenbarger B, White N, Perez CF, MacDonald GN, Stodola T, Bunnell BA, Ledebur HC, Lasky LC. 2005. Transgene expression after stable transfer of a mammalian artificial chromosome into human hematopoietic cells. Exp Hematol 33:1470–6.

Viader A, Blankman JL, Zhong P, Liu X, Schlosburg JE, Joslyn CM, Liu Q-S, Tomarchio AJ, Lichtman AH, Selley DE, Sim-Selley LJ, Cravatt BF. 2015. Metabolic Interplay between Astrocytes and Neurons Regulates Endocannabinoid Action. Cell Rep 12:798–808.

Volterra A, Meldolesi J. 2005. Astrocytes, from brain glue to communication elements: the revolution continues. Nat Rev Neurosci 6:626–40.

Vuksic M, Del Turco D, Bas Orth C, Burbach GJ, Feng G, Müller CM, Schwarzacher SW, Deller T. 2008. 3D-reconstruction and functional properties of GFP-positive and GFP-negative granule cells in the fascia dentata of the Thy1-GFP mouse. Hippocampus 18:364–75.

Wallace MJ, Blair RE, Falenski KW, Martin BR, DeLorenzo RJ. 2003. The endogenous cannabinoid system regulates seizure frequency and duration in a model of temporal lobe epilepsy. J Pharmacol Exp Ther 307:129–37.

Walter L, Stella N. 2003. Endothelin-1 increases 2-arachidonoyl glycerol (2-AG) production in astrocytes. Glia 44:85–90.

Wang X, Miyares RL, Ahern GP. 2005. Oleoylethanolamide excites vagal sensory

neurones, induces visceral pain and reduces short-term food intake in mice via capsaicin receptor TRPV1. J Physiol 564:541–7.

Ward WW, Cormier MJ. 1979. An energy transfer protein in coelenterate bioluminescence. Characterization of the Renilla green-fluorescent protein. J Biol Chem 254:781–8

Wilson RI, Nicoll RA. 2001. Endogenous cannabinoids mediate retrograde signaling at hippocampal synapses. Nature 410:588–92.

Witter M. 2012. The Mouse Nervous System. Elsevier

Witter MP, Amaral DG. 2004. The Rat Nervous System. Elsevier

Witter MP. 2007. The perforant path: projections from the entorhinal cortex to the dentate gyrus. Prog Brain Res 163:43–61.

Wittner L, Henze DA, Záborszky L, Buzsáki G. 2007. Three-dimensional reconstruction of the axon arbor of a CA3 pyramidal cell recorded and filled in vivo. Brain Struct Funct 212:75–83.

Wu S-X, Goebbels S, Nakamura K, Nakamura K, Kometani K, Minato N, Kaneko T, Nave K-A, Tamamaki N. 2005. Pyramidal neurons of upper cortical layers generated by NEX-positive progenitor cells in the subventricular zone. Proc Natl Acad Sci U S A 102:17172–7.

Yi C-X, Habegger KM, Chowen JA, Stern J, Tschöp MH. 2011. A role for astrocytes in the central control of metabolism. Neuroendocrinology 93:143–9.

Zerucha T, Stuhmer T, Hatch G, Park BK, Long Q, Yu G, Gambarotta A, Schultz JR, Rubenstein JLR, Ekker M. 2000. A Highly Conserved Enhancer in the Dlx5/Dlx6 Intergenic Region is the Site of Cross-Regulatory Interactions between Dlx Genes in the Embryonic Forebrain. J Neurosci 20:709–21.

Zhang J-P, Xu Q, Yuan X-S, Cherasse Y, Schiffmann SN, de Kerchove d'Exaerde A, Qu W-M, Urade Y, Lazarus M, Huang Z-L, Li R-X. 2013. Projections of nucleus accumbens adenosine A2A receptor neurons in the mouse brain and their implications in mediating sleep-wake regulation. Front Neuroanat 7:43.

Zimmer A. 2015. Genetic Manipulation of the Endocannabinoid System. Handb Exp Pharmacol. Springer International Publishing 231:129-83